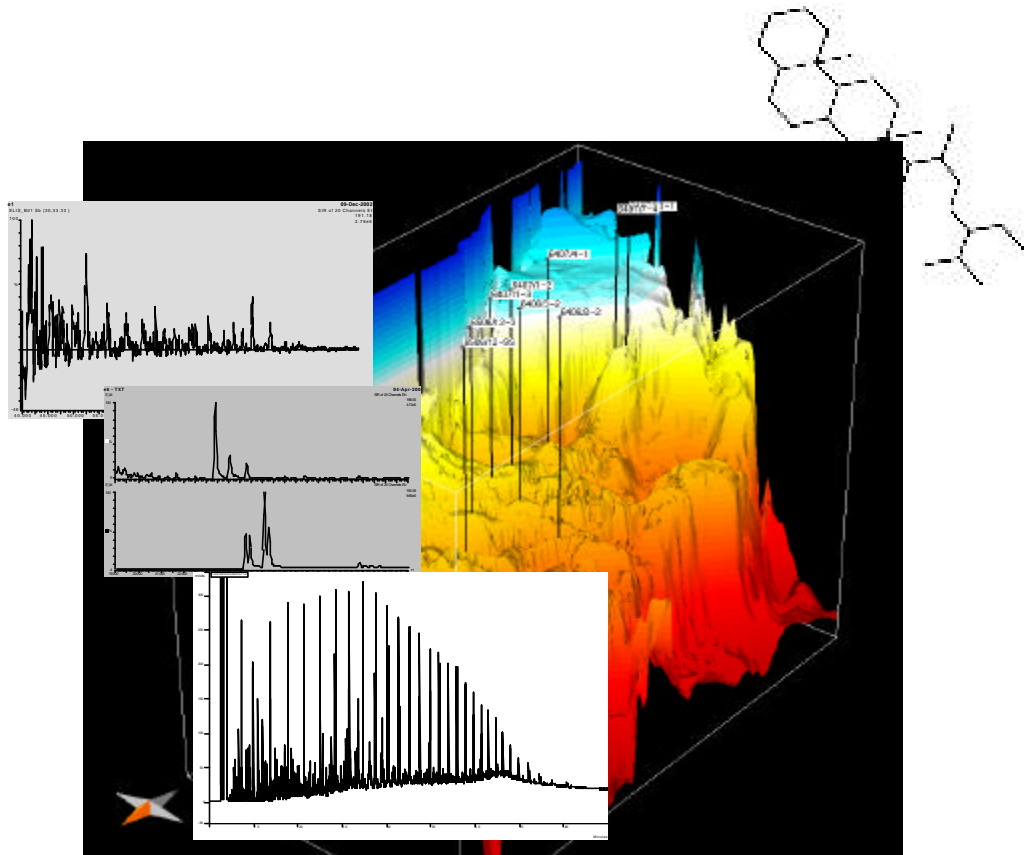

A comparison of petroleum from reservoirs and petroleum inclusions in authigenic mineral cements – Haltenbanken



Elisabeth Bøhle Sletten
University of Oslo, department of geology
2003



Acknowledgements

I would like to thank my supervisor, prof. Dag A. Karlsen for giving me the opportunity to explore the “forest” of biomarkers and other geochemical components, and for giving me input and help when I needed it the most. Kristian Backer-Owe get my gratitude for helping me through the difficulties in the lab and giving constructive comments on my thesis. I also got extensive help from Jon Erik Scheie during the last part of my study.

Statoil, and John Scotchmer in particular is gratefully acknowledged for financial support. Geologists in Statoil, NPD and Hydro have been helpful providing geological information about my study area. The study could not have been performed without the samples gathered from the Norwegian Petroleum Directorate.

My family and friends get a big hug and lots of kisses for always being there for me. If I needed to get my mind off geology, was feeling blue or just needed to talk, everyone has been there to help, you are all great! I would also like to give a big smile and thanks to my fellow students, we had a lot of great times.

University of Oslo, 25/9/2003

Elisabeth B. Sletten

No spring, nor summer beauty hath such grace
As I have seen in one autumnal face
-John Donne-

Table of contents

1. Introduction	2
2. Geological setting	4
2.1. Regional geology	5
2.2. The Haltenbanken Region.....	6
2.3 The fields.....	13
3. Analytical methods and the sample set	18
3.1. TLC-FID Iatroscan.....	19
3.2. Gas Chromatography-Flame Ionization Detector (GC-FID) – analysis of oils and extracts	20
3.3. Gas Chromatography - Mass Spectrometry (GC-MS).....	21
3.4. Microscopy.....	23
3.5. Facies and maturity parameters.....	24
3.6. The sample set.....	36
4. Results	38
4.1. Iatroscan TLC-FID oils and extracts	39
4.2. GC-FID oils and extracts	42
4.3. GC-MS oils and extracts	48
4.4. Microscopy.....	53
5. Discussion and conclusions	80
5.1. Problems and limitations in the sample set.....	81
5.2. Biomarker parameters: Inclusions versus reservoir oil/extract (south- north)	82
5.3. Comparing the fields.....	90
6. Summary and conclusions	98

1. Introduction

Petroleum explorationists have a large number of tools available to get a better understanding of the processes in the subsurface. They range from a more global understanding of basins to regional seismic studies and all the way down on micro scale when observing geochemical components like hopanes and steranes. Understanding the movement and origin of the hydrocarbons are important aspects in the exploration process.

Petroleum geochemistry, defined by Hunt (1996) is the application of chemical principles to the study of origin, migration, accumulation and alternation of petroleum, oil and gas, and the use of this knowledge in exploring for and recovering petroleum.

The use of petroleum inclusions in petroleum and reservoir geology is a relatively new tool utilized to get a better understanding of the petroleum generation and migration, paleo fluid distribution and facies and maturity of the source rocks. Fluid inclusions are tiny quantities of liquid, vapour, or a mixture of these phases, trapped in mineral cement formed after deposition (diagenetic). Various sources of evidence suggest the fluid inclusions to preserve the original composition of the hydrocarbons, and they can therefore give valuable information about several important aspects of petroleum genesis and migration. Fluid inclusions can give an answer to whether there has been one or several hydrocarbon pulses in relation to field filling and if all the hydrocarbons originate from the same source rock, or if there have been a shift in source through geologic time. They can also be a powerful tool when reconstructing the pressure – temperature (P-T) conditions of a trap, which plotted together with time, is a key parameter for the evaluation of the oil potential of a sedimentary basin. Also the time for the arrival of hydrocarbons relative to sedimentation and burial in a structure may be calculated from fluid inclusion.

Hydrocarbons contain a small amount (~1% and less) of molecules referred to as biomarkers or geochemical fossils. The biomarkers are the fingerprint of the source rock and have undergone little or no changes during maturation and migration. They are described by Tissot and Welte (1978) to be molecules synthesized by a plant or animal where the molecule is unchanged or have suffered only minor subsequent changes. It is knowledge about the kinetic and chemical properties of these compounds with high molecular weight, which is the key to their use in organic geochemistry in petroleum geology. The knowledge makes it among other things possible to decide any genetic relationship between petroleums, the amount of hydrocarbons expelled and the quality and maturity of the source rock.

Biomarkers have been used in several studies of different petroleum accumulations in the Haltenbanken region, e.g. Karlsen et al. (1995). However most of these studies focus on the oils and condensates and little material have been published on inclusions in the present and paleo reservoir sandstones. This study represents the first attempt to systematically study the C₁₅₊ fraction trapped in diagenetic inclusions and produced oils of various traps in the

Haltenbanken Area, including selected samples from the following fields; Njord, Smørbukk, Smørbukk South, Lavrans, Tyrihans North and South, Trestakk and well 6407/4-1. The inclusions and oil/condensate/extract from each field will be compared and similarities and differences in maturity and facies between different biomarkers and “medium range” parameters will be discussed. Then the fields will be compared to each other to determine if there is any geographic control on the geochemistry in the area.

This thesis aims at answering the following questions:

- To determine if it is possible to extract hydrocarbons in the range C_{15+} from inclusions.
- Is there any systematic maturity difference between fluid inclusions and trapped hydrocarbons and/or is there a difference between mediumrange parameters such as methyl dibenzothiophene and phenantrenes compared to hopanes and steranes?
- Is there any difference in organic facies between the fluid inclusions and the trapped hydrocarbons?
- Assuming there is a difference in maturity and/or facies between the fluid inclusions and trapped hydrocarbons is the difference similar in the various traps? And is there any geographic distribution?

2. Geological setting

The object of this chapter is to give a short introduction and description of the geological setting in the Haltenbanken Area, both stratigraphic and tectonic. The 7 fields/discoveries represented in this study will be described in general with emphasis on features important to oil exploration.

- 2.1. Regional geology
- 2.2. The Haltenbanken Region
- 2.3. The fields

2.1. Regional geology

The eastern North-Atlantic continental margin, including the Norwegian Sea, has undergone multiple rift events throughout its evolution since the Carboniferous (Arbenz, 1992; Hinz et al., 1993; Brekke et al., 1999). The Mid-Norwegian Margin is a rifted passive continental margin in the Norwegian Sea between 62°N and 69°30'N (Blystad et al., 1995), superimposed on the Caledonian suture between the Greenland and Fennoscandian cratons (Bukovics et al., 1984). The major plate tectonic episodes, the Caledonian orogeny and the break up of the North Atlantic divide the tectonic history of the area into three epochs:

The pre-Late Devonian epoch ended with the final closure of the Iapetus Ocean (Proto Atlantic) during the Caledonian Orogeny in Late Silurian and Early Devonian time.

Late Devonian to Paleocene was a period of episodic extensional deformation culminating with the continental separation between Eurasia and Greenland at the Paleocene-Eocene boundary.

The Earliest Eocene to Present was a period of active sea-floor spreading between Eurasia and Greenland (Blystad et al., 1995).

The Mesozoic rift systems are significantly influenced by the Caledonian orogeny but only the latest major extensional events can be mapped with confidence from the available data. These are the major Late Jurassic/Early Cretaceous and the early Tertiary rifting events (Planke et al., 1991) from the second epoch and can be seen as a series of rifting episodes. The three epochs are in the Late Carboniferous and Late Permian, in the Late Jurassic and Early Cretaceous, and in the Late Cretaceous and earliest Tertiary (Blystad et al., 1995). Prior to this, the epoch was dominated by sinistral shear along the Caledonian Iapetus suture, creating intramontane basins filled with thousands of meters of coarse sediments (Ziegler et al., 1986) e.g. the Hornhelen Basin in Western Norway.

The Late Permian rifting episode is assumed to have created large subsiding half-grabens filled with Permian clastics and carbonates as in the eastern parts of Greenland, although the seismic evidence for this is sparse (Bukovics and Ziegler, 1985). In Middle to Late Triassic time some block faulting took place and the basins were filled with extensive redbeds with evaporitic halite intervals (Jacobsen and van Veen, 1984). The latest Bathonian was a time of transition into the Late Jurassic-Early Cretaceous rifting episode (Blystad et al., 1995). This episode strongly influenced the whole Mid-Norway region. The Møre and Vøring Basins began to subside rapidly, whilst the Trøndelag Platform only experienced minor subsidence. Deep water conditions were established in the Norwegian-Greenland rift system in this period (Bukovics and Ziegler, 1985). The development of rotated fault blocks and subsiding sub-basins created stagnant bottom waters and an ideal depositional environment for organic-rich shale (Gage and Dore, 1986). The Møre and Vøring Basins as a whole started to subside regionally together with the Halten Terrace and the Trøndelag Platform during Late Cretaceous and the major faulting activity died out, indicating a gradual decreasing in the

rifting activity (Bukovics and Ziegler, 1985). The Late Cretaceous and earliest Tertiary rifting episode caused new block faulting and increased subsidence in the Vøring Basin (Blystad et al., 1995).

The last epoch of tectonic activity was the beginning of the opening of the Norwegian Sea, development of a passive margin and generation of oceanic crust in the Norwegian-Greenland Sea which started in early Tertiary and continuing today (Arbenz, 1992). This active spreading changed the regional stress regime from extensional to weakly compressional. The last important tectonic period started in the Neogene, possibly in the latest Miocene to early Pliocene, and created an up to 1500 m thick Plio-Pleistocene prograding succession across the shelf (Blystad et al., 1995).

2.2. The Haltenbanken Region

Haltenbanken is situated on the Mid-Norwegian Margin (figure 2.1.). Three pronounced fault trends are recognized in the area: N, NE and NW (Aasheim and Larsen, 1984). Predominant structural features at base Cretaceous (BCU) level are the Halten Terrace, the Trøndelag Platform, Nordland Ridge and the Vøring Basin (Whitley, 1992).

The central part of the Haltenbanken, the Halten Terrace, was formed during the Middle Jurassic to Early Cretaceous extensional event and is an approximately 80 km broad rhombic shaped zone within the Kristiansund-Bodø Fault Complex. It is a down faulted step between the Trøndelag Platform and the Vøring Basin and was formed in a pull-apart basin in a dextral, strike-slip faulting regime. Faulting was initiated in the Early Jurassic, culminating in widespread tectonic activity in the Late Jurassic and Early Cretaceous (Provan, 1992). The latter phase, often referred to as the Cimmeridgian tectonic phase, resulted in widespread footwall uplift and erosion and tilting of the Jurassic fault blocks (Whitley, 1992).

To the north, the Halten Terrace passes into the narrower Dønna Terrace, and to the south the displacement is concentrated within the narrow Klakk Fault Complex (Ehrenberg et al., 1992). To the east the terrace is separated from the Trøndelag Platform by the Kristiansund-Bodø Fault Zone, and to the west the West Haltenbank High separates the terrace from the deeper Møre-Vøring Basin.

2. Geological setting

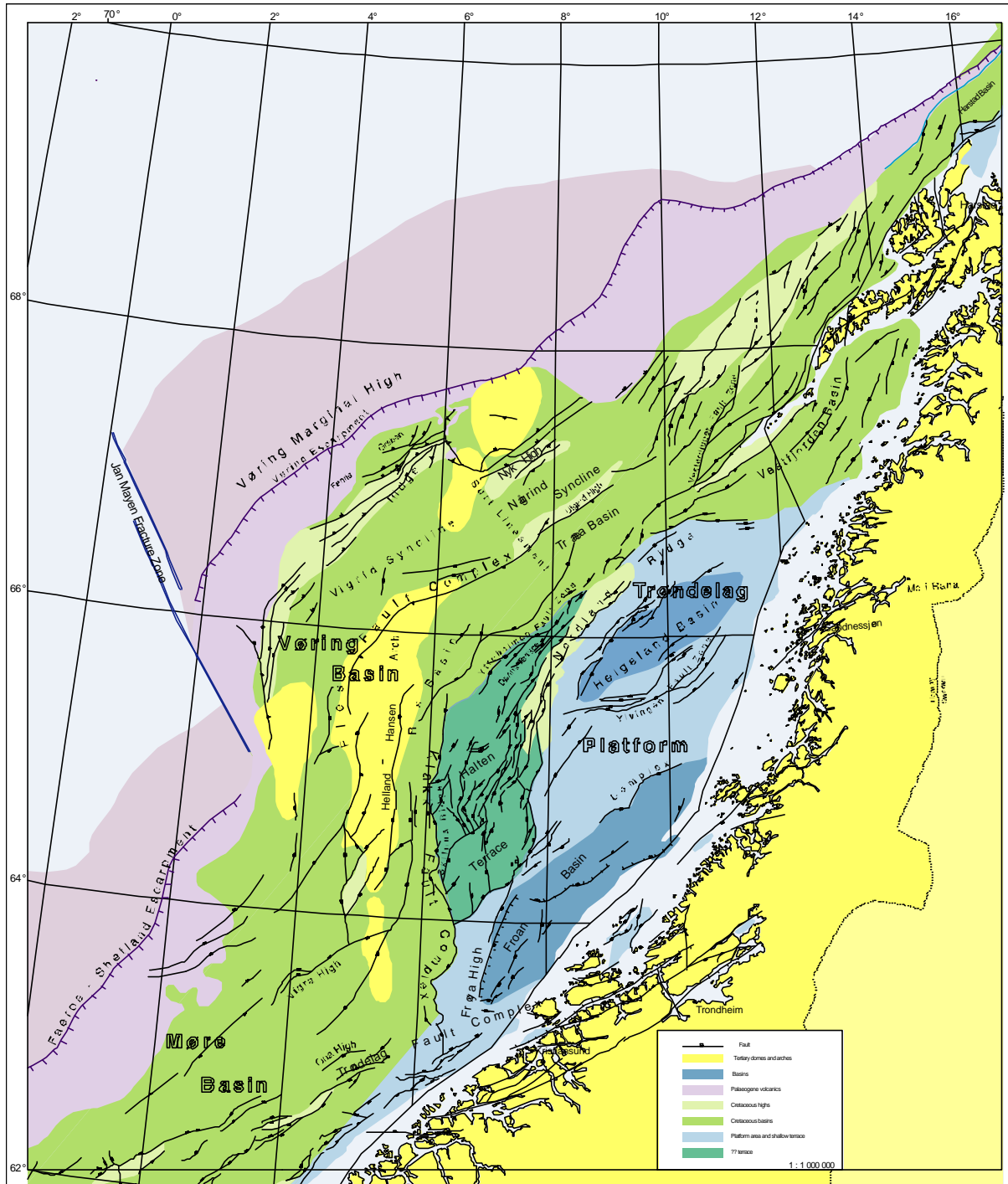


Figure 2.1. The Haltenbanken Area with structural elements (Blystad et al., 1995).

2.2.1. Stratigraphy at Haltenbanken

Pre-Triassic sediments have not been drilled in the Haltenbanken wells but from seismic sections (Ehrenberg et al., 1992) identifies thick Devonian to Carboniferous deposits. This

chapter will give a general description of the deposits from Triassic to Quaternary in the Haltenbanken Area. Figure 2.2. shows the general lithostratigraphy of the Norwegian Sea.

Triassic

The Triassic sediments in Haltenbanken is genetically related to the North Sea and the Norwegian-Danish Basin (Jacobsen and van Veen, 1984). Because of eustatic lowstand, continental strata (red beds) were deposited over the Halten terrace and the Trøndelag platform during the middle Triassic to the Early Jurassic. The deposits consist of red siltstones, shales and thin sandstones accumulated in a fluvial setting (Ehrenberg et al., 1992). The Early Triassic deposits consist mainly of shale, and sand- and siltstones interbedded with shale (grey beds). Above this sequence a thick unit of evaporites, shales and halite was deposited. The two thick halite units (each 400 m thick) of Middle and Late Triassic age probably represent incursion from predominantly marine area of the Barents shelf along arms of the Atlantic rift system (Whitley, 1992).

Jurassic

Upper Triassic and Jurassic sediments can only be confidently mapped on the inner part of the Mid-Norwegian shelf, where Cretaceous subsidence was low to moderate (Bøen et al., 1983). The Lower Jurassic is represented by the Båt Group deposited in a generally transgressive situation. The Båt Group is divided into three formations; Åre, Tilje and Ror (figure 2.2.). The Middle Rhaetian (Upper Triassic) to Pliensbachian (Lower Jurassic) Åre Formation consists of sandstones, shales and coals representing an extensive delta-plain development (Ehrenberg et al., 1992). The sediments range from mainly fluvial in the bottom to some intercalated marine beds (Heum et al., 1986) in the upper part. In the 490 m thick unit described by (Ehrenberg, 1990) there are no major hiatus, and the Jurassic part seems to overlie the Triassic conformably. The coals in the Åre Formation are estimated to have a large hydrocarbon source potential (Heum et al., 1986). It is considered to be an important gas-prone source rock with possible oil generation potential (Whitley, 1992). Because of the low sand content in the Åre Formation it is considered to have a generally poor reservoir quality (Karlsson, 1984).

The transition from the Åre Formation to the overlying Tilje Formation is gradual. A transgression forces the deltaic deposition system to retreat towards the east and is followed by an increased sand influx in the west. Bukovics et al. (1984) ascribes the increase in the sand influx to be related to the uplift and erosion of a tectonically active element in the west, possibly the Haltenbanken High. The Tilje Formation is 75 to 150 m thick where the unit have maximum thickness in the west and is thinning towards the east. The sediments are delta plain – delta front deposits (Dalland et al., 1988), and the formation is considered to have been deposited in marine near shore to shallow offshore conditions. The reservoir properties of the formation are gradually changing due to the wide lateral distribution, but Fagerland (1990) regarded them as generally good.

2. Geological setting

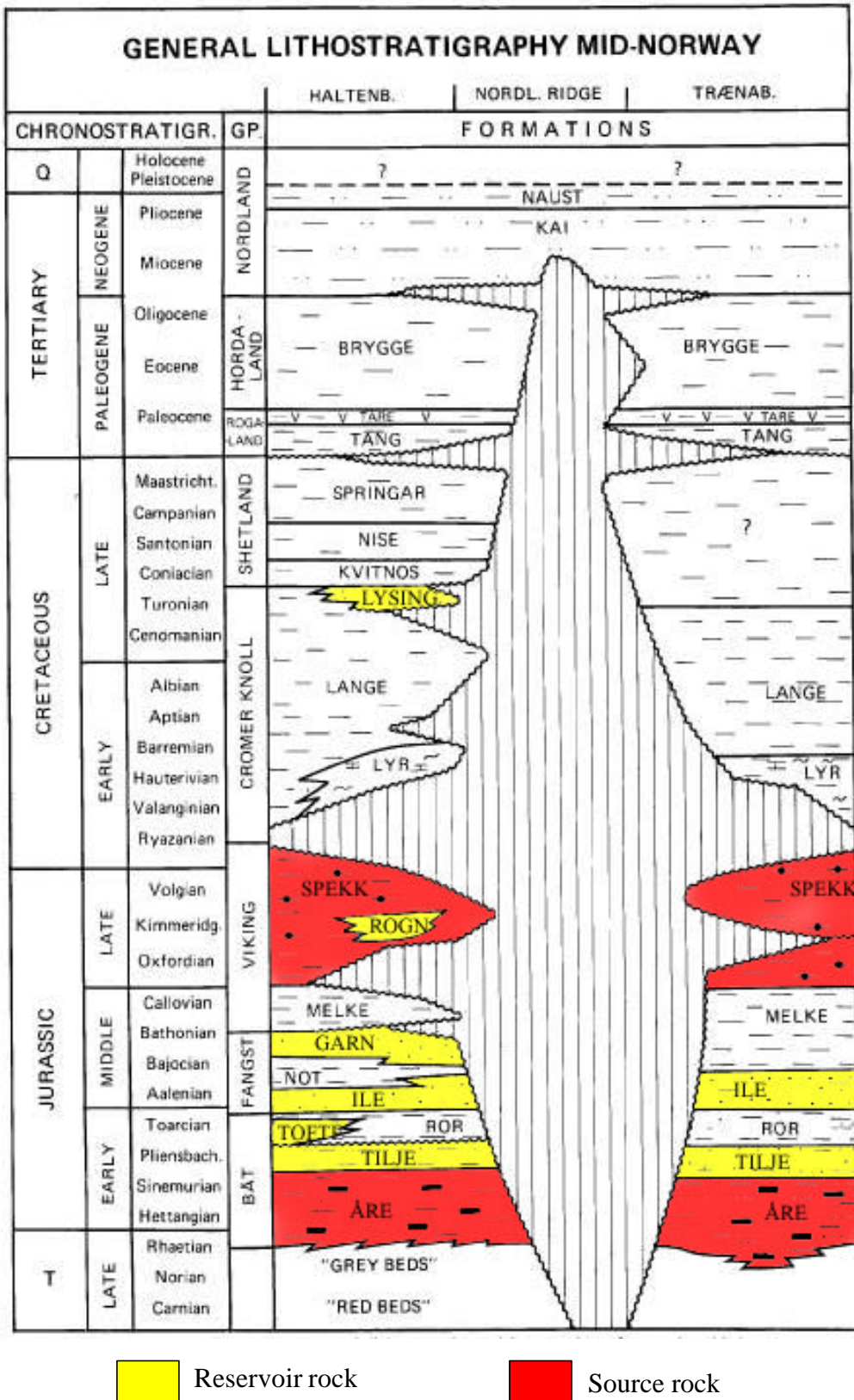


Figure 2.2. Generalized time- and lithostratigraphic section from the Halten Terrace to the Trænabanken area indicating the main reservoir and source rocks (Karlsen et al., 1995).

Following the deposition of the Tilje Formation, a strong transgression and open marine conditions of the entire Haltenbanken area resulted in the deposition of the Ror Formation. The Ror Formation is a 53 to 73 m thick, over-all upward coarsening unit consisting of marine shales and mudstones with several upward-coarsening storm deposited sandstone beds (Ehrenberg et al., 1992).

A regression in the Middle Jurassic produced the coastal deposits in the Fangst Group, comprising the Ile, Not and Garn Formations. The sandy deposits were caused by clastic influx from regional updoming during the same major sea level lowstand as the Brent Group in the northern North Sea (Ehrenberg et al., 1992; Whitley, 1992). The Fangst Group was deposited in response to rapid changes in relative sea level in a cyclic transgressive/regressive way. The cyclicity is expressed by the large scale transition from marginal marine deposits (Ile Formation) via the deeper marine Not Formation into the shallow marine Garn Formation. The Ile Formation is a 60 to 82 m thick series of tidally influenced nearshore marine sands and thinner bioturbated shale/siltstone intervals (Ehrenberg et al., 1992) deposited in the Late Toarcian to Early Bajocian. The transition from the underlying Ror Formation is easily seen as an extensive carbonate cemented bed interpreted to be a hardground (Karlsson, 1984). The sands in the Ile Formation are considered to have good reservoir quality.

The transition to the overlying Not Formation is represented by a 10 cm thick transgressive conglomerate lag bed. The Not Formation is deposited in Aalenian to Bajocian and consists of marine shelf sediments, 24-34 m thick. The formation shows a coarsening upward trend from mainly shales at the base, grading upward into highly bioturbated siltstones and at the top fine-grained sandstone. Heum et al. (1986) believes the source rock potential to be of no importance.

A sharp erosional contact separates the Not Formation from the overlying Garn Formation. The Garn Formation varies in thickness from 14 to 114 m reflecting varying depositional thickness and local erosion (Ehrenberg, 1990). It is thickest in the south-western parts and thins towards the central and northern parts of the Halten Terrace. This Formation is an important reservoir unit which can give good porosity and permeability values, eg. ~22% porosity at 4.7 km burial (Rønnevik, 1998).

In the Upper Jurassic the Viking Group, including Melke, Spekk and Rogn Formations, was deposited. The Melke and Spekk formations are marine shales deposited during the major transgression beginning at the end of the Middle Jurassic and continuing into the Early Cretaceous.

The Melke Formation consists of 117-282 m of “cold” shale with silt- and claystones interbedded with some fine-grained sandstone layers and carbonate cemented horizons and is equivalent to the Heather Formation in the northern North Sea. The depositional environment is interpreted to be open marine. The formation is moderately organic-rich (generally 1 to 4% TOC) (Ehrenberg et al., 1992) but because of low hydrogen index (HI) it is believed to be of no importance as a source rock. However, its potential may be better in basin depressions.

The Late Jurassic transgression culminated with the deposition of the Spekk Formation in deeper water with anoxic bottom conditions (Whitley, 1992). The Spekk formation was

deposited in Oxfordian to Ryazanian and is an equivalent to the Kimmeridge Clay and Draupne Formations of the North Sea. It consists of highly radioactive shales and mudstones with a high content of organic carbon (generally 5 to 8% TOC) and high hydrogen index (HI → 800 mg HCs/g TOC) and is an important source rock in the area (Heum et al., 1986; Whitley, 1992).

The Late Jurassic Rogn Formation occurs as a lens of restricted lateral extent within the Spekk Formation in the Draugen Field (Provan, 1992) in the eastern parts of Haltenbanken. The unit was deposited due to erosion of Middle to Late Jurassic clastics exposed elsewhere on the Trøndelag Platform and is bounded by regional unconformities. It is a shallow marine bar deposit 40-50 m thick in the Draugen Field (Ellenor and Mozetic, 1986; Dalland et al., 1988) and shows a coarsening upward trend with shales and siltstones at the bottom and sandstones at the top. The reservoir quality is generally very good towards the top of the formation because of an increase in the sand content.

Cretaceous

Thick marine calcareous shales with occasional turbiditic sandstones (some with proven reservoir quality) were deposited during rapid subsidence in the Cretaceous (Ehrenberg et al., 1992; Whitley, 1992). The deposits are divided into two groups; the Cromer Knoll Group, 661-777 m thick (Lyr, Lange and Lysing Formations) and the Shetland Group, 869-922 m thick (Kvitnos, Nise and Springar Formations). The formations were deposited during a transgression and the marine shales onlap against the Kimmerian structures (Ehrenberg et al., 1992).

Tertiary

Tertiary deposition followed a regional Upper Cretaceous unconformity and thick marine shales were deposited on a passive continental margin. Tuffaceous sediments form a regional seismic marker (equivalent to the Balder Formation) at the Paleocene-Eocene boundary. The Tertiary stratigraphy is represented by the Rogaland Group consisting of the Tang and Tare Formations, the Hordaland Group with the Brygge Formation and one member of the Nordland Group, the Naust Formation (Dalland et al., 1988).

Quaternary

The Haltenbanken area underwent rapid subsidence from the Late Pliocene throughout the Quaternary. The Nordland Group represented by the Naust formation is a thick sequence of alternating glaciomarine grey clay and poorly sorted sand (Whitley, 1992).

2.2.2. Tectonic and burial history

During Late Triassic and Early Jurassic the sediments were deposited in a subsiding basin where the only tectonic activity was the development of down-to-the-west growth faults.

Middle Jurassic was a period of no recorded tectonic activity, followed by the Kimmerian rifting at the transition between Jurassic and Cretaceous. The rifting strongly affected the

Mid-Norwegian shelf with erosion of the top of the rotated fault blocks and a widespread unconformity. During Early Cretaceous, the Møre and Vøring basins subsided rapidly while the more stable Trøndelag Platform underwent only limited subsidence. In Mid-Cretaceous the major faulting activity ceased, indicating a gradual decrease in rifting activity (Bukovics and Ziegler, 1985). During Late Cretaceous, the Møre and Vøring Basins as a whole started to subside regionally together with the Halten Terrace and Trøndelag Platform. This can be related to the gradual cooling of the thermal anomaly (ref. McKenzie, 1978) that was initiated by the Late Cimmerian tectonic phase.

Late Cretaceous and Early Tertiary rifting episodes caused new block faulting and increased subsidence in the Vøringen Basin (Blystad et al., 1995). The rifting was centred on the break-up-axis of the Greenland and Fennoscandian cratons and represents the initial stage of sea floor spreading in the Iceland Sea. Haltenbanken then developed as a passive continental margin where the subsidence was controlled by lithospheric cooling, contraction and loading of water and sediments.

Rapid burial of the Halten Terrace and Trøndelag Platform started in Late Pliocene and continued through the Quaternary. During this period deposition of approximately 1 km glaciomarine clastics together with rapid subsidence resulted in deepening and heating of the underlying strata throughout the Haltenbanken area (Ehrenberg et al., 1992). This event accelerated hydrocarbon generation and migration, with the result that most of the petroleum today found in traps at Haltenbanken was generated after 3.0 M.Y. b.p. Deposition of these Late Pliocene-Quaternary clastics also created overpressure in the Jurassic reservoir section in the deeper western part of the Haltenbank Terrace. The result was in cases that hydrocarbons were lost due to fracturing of the sealing shaley cap rocks.

2.2.3. Source rocks

The term source rock refers here to a unit of sedimentary rock with sufficient amounts of organic matter, which during burial generate and release commercial quantities of petroleum. The term includes coals, shales and other organic rich sediments. The main source rocks in the Haltenbanken region are the Spekk (shale) and Åre (coal and shale) Formations of Jurassic age.

The Spekk Formation, a marine hot shale with high radioactivity and 5 to 8% TOC, is an equivalent to the Draupne and Kimmeridge Clay Formation in the North Sea and characterised as a fairly rich oil-prone source rock (Heum et al., 1986). It contains kerogen which varies from Type II to type III (Whitley, 1992). Karlsen et al. (1995) rated it to be overmature towards the Vøring Basin in the west and immature in the Trøndelag Platform in the east. Primary migration is described to start at a maturity level of 0.7% vitrinite reflectance equivalent (VRE), corresponding to a burial of ca. 3900 m (Heum et al., 1986). Based on the most typical thickness, the Spekk Formation in Haltenbanken has been calculated to have a generative capacity of 7 to 20 million m³ of light oil per km². This

formation seems to have generated the bulk of C₁₅₊-hydrocarbons in the Haltenbanken area (Pittion and Gouadain, 1985; Karlsen et al., 1995).

The Åre Formation in the Haltenbanken area contains both coals and shales able to generate mainly condensate, but also oil, wet gas and methane. The organic matter is dominated by terrestrially-derived humic material classified as type III and type IV kerogen (Cohen and Dunn, 1987; Hvoslef et al., 1988; Khorasani, 1989; Odden et al., 1998). Primary migration starts at 0.65% VRE in the coaly sequences, corresponding to a burial depth of ca 3450 m, and at 0.85 VRE in the paralic shales. Total potential is estimated to 10 to 25 million m³ oil and condensate, and at least the same amount of gas, per km² (Heum et al., 1986). The Åre Formation is assumed to be the most important source rock in the Haltenbanken area when total amounts of hydrocarbons generated through geologic time are considered. Mo et al. (1989) consider the Åre Formation to be far more important volumetrically in terms of hydrocarbon generation than the Spekk Formation, but this is strongly debated and not generally accepted.

Each field in this study is discussed below with a closer focus at the source and reservoir rocks.

2.3 The fields

8 fields/discoveries from the Haltenbanken Area are presented in this study. Below follows a short description of the main elements of the different fields.

2.3.1. Trestakk

Trestakk is a small oil discovery located in block 6406/3 west on the Halten Terrace. The main reservoir is in the Garn Formation located in a rotated NNE-SSW trending fault block. The Garn Fm. in Trestakk generally has limited reservoir quality due to the large burial depth of the Trestakk field. There is hardly any published material on the Trestakk Field.

2.3.2. Tyrihans

The Tyrihans discovery is mainly located in block 6407/1 and comprises of two structures - Tyrihans North and Tyrihans South which extends into block 6406/3. The Tyrihans South trap is an anticlinal structure which towards the north transforms into a horst structure (Tyrihans North) across a saddle area (Larsen et al., 1987).

The reservoir in the Tyrihans field is sandstones from the upper part of the Middle Jurassic Garn Formation. The formation was succeeding a relative sea level fall and was deposited in an upper shoreface environment with variable degree of tidal influence. Sandstones constitutes major part of the Garn formation with generally medium to good reservoir quality in the Tyrihans fields, and it is further subdivided into four subzones; Garn 1, 2, 3 and 4.

2. Geological setting

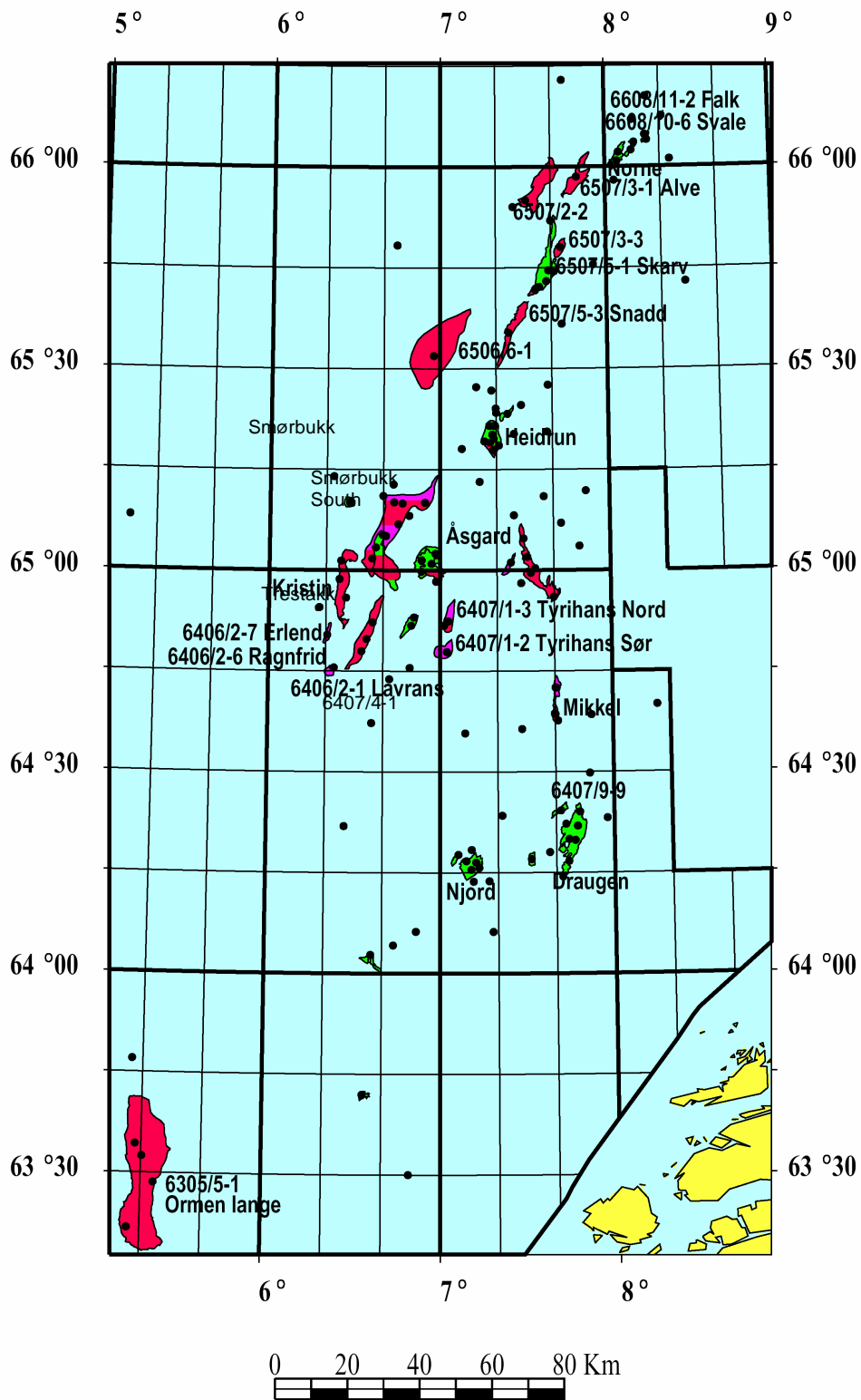


Figure 2.3. The fields in the Haltenbanken Area (Blystad et al., 1995).

The main source rock in the Tyrrihans region is thought to be the anoxic shales of the Spekk Formation, equivalent to the Draupne and Kimmeridge Clay Formation in the North Sea.

Karlsen et al. (1995) suggested that the geochemistry of the Tyrihans North and South traps indicate that Tyrihans North was filled from a more carbonate rich Spekk formation as compared to Tyrihans South. Thus, the traps were filled from separate basins. But also the Åre Formation may also have contributed with some hydrocarbons to the field. The hydrocarbon finds are mainly gas in the Tyrihans South and oil in the Tyrihans North structure. The filling history and maturity in the field is not widely discussed, but the maturities have by Karlsen et al. (1995) been rated from low to moderate based on biomarker analysis.

2.3.3. Lavrans

The Lavrans discovery is in block 6406/2 in the southern part of the Haltenbanken Area. The hydrocarbon trap lies in a rotated fault block, bounded to the east by the Trestakk-fault and to the west by a graben (an extended part of the Smørbukk-fault). The main reservoir units are the Ile Formation in the Fangst group and the Tofte Formation in the Båt Group, furthermore the Tilje Formation can be a potential reservoir rock in some parts of the Lavrans Field.

The gas condensate (average GOR is 3000) in Lavrans is sourced mainly from the Spekk Formation, but the shales in the Melke Formation may also have generated a small amount of hydrocarbons. Hydrocarbons have migrated into the structure from the around lying grabens, mainly where there is contact between the source and reservoir rock (Bang, 1998; Bergan, 1999).

2.3.4. Njord

The Njord field is situated on the mid-Noway shelf in blocks 6407/7 and 6407/10.

Main development of the Njord structure occurred during the Late Jurassic by downfaulting and rotation of a large hanging-wall block along a major listric shaped fault plane belonging to the Vingereie fault complex which separates the Njord structure from the Frøya high to the South-East (Lilleng and Gundestø, 1997).

The main reservoir is the Tilje formation, where the tidal channels have the best reservoir quality. A higher marine influence towards the top of the formation results in the transition to the marine Spekk formation. The Njord field is sourced from multiple kitchen areas, but the Spekk formation source rock can explain the main hydrocarbon charge. The westernmost part of the field is sourced from the kitchen area to the west of the field, whereas the eastern part of the field is sourced from the Gimsan Basin to the east (Hydro, 2003).

2.3.5. Smørbukk / Smørbukk South fields

The Smørbukk and Smørbukk South hydrocarbon fields are located in the north-west part of the Halten Terrace mainly in block 6506/12, but Smørbukk extends into block 6506/11 and parts of Smørbukk South is in block 6406/3-3.

The Smørbukk field lies at the crest of a southeast-dipping fault block, bounded to the west by a major normal fault and to the north by an east-west trending graben that transects the crest of the fault block (Ehrenberg et al., 1992). The trap is a complicated faulted anticline which is divided into a northern and a southern segment by a central graben structure. The two segments are not in pressure communication with one another and hydrocarbons are only found in the southern segment.

The hydrocarbon accumulations are trapped in multiple zones of mainly regressive sandstone bodies separated by transgressive shale units that form vertical production barriers. The reservoir sands were deposited in Lower to Middle Jurassic and have been buried to more than 4500 m. Half the in-place liquid reserves in Smørbukk are accumulated in the Lower Jurassic Tilje Formation. This formation varies from 119 to 151 m in thickness and consists mainly of tidally influenced nearshore marine sandstones with thinner layers of offshore shale and bioturbated siltstones (Ehrenberg et al., 1992). The Middle Jurassic Garn Formation deposited in a fan delta or delta front environment contain also large gas condensate accumulations.

Fluids in the Smørbukk reservoirs are mainly rich gas condensates and volatile oils derived from both the Åre and the Spekk Formation (Aasheim et al., 1986; Ehrenberg et al., 1992). Karlsen et al. (1995) suggested the hydrocarbons mainly to be derived from the oil-prone source rock of the Spekk Formation rather than the coals of the Åre Formation. In the northern part of the field the reservoir is dry, presumably because of high overpressure. Hydrocarbons found in the reservoir show difference in maturity, the petroleum in the north-east being less mature than the petroleum in the southern parts. Together with the fact that the least mature petroleum is located in the shallowest parts of the structure, this indicate filling of the reservoir from the south and east. The many petroleum heterogeneities in the Smørbukk indicate a complex history with several filling episodes, and reflect low degree of intra-reservoir petroleum communication (Angard, 1996).

The Smørbukk South field is located south-east of the Smørbukk field in block 6506/12 and 6406/3-3. Separating the Smørbukk South field from the main Smørbukk field is a NNE-SSW trending syncline at the base Cretaceous level (Corfield and Sharp, 2000). The field is an anticlinal structure formed due to movement of the underlying Triassic salt and bounded to the east by a major, complex fault.

The field is buried to the same depth and share the same stratigraphy and lithology as the Smørbukk field. Petroleum accumulations occur mainly in the fan delta or delta front deposits of the Garn Formation and are mainly light oils rather than gas condensate. The Spekk, Melke and Åre Formations have been recognized as the regional source rock in the drainage area of the Smørbukk South structure (Forbes et al., 1991). Because of the maturity gradient in the

reservoir it has been suggested that the petroleum migrated into the field from the west (Angard, 1996).

The term Åsgård refers today to the linked up and developed Smørbukk, Smørbukk South and Midtgard structures.

2.3.6. The well 6407/4-1 discovery

The discovery is located between the Njord field and Tyrihans South (see figure 2.3.). There is little published material on the condensate discovery, but Karlsen et al. (1995) indicated it to be a medium overpressured trap.

3. Analytical methods and the sample set

Analytical methods used in geochemical studies and correlations have over the last 60 years developed tremendously and there has been an increase in both the number and diversity. Correlation techniques based on geochemical properties can be divided into two main groups based on whether they are to describe the whole sample (bulk parameters) or detailed chemical characteristics (specific properties). The bulk parameters describe gross composition properties of the whole oil or total extract using for example percentage amount of aromatic hydrocarbons, polar compounds and saturated hydrocarbons (Iatroscan, TLC-FID). The specific properties describe the sample on molecular level using for example GC-MS or GC-FID to give a chemical characterisation of specific sample fractions.

The following section will describe the analytical methods used in this study and how they are used to calculate different facies and maturity parameters.

- 3.1. TLC-FID Iatroscan
- 3.2. GC-FID
- 3.3. GC-MS
- 3.4. Microscopy
- 3.5. Maturity and facies parameters
- 3.6. The sample set

3.1. TLC-FID Iatroscan

Iatroscan analysis involves thin-layer chromatography and flame ionization detection (TLC-FID analysis) of petroleum fractions. It provides for a rapid and relatively accurate method for the quantification of saturated hydrocarbons, aromatic hydrocarbons and the polar fraction (resins and asphaltenes) in solvent extracts of petroleum source rocks, reservoir rocks and crude oils (Karlsen and Larter, 1989). The varying proportions of saturated and aromatic hydrocarbons and polar compounds can be used to characterise the petroleum populations in the reservoir (Bhullar et al., 2000) and differentiate between migrated hydrocarbons, *in-situ* generated hydrocarbons and also diesel drilling fluids (Karlsen and Larter, 1991). This technique is suitable to screen large sample volumes from petroleum reservoirs to obtain information for selection of samples for high-resolution analysis.

In this study both extracted rock samples and crude oils were analysed (13 samples in addition to the standard oil NSO-1) by a Iatroscan TH-10, MK IV (Iatron inc., Tokyo) instrument equipped with a flame ionization detector (FID) and interfaced with an electric integrator (Perkin-Elmer LCI-100) used for rod scanning and quantification (Karlsen and Larter, 1991 describes the method). The components were separated using silica rods, type Chromarods-S III (pore diameter 60 Å, particle size 5µm).

The rock samples were crushed and the hydrocarbons extracted by adding 5 ml of DCM:MeOH (93:7 VOL%) in glass vials. The samples were placed in the dark for 2 weeks and shaken five times during the period. The crude oil samples was diluted by adding 2 ml of DCM:MeOH(93:7 VOL%) to 2 ml of sample in glass vials.

All of the samples were then systematically applied (3 µl) to a fixed point near the base of the chromarod. 8 out of 10 rods were used for the samples (2 rods pr. sample), as the remaining 2 were used for test runs, one with the NSO-1 and the other blank.

To develop the Chromarods, solvents of different polarity were used to separate saturated hydrocarbons, aromatic hydrocarbons and polar compounds. The rods were placed in normal-hexane (35 min) causing the saturated hydrocarbons to rise to the uppermost part of the rods. After air drying the rods were placed in toluene (12 min) causing the aromatic hydrocarbons to move to the middle of the rods. Then the Chromorods were placed in the Iatroscan instrument, the scanning speed was 30 sec/scan, and pure grade hydrogen (180 ml/min) and air (2.1 l/min) supplied by a pump were used for the detector.

3.2. Gas Chromatography-Flame Ionization Detector (GC-FID) – analysis of oils and extracts

Gas-chromatographic analysis is used for quantification of individual hydrocarbon components and is usually carried out on whole oils, total extracts or saturated and aromatic hydrocarbon fractions of crude oils and bitumens. The GC-FID (figure 3.1.) instrument is used for geochemical screening of samples to obtain information about the n-alkanes and isoprenoid distributions. Information about “steranes” and “terpanes” may also in some cases be obtained.

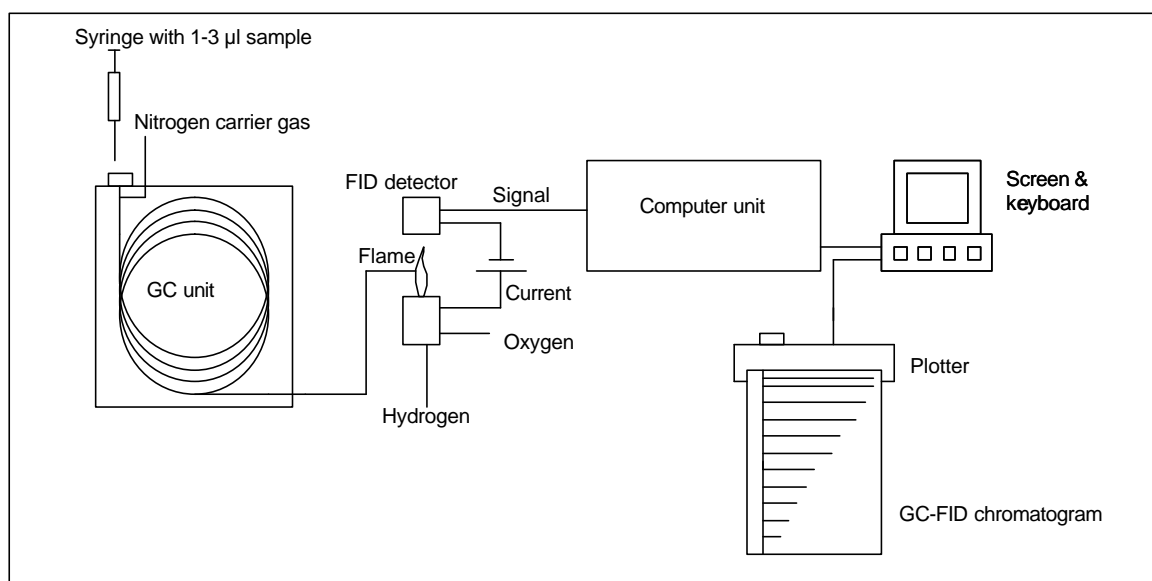


Figure 3.1. The GC-FID instrument (Pedersen, 2002).

Some of the most common parameters in organic petroleum geochemistry studies are based on data collected by the GC-FID. The parameters include:

- ◆ Carbon Preference Index (CPI) or Improved Odd Even Preference (OEP)
- ◆ pristane/n-C₁₇
- ◆ phytane/n-C₁₈
- ◆ pristane/phytane (Pr/Ph)

These parameters are mainly used as maturity and facies indicators, but GC-FID chromatograms may also be applied for general fingerprinting of the samples.

The GC-FID instrument used in this study was a Varian Capillary Gas Chromatograph Model 3500 with a 50 m length HP Ultra-1 column, which had a 0.2 mm internal diameter and 0.33µm film thickness. Temperature programming was 80°C for 1 min, then an increase of 4.5°C/min to a final temperature of 320°C held for 20 min (total time 79.33 min). Pressure

was 45 psi, the split flow through vent was 16 ml/min, the injector had a temperature of 300°C and the detector temperature was 330°C. The analysis was performed with nitrogen carrier gas and split injection.

3.3. Gas Chromatography - Mass Spectrometry (GC-MS)

The GC-MS instrument was used to analyse compounds in oils and the petroleum in fluid inclusions. It was used both to analyse biomarkers in oils and fluid inclusions, and for analysis of the n-alkane distribution, pristane and phytane in the fluid inclusions.

3.3.1. Disintegration and cleaning of sandstones

The sand samples was crushed manually to individual grains which first was treated with chromic acid and washed with water to remove any clay and organic matter from the grains (Karlsen et al., 1993). Second, residuals and non-extractable organic matter was removed from the fissures and cracks with hydrogen peroxide. Finally, the samples were treated with Soxtec to remove any possible bitumen from the grain surface and fissures opened after the first two treatments. Karlsen et al. (in prep) believes the combined acid and H₂O₂ treatment helps to oxidize more effectively organic matter residing in fissures and cracks then can be done by either method alone.

3.3.2. Fluid inclusions

To extract the fluid from the inclusions in the sandstones, the sand was pulverized together with cyclohexane in an agate mortar, transferred together with the pulverised sand to 16 dr. glass vials. It was left to vaporize to 1/6 of the volume and then prepared for analyse on the GC-MS.

When analysing the pristane, phytane and n-alkane distribution the sample was taken when half the fluid was vaporized, but for biomarker detection the sample is treated with molecular sieve like described below. This means that every fluid inclusion sample received two GC-MS runs, one sieved and one not sieved ($m/z = 85$).

3.3.3. Molecular Sieving

For many years organic geochemists have been using 5Å molecular sieves to separate n-alkanes from other saturated hydrocarbon components of petroleum (Eglinton and Murphy, 1969). The main purpose for carrying out this separation is to remove the n-alkanes (straight chained hydrocarbons) and polar compounds. The n-alkanes comprise a major proportion of most petroleum and if present in the sample they will interfere with the signals from the biomarkers. By removing n-alkanes the biomarker signals will be enhanced relative to the interference from n-alkane fragments.

In this study 5Å silicalite UOP MHS2-420LC (a synthetic zeolitic form of silica) was used to remove the n-alkanes and polar compounds from the samples.

3.3.4. Gas Chromatography - Mass Spectrometry (GC-MS)

A GC-MS system forms an instrument capable of separating mixtures into their individual components, identifying and then providing quantitative and qualitative information on the amount and chemical structure of each compound (McMaster and McMaster, 1998). The GC-MS is a combination of a gas chromatograph (GC) for compound separation and mass spectrometer (MS) using ionization and mass analysis for detection and identification of the components (see figure 3.2.). The GC-MS uses the relative GC retention times, elution patterns and the mass spectral fragmentation patterns to detect and provisionally identify compounds.

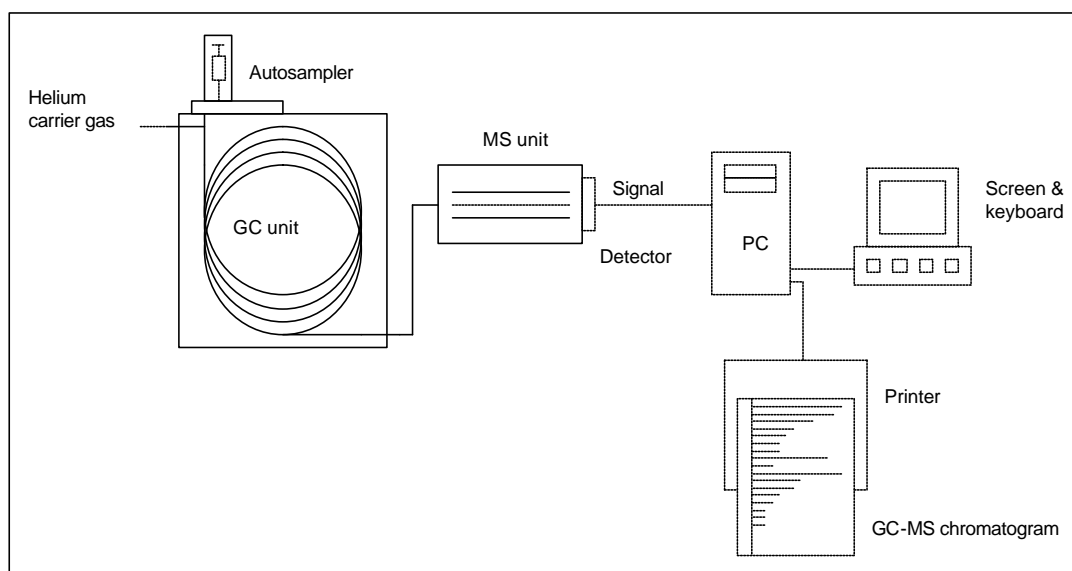


Figure 3.2. The GC-MS instrument (Pedersen, 2002).

The GC-MS instrument used in this study was a Fisons MD800 quadrupole-instrument with a 50 m long Chompack, WCOT, CP-sil 5 CB LOW BLEED/MS column, which had a 0.32 mm internal diameter and 0.40 μm film thickness. The injection was done using a CTC A200S autosampler with a sample volume of 4 μm . The starting temperature was 80°C (1 min), then an increase of 10°C/min to a temperature of 180°C, and then 1.7°C/min to a final temperature of 310°C held for 30 min.

The GC-MS was used in this study to monitor the ions with a mass/charge (m/z) ratio of 85, 178, 191, 192, 198, 217, 218, 231 and 253.

Monitoring of these ions will give information about the n-alkane distribution and the most common biomarkers and related compounds used to establish the maturity, source and facies of the petroleums in this study.

3.4. Microscopy

Fluorescence microscopy is a well established technique for petrographic studies of petroleum fluid inclusions. When exposed to ultraviolet (UV) light, petroleum emits light in the visible range, making it possible to separate them from aqueous fluids which are non-fluorescent (Munz, 2001). The fluorescent colour of petroleum inclusions reflects the composition. The main fluorescing components in petroleum are aromatic hydrocarbons (Hagemann and Hollerbach, 1986; Khorasani, 1987), and NSO compounds. Sellwood et al. (1993) described the general fluorescence response for different gravity oils (see figure 3.3) and made it possible to indicate the oil type visually.

The most common occurrence of petroleum inclusions in clastic reservoirs is in secondary quarts (Munz, 2000). The precipitation of quarts cement in sandstones is controlled by a rise in temperature (Walderhaug, 1994). Hence it is likely to believe that during rapid subsidence most of the inclusions will be formed at great depths. And when subsidence is low inclusions will be formed at several levels during burial. The amount of inclusions is determined by observing the sample through the microscope. The scale used in this study is subjective, 1 indicate a low number of inclusions and 5 a high number.

The microscope used in this study is a Nikon Microphot-SA with an excitation filter (EX) 405/10. All the samples viewed in the microscope were cleaned as described in chapter 3.3.1. to remove any residuals from the surface of the grain.

FLUORESCENCE WAVELENGTH (nm)	A.P.I.	FLUORESCENCE COLOUR	OIL TYPE
560	19	FULL YELLOW YELLOW/RED	LOW MATURITY OILS
548	25	GREEN	_____
528	33	GREEN/BLUE	OILS
494	44	BLUE	_____
450	50+	VIOLET	CONDENSATES

Figure 3.3. General fluorescence response to different gravity oils under ultra violet light (Sellwood et al., 1993).

3.5. Facies and maturity parameters

3.5.1. Iatroscan TLC-FID

Saturated hydrocarbons/aromatic hydrocarbons

The saturated hydrocarbons/aromatic hydrocarbons (SAT/ARO) mainly reflects source rock quality and maturity (Cornford et al., 1983; Clayton and Bostick, 1986). The ratio increase with increasing thermal maturity, but will also increase in the gas-phase of phase-fractionated petroleum during the migration to shallower depths.

3.5.2. GC-FID oils and core extracts

The GC-FID analysis of oils and core extracts have been used to analyse $C_4 - C_{30}$ alkanes with the emphasis placed on the C_{15+} compounds. The n-alkane distribution together with n- C_{17} , n- C_{18} , pristane and phytane (figure 3.4.) can give valuable information about source and depositional facies, maturity and biodegradation.

n-alkane patterns

The n-alkane patterns can be used to classify chromatograms, giving valuable information about the facies and maturity of the samples (Peters and Moldowan, 1993). Four distinct groups are recognized:

- ◆ Normal “North Sea” petroleums and core extracts; a decrease in peak height with increasing carbon number creating a concave curve in the chromatogram.
- ◆ Light end biased extracts; a higher relative concentration of low molecular weight n-alkanes compared to the “normal” pattern in this range.
- ◆ Heavy end biased extracts; concentration of n-alkanes dominate the high carbon number side.
- ◆ Bimodal extracts; the peaks in the chromatogram have to maxima groups with a minimum in between.

Carbon Preference Index (CPI)

CPI was first introduced by Bray and Evans (1961) and can be used to indicate the thermal maturity of an oil or extract. CPI values significantly above or below 1.0 indicate the oil or extract is thermally immature. Values close to 1.0 suggest, but do not prove an oil or extract to be thermally mature (Peters and Moldowan, 1993). A limitation of CPI is the influence of the type of kerogen the hydrocarbons are derived from. Values below 1.0 indicate carbonate facies, while values higher than 1.0 indicate lacustrine environment or siliclastic source rocks. But despite its limitations, used together with another independent index, it is a valuable qualitative indicator of the maturation of source rocks.

In this study two CPI values were used to evaluate if the oils and extracts had the same odd/even distribution for both short- and longer-chained n-alkanes:

$$\text{CPI 1} = \frac{C_{21} + C_{23} + C_{25}}{C_{22} + C_{24} + C_{26}}$$

$$\text{CPI 2} = \frac{2 \times C_{31}}{C_{30} + C_{32}}$$

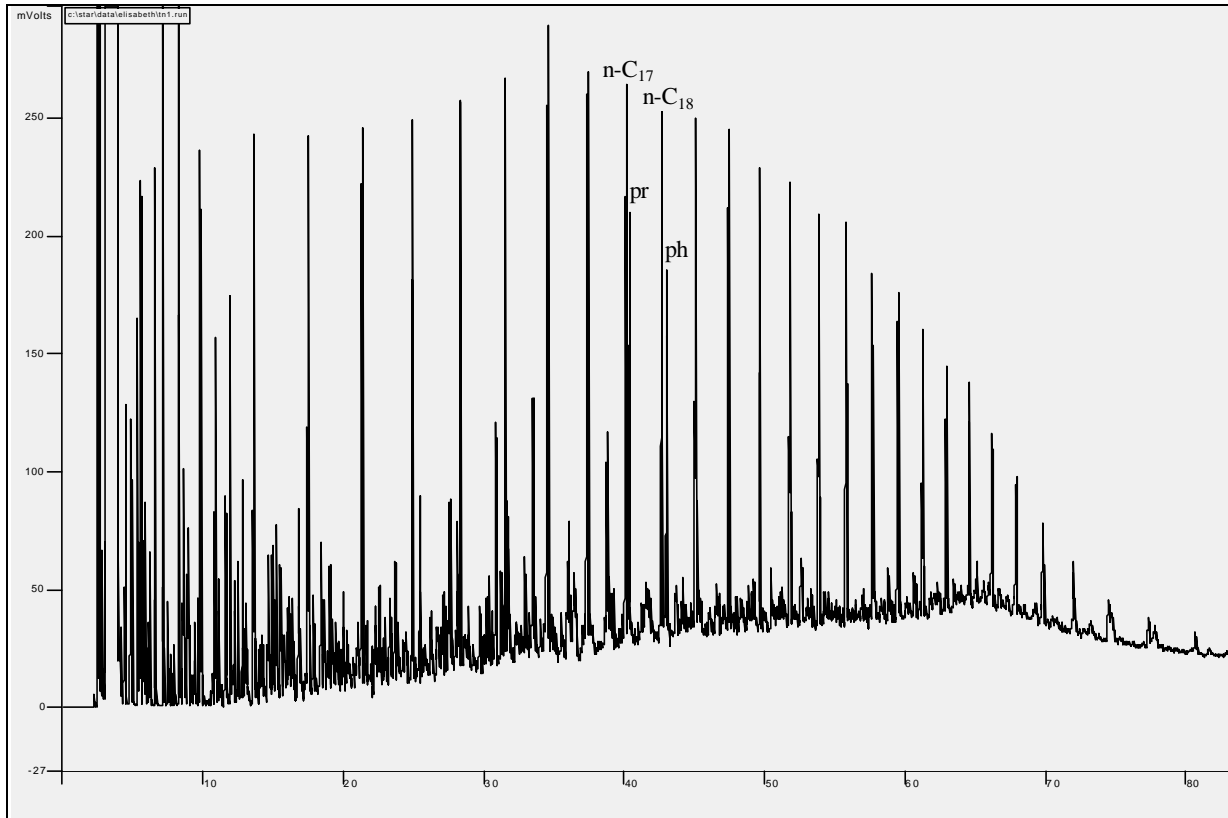


Figure 3.4. The GC-FID trace for TN1 (see table 3.1. for identification) with the n-C₁₇, n-C₁₈, pristane and phytane peaks identified. The shortening of the peaks in the left side of the chromatogram (C₈ – C₁₄) can be caused either by biodegradation, water washing or phase fractionation.

Pristane/Phytane

Pristane and phytane are isoprenoid isoalkanes derived from the phytol side-chains in chlorophyll (Tissot and Welte, 1978). Whether the phytol transforms into pristane or phytane is determined by the environment of deposition. Therefore the parameter is used to indicate what type of organic facies (kerogen) the sediments contain. Pr/Ph < 3 indicates type I/II kerogen, deposition of marine algae in anoxic environment. Pr/Ph > 3 indicates type III kerogen or coal, deposition of terrestrial material in an oxidising environment. The numbers must be supported by other data to be conclusive. However, substantial amounts of phytane is also derived from bacteria (Peters and Moldowan, 1993)

The ratio can also be used as a maturity indicator because it typically increase with increasing maturity (Alexander et al., 1981), but because pristane and phytane during diagenesis can be derived from sources other than phytol e.g. bacterial membranes (ten Haven et al., 1987) the ratio should be used together with other parameters.

Pr/n-C₁₇ and Ph/n-C₁₈

These two parameters are used as an addition to other parameters to determine source rock facies, maturity and the level of biodegradation of hydrocarbons. Low ratios indicate a more mature sample, because the isoprenoids will break down earlier than n-alkanes during maturation this is because tertiary carbon-carbon bonds have lower stability than primary and secondary carbon bonds. The ratios can be used together with other parameters to rank related, nonbiodegraded oils and bitumens based on thermal maturity. But care should be taken because organic input and biodegradation may affect the ratio (Peters and Moldowan, 1993).

Peak name	Identity
n-C ₁₇	C ₂₀ triaromatic steroid (TA)
n-C ₁₈	C ₂₈ triaromatic steroid (TA)
pr	Pristane
ph	Phytane

Table 3.1. Identified peaks from the GC-FID and GC-MS m/z=85 chromatogram describing the n-alkane distribution.

3.5.3. GC-MS

The GC-MS was used in this study to monitor the ions with a mass/charge (m/z) ratio of 85, 178, 191, 192, 217, 218, 231 and 253. Peaks are identified from the chromatograms (see table 3.1.-3-4. and figure 3.5.-3.11.) and used to calculate the parameters below:

- 1) $18a(H)\text{-trisorneohopane} / (18a(H)\text{-trisorneohopane} + 17a(H)\text{-trisorhopane}) = Ts/Ts + Tm$ (Seifert and Moldowan, 1978; MacKenzie, 1984)
- 2) $\text{diahopane} / (\text{diahopane} + \text{normoretane})$ (Cornford et al., 1986). Diahopane = hopane x (Moldowan et al., 1991)
- 3) $22S / (22S + 22R)$ of C₃₁ 17a(H), 21β(H)-hopanes
- 4) $C_{30}\text{-hopane} / (C_{30}\text{-hopane} + C_{30}\text{-moretane})$ (Mackenzie et al., 1985)
- 5) $29Ts / (29Ts + \text{norhopane})$ (Moldowan et al., 1991)
- 6) $\text{bisnorhopane} / (\text{bisnorhopane} + \text{norhopane})$ (Wilhelms and Larter, 1994)
- 7) $C_{23}\text{-}C_{29}$ tricyclic terpanes/ C_{30} αβ-hopane (modified from Mello et al., 1988)
- 8) C_{24} tetra cyclic terpanes/ C_{30} αβ-hopane (Mello et al., 1988)
- 9) hopane/sterane from the C_{30} αβ-hopane and regular C_{29} sterane (MacKenzie et al., 1984)

- 10) $\beta\beta/(\beta\beta + \alpha\alpha)$ of C_{29} (20R + 20S) sterane isomer (Mackenzie et al., 1980)
- 11) $20S/(20S + 20R)$ of C_{29} 5 α (H), 14 α (H), 17 α (H) steranes (Mackenzie et al., 1980)
- 12) Diasterane/(diasterane + regular sterane) (Mackenzie et al., 1985)
- 13) % C_{27} of $C_{27} + C_{28} + C_{29}$ $\beta\beta$ -steranes (Mackenzie et al., 1985)
- 14) % C_{28} of $C_{27} + C_{28} + C_{29}$ $\beta\beta$ -steranes (Mackenzie et al., 1985)
- 15) % C_{29} of $C_{27} + C_{28} + C_{29}$ $\beta\beta$ -steranes (Mackenzie et al., 1985)
- 16) $C_{20}/(C_{20}+C_{28})$ triaromatic steroids (TA) (Mackenzie et al., 1985)
- 17) C_{28} TA/(C_{28} TA + C_{29} MA) (Peters and Moldowan, 1993)
- 18) Methylphenantrene ratio, MPR (Radke et al., 1982b)
- 19) Methylphenantrene index 1, MPI 1 (Radke et al., 1982a)
- 20) Methylphenantrene distribution factor (F1 or MPDF) (Kvalheim et al., 1987)
- 21) Methylthiophene ratio (MDR) (Radke, 1988)
- 22) Calculated vitrinite reflectivity, $R_{m(1)}=1.1*\log_{10} MPR + 0.95$ (Radke, 1988)
- 23) Calculated vitrinite reflectivity, % $R_o=0.6*MPI\ 1 + 0.4$ (Radke and Welte, 1983)
- 24) Calculated vitrinite reflectivity, % $R_o=2.242*MPDF - 0.166$ (Kvalheim et al., 1987)
- 25) Calculated vitrinite reflectivity, $R_{m(2)}=0.073*MDR + 0.51$ (Radke, 1988)
- 26) 3-methylphenantrene/4-methylthiophene (Radke et al., 2001)
- 27) MDBTs/MPs (Radke et al., 2001)

From chromatogram $m/z = 191$ it is possible to calculate the following parameters from identification of terpanes and triterpanes:

1: $T_s/(T_s + T_m)$, maturity parameter with maximum value 1 (peak A and B). With increasing maturity the 17 α (H)-trisnorhopane (T_m) decrease compared to 18 α (H)-trisnorhopane (T_s). T_m is believed to represent the biologically produced structure. The T_m/T_s ratio begins to decrease quite late during maturation ($>0.9\%R_o$) (Waples and Machihara, 1991), but may be used through the entire oil window. The ratio is greatly affected by facies, but is a useful non-quantitative indicator of relative maturity when used on oils of uniform or common organic facies.

2: diahopane/(diahopane + normoretane), maturity parameter (peak X and D respectively). Peters and Moldowan (1993) assume there is a relationship between maturity and this ratio, high ratios indicate high maturities. In addition the peak X indicates terrestrial input.

3: $22S/(22S + 22R)$ of C_{31} 17 α (H), 21 β (H)-hopanes, maturity parameter with equilibrium reached at 0.6 (peak G and H).

The 17 α (H)-extended hopane has two isomers, S and R which behave differently during maturation. 22S is the most stable and will increase when the source rock gets more mature causing an increase in the ratio. The equilibrium is reached fast, thus the range of the ratio is limited to immature samples at the start of oil genesis.

4: C_{30} -hopane/(C_{30} -hopane + C_{30} -moretane), maturity parameter (peak E and F). C_{30} -moretane is thermally less stable than C_{30} -hopane and the ratio will increase during maturation. The loss of C_{30} -moretane occurs at relatively low maturity, thus the range of the ratio is limited to immature samples and extracts.

5: 29Ts/(29Ts + norhopane), maturity parameter (peak 29Ts and C).

The abundance of 29Ts relative to norhopane is related to thermal maturity, thus the ratio will increase with an elevation of the temperature.

6: bisnorhopane/(bisnorhopane + norhopane), facies parameter (peak Z and C).

Bisnorhopane is believed to indicate anoxic conditions (Peters and Moldowan, 1993), but is also affected by maturity. With increasing maturity the norhopane peak rises relative to bisnorhopane due to reduction in the amount of bisnorhopane. When comparing two samples an immature sample may give a more anoxic impression than a more mature sample.

7: C_{23} - C_{29} tricyclic terpanes/ C_{30} $\alpha\beta$ -hopane, maturity parameter (peak P, Q, R, T, U, V and E).

With increasing maturity the amount of C_{23} - C_{29} tricyclic terpanes will increase relative to the C_{30} $\alpha\beta$ -hopane. The parameter is strongly influenced by evaporative fractionation and phase fractionation (Karlsen et al., 1995), but is valid through the whole oil window.

8: C_{24} tetracyclic terpanes/ C_{30} $\alpha\beta$ -hopane, maturity parameter (peak S and E).

The C_{24} tetracyclic terpanes can be compared to C_{30} $\alpha\beta$ -hopane for estimating maturity, as the amount of C_{24} will increase relative to C_{30} with thermal maturity (Peters and Moldowan, 1993).

Parameter 9 is calculated from both chromatograms $m/z = 191$ and $m/z = 217$.

9: hopane/sterane ratio from the C_{30} $\alpha\beta$ -hopane, facies parameter (peak E from chromatogram $m/z = 191$ and q, r, s and t from chromatogram $m/z = 217$)

The parameter is based on the knowledge that hopanes are derived from bacteria and steranes from algae and plants. A low hopane/sterane ratio indicate marine, algae dominated organic matter, while a high ratio may point to bacteria rich facies, bacterially reworked organic matter or a special terrestrial input (Peters and Moldowan, 1993). In a sample set with more or less uniform organic facies, the hopane/sterane parameter will be more influenced by maturity than by facies, hopanes being more thermally stable than steranes.

Six isomers of diacholestanes and ethyl-cholestanes are identified from the $m/z = 217$ ion chromatogram and are used to calculate the following parameters:

10: $\beta\beta$ /($\beta\beta$ + $\alpha\alpha$) of C_{29} (20R + 20S) sterane isomer, maturity parameter with maximum equilibrium ratio of 0.7(peak q, r, s and t).

During maturation the $\beta\beta$ -isomer increases compared to the $\alpha\alpha$ -isomer. The parameter is valid to peak oil generation, but it may be affected by the mineralogy in the rock.

11: $20S/(20S + 20R)$ of C_{29} 5a(H), 14a(H), 17a(H), maturity parameter with maximum equilibrium ratio at 0,5 (peak q, r, s and t).

20R converts to 20S during maturation and reaches equilibrium in the middle of the oil window. The parameter is not only affected by maturity, but also facies, biodegradation and weathering.

12: Diasterane/(diasterane + regular sterane) is a facies and maturity parameter with maximum ratio at 1.0 (peak a, b, q, r, s and t).

Thermal cracking during maturation causes the amount of diasteranes to increase relative to the regular steranes. The parameter is valid through the whole oil window. Oils from carbonate source rocks may have lower ratios than oils from clastic source rocks (Peters and Moldowan, 1993). Presence of diasteranes is indicative of a siliclastic source rock.

Parameters **13** (peak i), **14** (peak o) and **15** (peak s') are relative percentages of the C_{28} , C_{29} , and C_{30} $\beta\beta$ -steranes calculated from the $m/z = 218$ ion chromatogram. Plotted in a ternary diagram they can indicate organic facies.

Scanning of the ions $m/z = 231$ and $m/z = 253$ gives data to allow calculation of:

16: $C_{20}/(C_{20}+C_{28})$ triaromatic steroids (TA), maturity parameter (peaks a1 and g1).

With increasing maturation the amount of C_{20} increases relative to C_{28} . The parameter is valid through the whole oil window, but is sensitive to phase fractionation (Karlsen et al., 1995).

17: $C_{28} TA/(C_{28}TA + C_{29} MA)$, maturity parameter with maximum ratio of 1.0 (peak g1 and H1).

Monoaromatics (MA) are during thermal maturation rearranged to triaromatics (TA), and the ratio between the two molecules is used to estimate maturity and possibly phase fractionation. The parameter is valid to peak oil generation.

Identification of tricyclic aromatic hydrocarbons from the $m/z = 178$, 192 and $m/z = 198$ & 192 is applied in the following parameters.

The three following parameters are calculated from the amount of phenanthrene and the four isomers of methylphenanthrene (1, 2, 3 and 9). The number assigns the location of the methyl group ($-CH_3$). During maturation the thermally more stable 3-MP and 2-MP will survive to a larger extent than 9-MP and 1-MP, which will deplete more rapidly. Comparison between these parameters and parameters derived from steranes and hopanes may give valuable information.

18: Methylphenanthrene ratio (MPR), maturity parameter (peak 1 and 2)

$$\text{MPR} = \frac{[2 - \text{MP}]}{[1 - \text{MP}]}$$

19: Methylpenantrene index 1 (MPI 1), maturity parameter (peak P, 1, 2, 3 and 9)

$$\text{MPI 1} = 1,5 * \left(\frac{[2 - \text{MP}] + [3 - \text{MP}]}{[\text{P}] + [1 - \text{MP}] + [9 - \text{MP}]} \right)$$

20: Methylphenantrene distribution factor (F1 or MPDF), maturity parameter (peak 1, 2, 3 and 9)

$$\text{MPDF} = \frac{[2 - \text{MP}] + [3 - \text{MP}]}{[2 - \text{MP}] + [3 - \text{MP}] + [1 - \text{MP}] + [9 - \text{MP}]}$$

21: Methyl dibenzothiophene ratio (MDR), facies and maturity parameter (peak 4 and 1)

$$\text{MDR} = \frac{[4 - \text{MDBT}]}{[1 - \text{MDBT}]}$$

The relationship between the two isomers of methyl dibenzothiophene is controlled by maturity. The principle is the same as for methylphenantrene, where 4-MDBT is the most thermally stable of the two isomers. The amount of MDBT in oils may also indicate the sulphur contents in the oil/source rock, because the thiophene structure contains a sulphur atom.

Vitrinite reflectance has been calculated based on measurements of phenanthrene, methylphenanthenes and methyl dibenzothiophene using the formulas:

22: Calculated vitrinite reflectivity, maturity parameter (using parameter 18)

$$R_{m(1)} = 1.1 * \log_{10} \text{MPR} + 0.95$$

23: Calculated vitrinite reflectivity, maturity parameter (using parameter 19)

$$\%R_c = 0.6 * \text{MPI 1} + 0.4$$

24: Calculated vitrinite reflectivity, maturity parameter (using parameter 20)

$$\%R_o = 2.242 * \text{MPDF} - 0.166$$

25: Calculated vitrinite reflectivity, maturity parameter (using parameter 21)

$$R_{m(2)} = 0.073 * MDR + 0.51$$

26: 3-methylphenantrene/4-methyldibenzothiophene, facies parameter (peaks 3 and 4)

Used together with other parameters like Pr/Ph this parameter can indicate different organic facies, e.g. shale or carbonate facies and the relative amount of sulphur in the source rock.

27: MDBTs/MPs, facies parameter (peaks 1, 2, 3, 4 and 9 from chromatogram m/z = 178 + 192 and peaks 1, 2+3 and 4 from chromatogram m/z = 192)

Values above 1 indicating carbonate facies and values below 1 being shale facies. Used together with the pristane/phytane ratio it can also give information about the Eh/pH conditions in the depositional system.

The parameters described above are derived from different peaks and chromatograms. The following figures show the different peaks used and the tables give a short description of each peak.

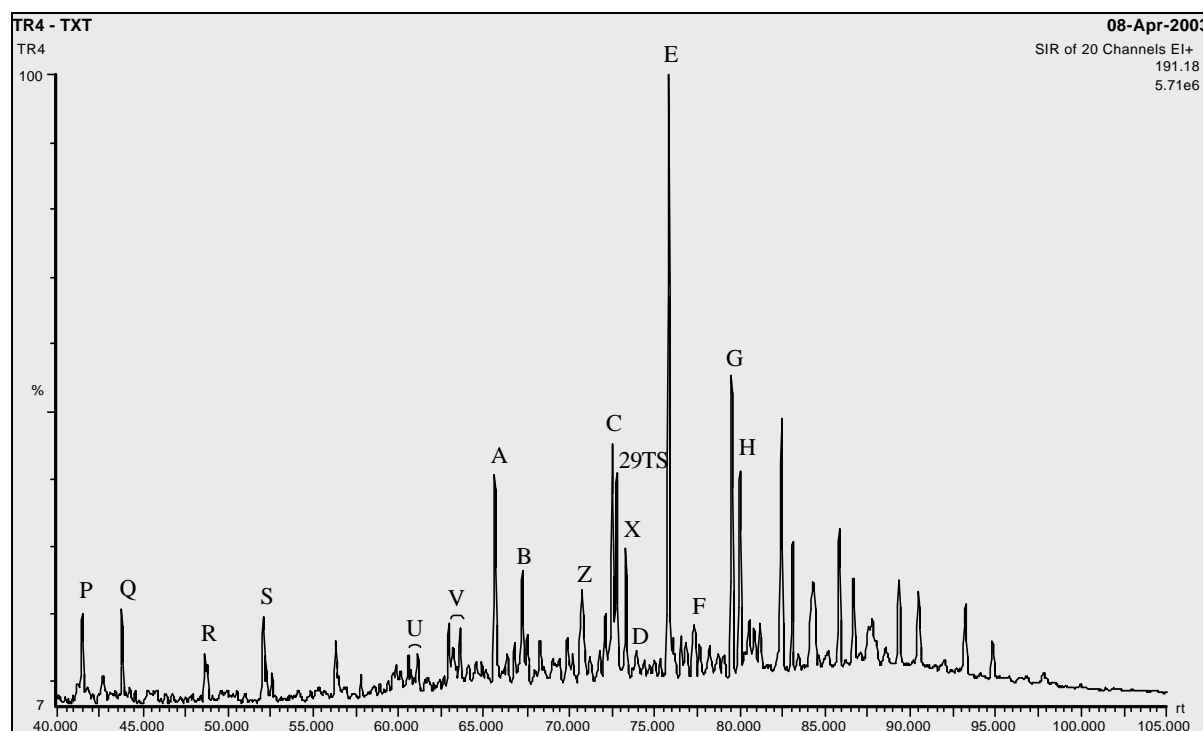


Figure 3.5. The m/z 191 chromatogram from the Trestakk sample TR4 showing the identified peaks of terpanes and triterpanes (see table 3.2. below for a detailed description).

Peak name	Stereochemistry	Identity	Composition
29TS		18a(H)-30-norneohopane	C ₂₉
A		18a(H)-trisnorehopane	C ₂₄ H ₄₄
B		17a(H)-trisnorehopane	C ₂₅ H ₄₆
C		17a(H), 21β(H)-norhopane	C ₂₉ H ₅₀
D		17a(H), 21β(H)-normoretane	C ₂₉ H ₅₀
E		17a(H), 21β(H)-hopane	C ₃₀ H ₅₂
F		17a(H), 21β(H)-moretane	C ₃₀ H ₅₂
G	22S	17a(H), 21β(H)-homohopane	C ₃₁ H ₅₄
H	22R	17a(H), 21β(H)-homohopane	C ₃₁ H ₅₄
P		Tricyclic terpane	C ₂₃ H ₄₂
Q		Tricyclic terpane	C ₂₄ H ₄₄
R	(17R+17S)	Tricyclic terpane	C ₂₅ H ₄₆
S		Tetracyclic terpane	C ₂₄ H ₄₂
U		Tricyclic terpane	C ₂₈ H ₄₈
V		Tricyclic terpane	C ₂₉ H ₅₀
X		17a(H)-diahopane	C ₃₀ H ₅₂
Z		28, 30-bisnorhopane	C ₂₈ H ₄₈

Table 3.2. Triterpanes identified from the m/z = 191 chromatogram (figure 3.5.).

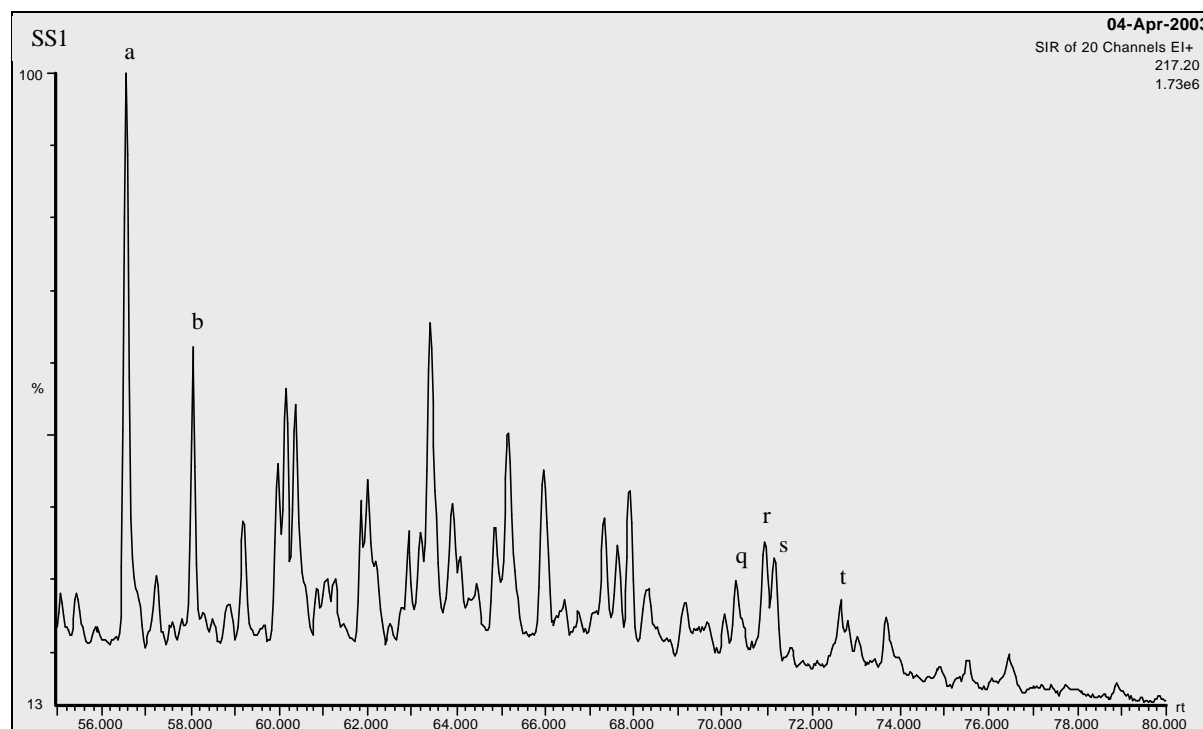


Figure 3.6. Sterane identification from the m/z=217 chromatogram from sample SS1 from Smørbukk South (see table 3.3. for more details). Note the higher relative amount of a and b compared to q, r, s and t indicating a mature oil.

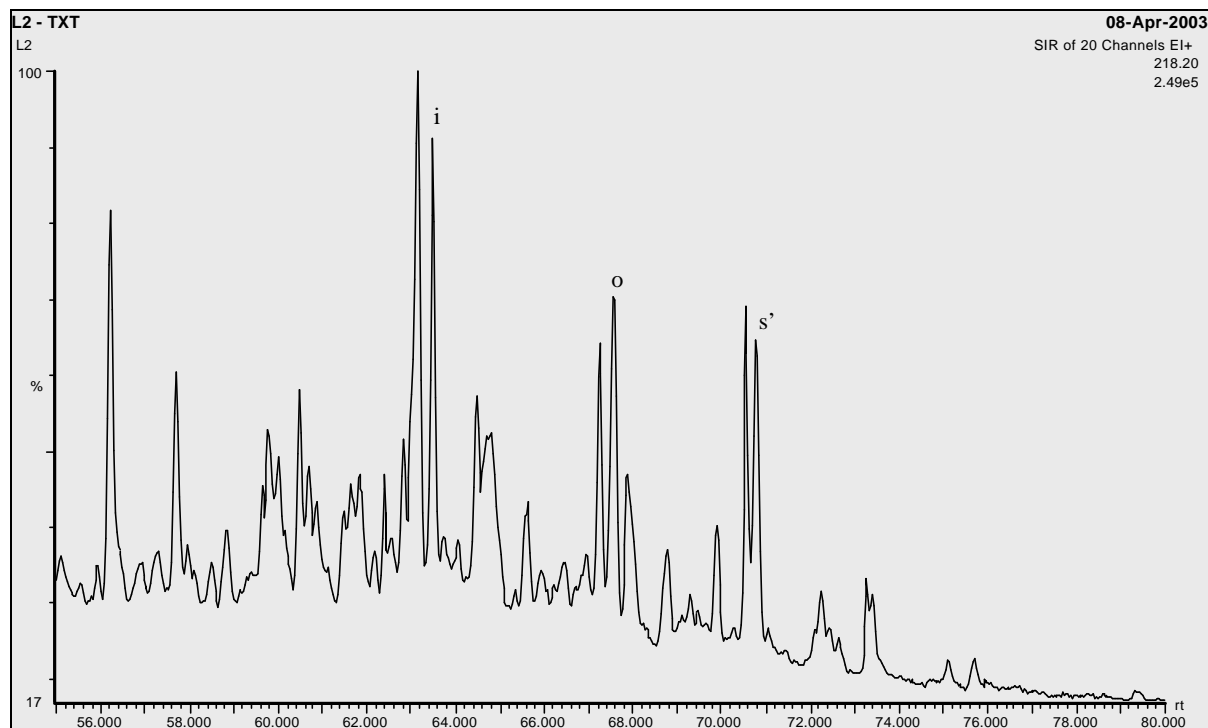


Figure 3.7. The $m/z=218$ chromatogram from inclusions in the Lavrans Field, (sample L2) showing the identified peaks (see table 3.3. for more detailed information).

Peak name	Stereochemistry	Identity	Composition
a	20S	13 β (H),17a(H)-dikolestane	$C_{27}H_{48}$
b	20R	13 β (H),17a(H)-dikolestane	$C_{27}H_{48}$
q	20S	14a(H),17a(H)-24-ethyl-kolestane	$C_{29}H_{52}$
r	20R	14 β (H),17 β (H)-24-ethyl-kolestane	$C_{29}H_{52}$
s	20S	14 β (H),17 β (H)-24-ethyl-kolestane	$C_{29}H_{52}$
t	20R	14a(H), 17a(H)-24-ethyl-kolestane	$C_{29}H_{52}$
i		C_{27} regular sterane	
o		C_{28} regular sterane	
s'		C_{29} regular sterane	

Table 3.3. Steranes identified from the $m/z = 217$ and $m/z = 218$ chromatograms (figure 3.6. and 3.7.).

3. Analytical methods and the sample set

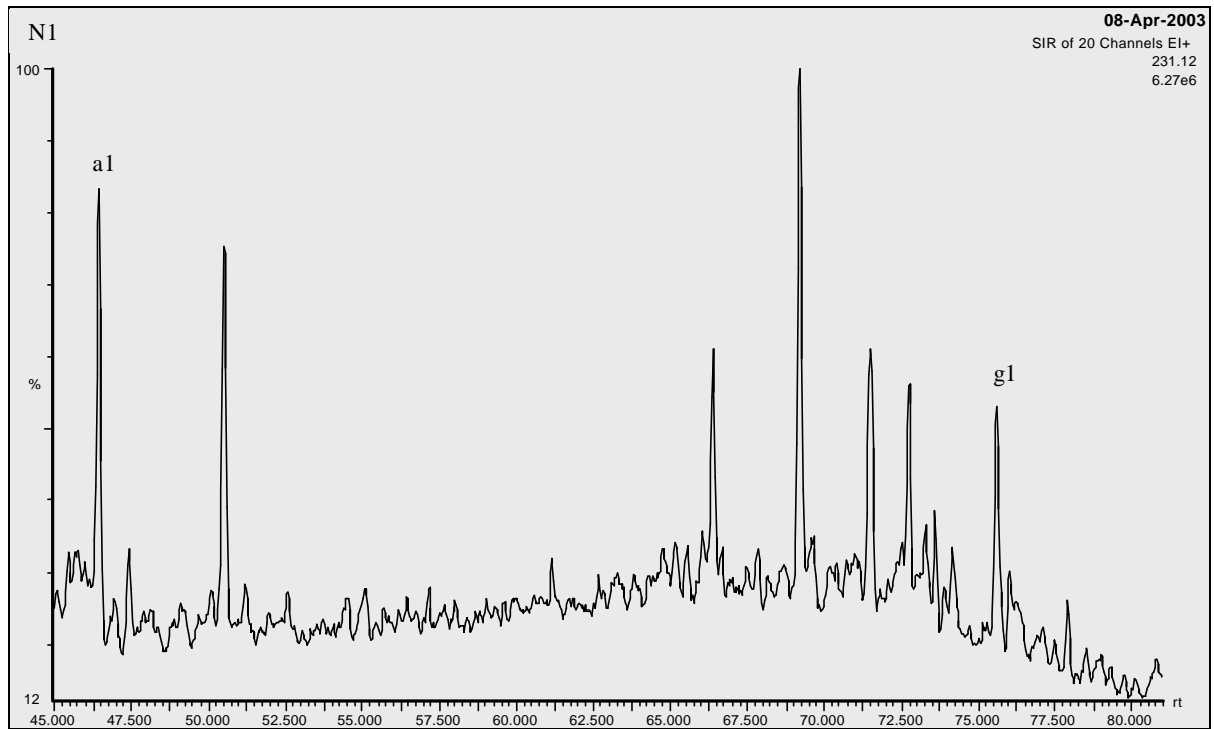


Figure 3.8. Oil sample N1 from the Njord Field showing the $m/z=231$ chromatogram and the identified peaks (see table 3.4. for more detailed information).

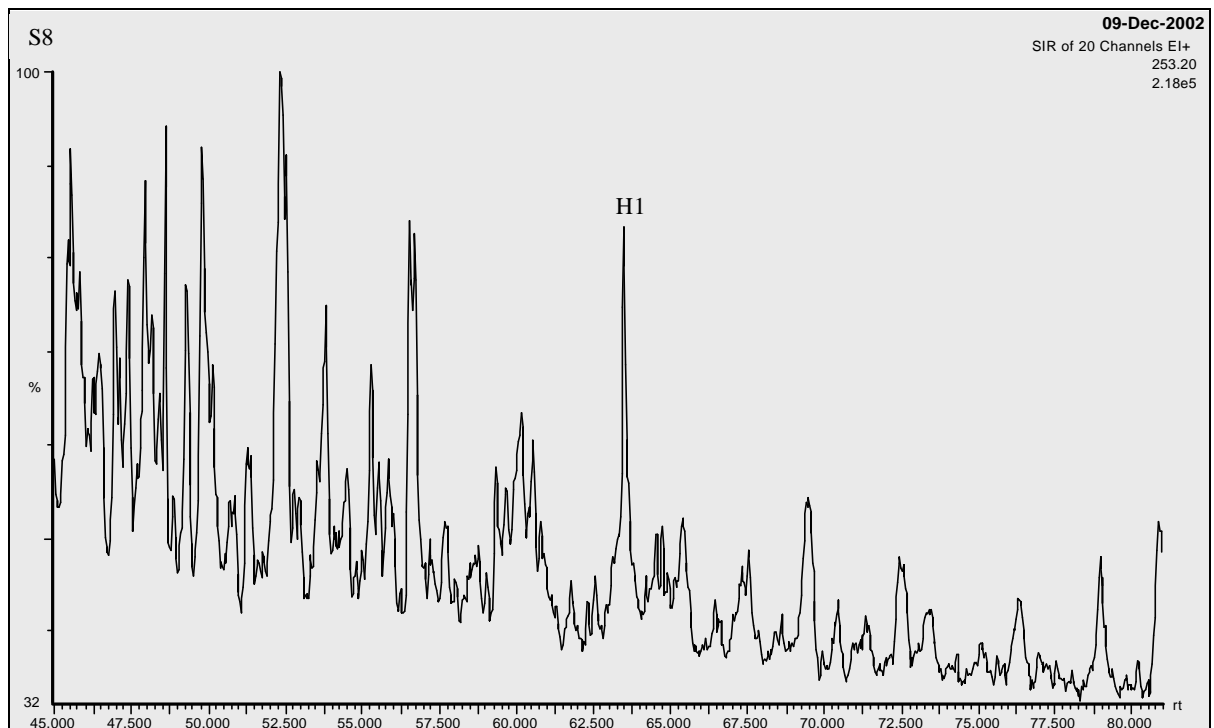


Figure 3.9. $M/z=253$ chromatogram from the Smørbukk Field (sample S8) showing the identified peaks (see table 3.4. for more details).

3. Analytical methods and the sample set

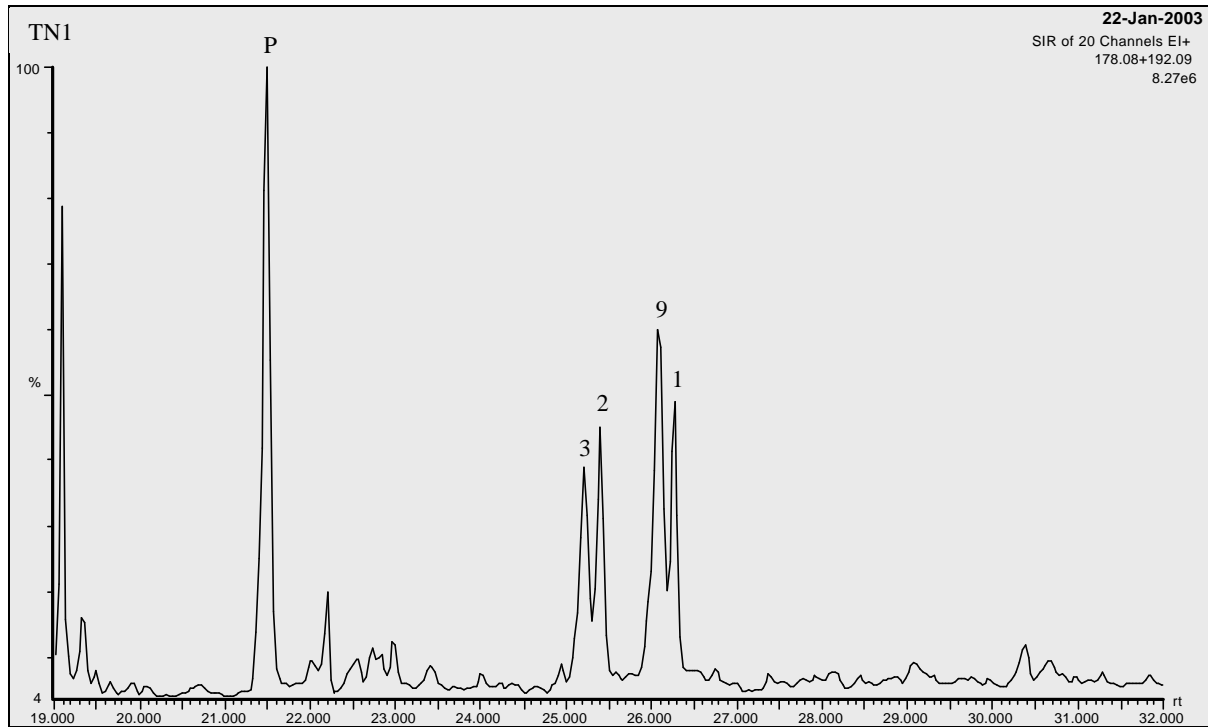


Figure 3.10. The $m/z=178+192$ combined chromatograms for the Tyrihans North oil sample TN1, showing the identified peaks (see table 3.5. for more details).

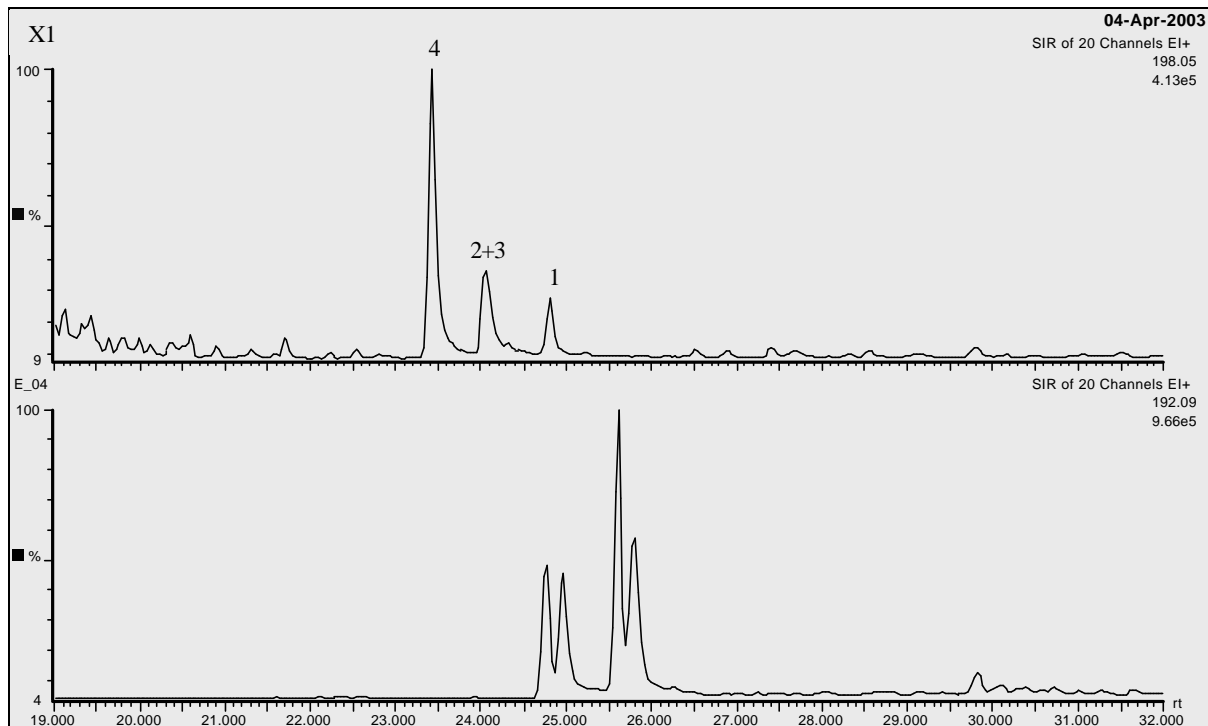


Figure 3.11. The chromatograms for $m/z=198$ and $m/z=192$ from the X1 oil sample showing the identified peaks (see table 3.5. for more details).

Peak name	Identity
a1	C ₂₀ triaromatic steroid (TA)
g1	C ₂₈ triaromatic steroid (TA)
H1	C ₂₉ monoaromatic steroid (MA)

Table 3.4. Triaromatic and monoaromatic steroids identified from m/z = 231 and m/z = 253 chromatograms (figure 3.8. and 3.9.).

Peak name	Identity
P	Phenantrene
1	1-methylphenantrene
2	2-methylphenantrene
3	3-methylphenantrene
4	4-methylphenantrene
9	9-methylphenantrene
1	1-methyldibenzothiophene
4	4-methyldibenzothiophene

Table 3.5. Phenantrene, methylphenantrene and dibenzothiophene identified from m/z = 178, m/z = 192 and m/z = 198 chromatograms (figure 3.10. and 3.11.).

3.6. The sample set

The sample set consists of 6 oil samples and 20 core samples from different wells in the Haltenbanken Area. All the samples are shown in tables 3.5., where i.e. the depths and formation to which the samples belong is listed.

Core samples are collected from sandstone units within the wells. Two core samples from the Garn Formation in Lavrans come from the 6406/2-2 well. In Trestakk the three core samples are from the Garn Formation in well 6406/3-2. From the Tyrihans trap the Garn Formation is sampled in both the North and the South structure, a total of 3 samples. From well 6407/4-1 (south of Tyrihans) there are three core samples from Garn. There is one sample from Njord (6407/7-4) and from the dry well 6407/10-1. From the Smørbukk Field there are a total of five core samples from the four different reservoir units (Garn, Not, Tofte and Tilje Formation). And from Smørbukk South there are two core samples from the Garn Formation.

The 6 oil samples are taken from 5 different fields: the Trestakk, Tyrihans North, 6407/4-1, Njord and Smørbukk South.

3. Analytical methods and the sample set

Sample code	Well/origin	Test	Depth (m)	Grain size	Formation	Field/discovery	Comment
L1	6406/2-2		4487		Garn	Lavrans B	sand
L2	6406/2-2		4492		Garn	Lavrans B	sand
N1	6407/7-4	DST 2A	2990-3008		Tilje	Njord	oil
N2	6407/7-4		3043+3038		Tilje	Njord	sand
S1	6506/12-9S		4416		Garn	Smørbukk	extract
S2	6506/12-9S		4416		Garn	Smørbukk	sand
S3	6506/12-9S		4472		Not	Smørbukk	extract
S4	6506/12-9S		4472		Not	Smørbukk	sand
S5	6506/12-9S		4634,8		Tofte	Smørbukk	extract
S6	6506/12-9S		4634,8		Tofte	Smørbukk	sand
S7	6506/12-9S		4672		Tilje	Smørbukk	sand
S8	6506/12-9S		4751,3		Tilje	Smørbukk	extract
S9	6506/12-9S		4751,3		Tilje	Smørbukk	sand
SS1	6506/12-3	DST 1	4222-4241		Tilje	Smørbukk South	oil
SS2	6506/12-3	DST 6	3162-3173		Lysing	Smørbukk South	oil
SS3	6506/12-3		3872	coarse	Garn	Smørbukk South	sand
SS4	6506/12-3		3872	fine	Garn	Smørbukk South	sand
TN1	6407/1-3	DST 1	3698-3703		Garn	Tyrihans North	oil
TN2	6407/1-3		3648	coarse	Garn	Tyrihans North	sand
TN3	6407/1-3		3648	fine	Garn	Tyrihans North	sand
TR1	6406/3-2	DST 2	3937-3995		Garn	Trestakk	oil
TR2	6406/3-2		3932	coarse	Garn	Trestakk	sand
TR3	6406/3-2		3932	fine	Garn	Trestakk	sand
TR4	6406/3-2		3954,5		Garn	Trestakk	sand
TS1	6407/1-2		3666,5		Garn	Tyrihans South	sand
X1	6407/4-1	DST 2			Garn		oil
X2	6407/4-1		3893	coarse	Garn		sand
X3	6407/4-1		3893	fine	Garn		sand
X4	6407/4-1		3893	ex coarse	Garn		sand
Y1	6407/10-1		2359,7				sand

Table 3.5. A list describing the sample data.

4. Results

Result accomplished during this study using different analytical methods will be presented in the following section. For a more detailed description of the methods used, see chapter 3. The interpretations and discussions of the results follow in chapter 5.

This chapter is constructed with a short description of the parameters for each field, followed by a presentation of the results in form of figures and tables.

- 4.1. Iatroscan TLC-FID oils and extracts
- 4.2. GC-FID oils and extracts
- 4.3. GC-MS oils, extracts and inclusions
- 4.4. Microscopy

4.1. Iatroscan TLC-FID oils and extracts

The data obtained from Iatroscan analysis of oils and core extracts are presented in this section. Table 4.1 gives the gross composition in terms of absolute yield and relative percentages of saturated hydrocarbons, aromatic hydrocarbons and polar compounds, the numbers given in the text are the average of two TLC-FID runs. Figure 4.1. illustrates the composition for all the samples.

Sample	Sample type	Rod	SAT ARO POL			Sample wt (g)	SAT ARO POL Tot ext				SAT%	ARO%	POL%	SAT%/ARO%	ARO%/POL%
			(mg/ml DCM)				(mg/g rock)								
N1	oil	1	3,953	0,929	0,458						74,0	17,4	8,6	4,3	2,0
		2	3,906	0,576	0,373						80,5	11,9	7,7	6,8	1,5
S1	core extr	1	0,227	0,072	0,199	2,5	0,909	0,286	0,795	1,991	45,7	14,4	39,9	3,2	0,4
		2	0,293	0,000	0,237	2,5	1,172	0,000	0,948	2,119	55,3	0,0	44,7	-	0,0
S3	core extr	1	0,326	0,098	0,150	2,5	1,305	0,391	0,599	2,295	56,8	17,0	26,1	3,3	0,7
		2	0,298	0,087	0,067	2,5	1,192	0,347	0,267	1,805	66,0	19,2	14,8	3,4	1,3
S5	core extr	1	0,190	0,105	0,211	2,5	0,760	0,418	0,842	2,020	37,6	20,7	41,7	1,8	0,5
		2	0,266	0,000	0,103	2,5	1,064	0,000	0,410	1,474	72,2	0,0	27,8	-	-
S8	core extr	1	2,675	0,363	0,658	2,5	10,700	1,452	2,633	14,784	72,4	9,8	17,8	7,4	0,6
		2	2,494	0,166	0,915	2,5	9,977	0,664	3,661	14,302	69,8	4,6	25,6	15,0	0,2
SS1	oil	1	2,969	0,840	0,680						66,1	18,7	15,1	3,5	1,2
		2	2,569	0,706	1,095						58,8	16,2	25,1	3,6	0,6
SS2	oil	1	4,331	0,610	0,304						82,6	11,6	5,8	7,1	2,0
		2	3,945	0,628	0,266						81,5	13,0	5,5	6,3	2,4
TN1	oil	1	2,523	1,221	2,337						41,5	20,1	38,4	2,1	0,5
		2	3,148	1,599	0,783						56,9	28,9	14,2	2,0	2,0
TR1	oil	1	2,894	1,037	0,867						60,3	21,6	18,1	2,8	1,2
		2	3,521	1,304	0,936						61,1	22,6	16,3	2,7	1,4
X1	oil	1	2,426	0,501	0,106						80,0	16,5	3,5	4,8	4,7
		2	2,509	0,645	0,659						65,8	16,9	17,3	3,9	1,0

Table 4.1. Gross composition in terms of absolute yield and relative percentages of the oils and core extracts from the Haltenbanken Area.

SAT = saturated hydrocarbons, ARO = aromatic hydrocarbons, POL = polar compounds (resins and asphaltenes). The units are given in mg extract/ml DCM and mg extract/g rock, - = not calculated because the %ARO or %POL = 0.

Njord Field (sample N1: oil)

The single sample from well 6407/7-4 has a high relative content of saturated hydrocarbons (77.1%), and only smaller amounts of aromatic hydrocarbons (14.8%) and polar compounds (8.2%), figure 4.1. The SAT/ARO ratio describing thermal maturity (see chapter 3.5.1. for further details) is relatively high in the Njord oil sample compared to the rest of the data set.

Smørbukk Field (samples S1, S3, S5, S8: core extract)

The extract samples in this well show a total yield, ranging from 1.747 to 14.543 mg/g rock with an average of 6.622 mg/g rock (see figure 4.2.). The sample S8 from the reservoir units in the Tilje Formation contains a higher amount of total extract (respectively 14, 543 mg/g rock) than the other three samples (see table 4.1). It also has a higher relative amount of saturated hydrocarbons with 71.1%. The sandstone samples have an average of 62.7% saturated hydrocarbons, 10.8% aromatic hydrocarbons and 26.5% polars. The SAT/ARO ratio increase from Not (S3), through Tofte, Garn and Tilje indicating a higher maturity in the Tilje core extract sample (see figure 4.3.).

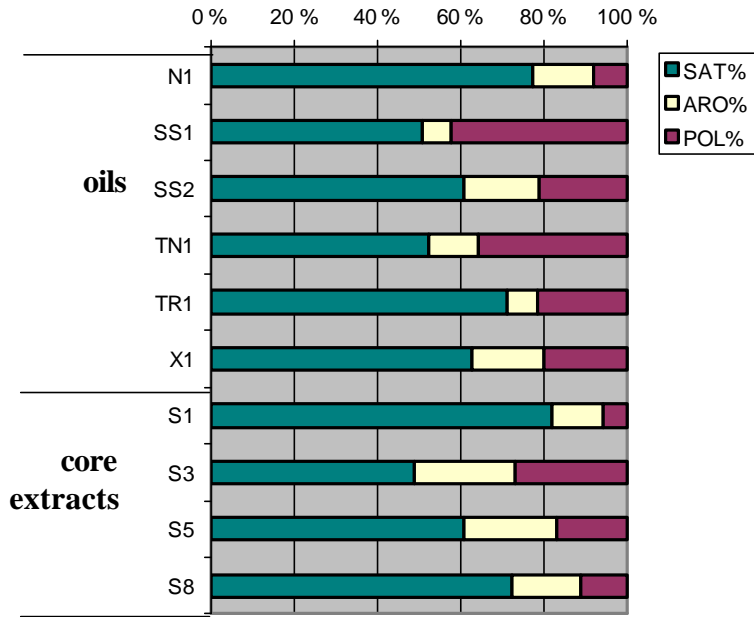


Figure 4.1. The bar diagram shows the percentage amount of saturated hydrocarbons, aromatic hydrocarbons, and polar compounds (resins and asphaltenes) of the oils and core extracts from the Haltenbanken Area.

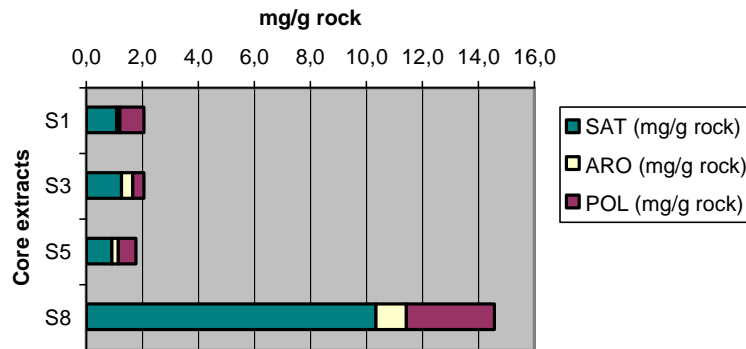


Figure 4.2. Bar diagram showing the total yield of the Smørbukk core samples, notice the much higher amount of total yield in the sample from the Tilje formation (S8). All units are reported in mg /gram rock.

Smørbukk South Field (samples SS1, SS2: oil)

The SS2 sample from the Lysing Formation has a 20% higher content of saturated hydrocarbons than the SS1 sample. But SS1 from the Tilje Formation have 15 % higher content of polar compounds, the average relative amount of saturated hydrocarbons is 72.3%, aromatic hydrocarbons is 14.9% and polars is 12.8%. The SAT/ARO ratio increase from the Tilje to the Lysing sample (see figure 4.3.).

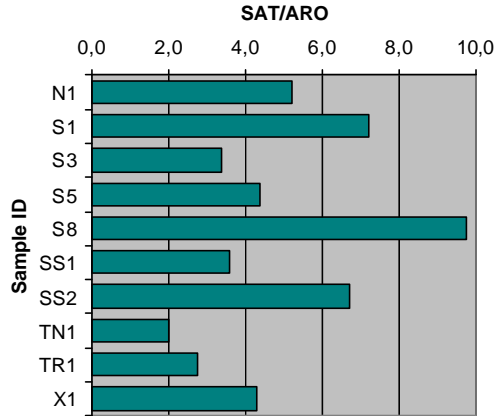


Figure 4.3. The saturated hydrocarbons/aromatic hydrocarbons ratio (SAT/ARO) mainly reflects maturity. Note the increase of the ratio in the Smørbukk core extracts from Not, through Tofte, Garn and Tilje. Both the Smørbukk South and the Njord oil also have a high SAT/ARO ratio, whilst the Tyrihans and Trastakk oils have lower ratios.

Trestakk discovery (sample TR1: oil)

The content of saturated hydrocarbons in the single oil sample from the Trestakk field is 60.8%, amount of aromatic hydrocarbons is 22.2% and polar compounds represent 17.1%. Together with the Tyrihans sample the Trestakk oil have the lowest SAT/ARO ratio in the sample set. The SAT/ARO ratio is among the lowest in the sample set.

Tyrihans discovery (sample TN1: oil)

The oil sample from the Garn Formation in well 6407/1-3 contains 48.8% saturated hydrocarbons, 24.3% aromatic hydrocarbons and 26.9% polar compounds. The sample plots closest to the centre of the ternary diagram in figure 4.4. The sample has the lowest SAT/ARO ratio in the data set.

6407/4-1 (sample X1: oil)

The oil sample from well 6407/4-1 contains 72.1% saturated hydrocarbons, 16.7% aromatic hydrocarbons and 11.2% polar compounds

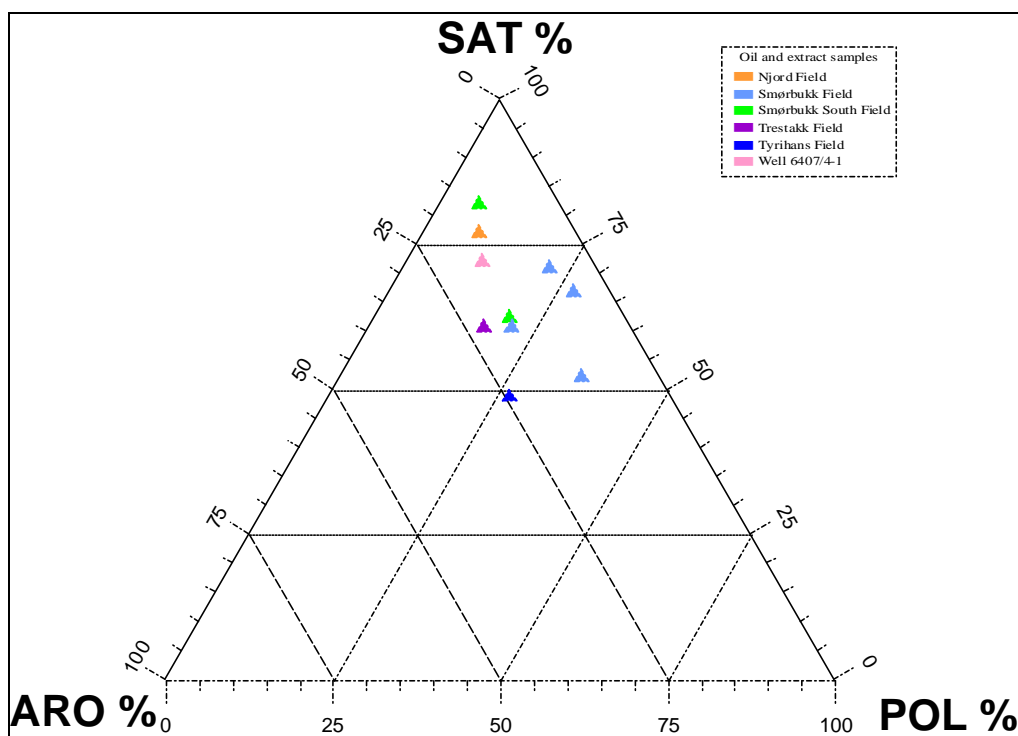


Figure 4.4. The relative SAP distribution of the oils and core extracts plotted in a ternary diagram. The trend is that the Tyrihans field have the lowest amount of saturated hydrocarbons, the samples from Smørbukk South show increasing saturated hydrocarbon content from Tilje to Lysing. The Smørbukk and Smørbukk South samples have the highest amount of polar compounds.

4.2. GC-FID oils and extracts

The extract and oil samples were analysed on GC-FID as described in Chapter 3.2. The GC-FID gives in this case information about the n-alkane and isoprenoid distribution, and can give information about the source rock facies and maturity of the sample (Peters and Moldowan, 1993). A normal n-alkane distribution for sandstone reservoir core extracts containing hydrocarbons from the Kimmeridge Formation is a bell shaped curve with maximum peak intensities in the C_{17} - C_{25} range, the lightest detectable n-alkanes occurring between C_{13} and C_{16} and with n-alkanes existing out to C_{35} (Skålnes, 1993).

The GC-FID traces for extracts and oils will be compared to GC-MS chromatogram $m/z=85$, used to monitor n-alkanes from fluid inclusions. The GC-FID analysis is not sensitive enough to detect the small amount of organic material in the fluid inclusions, therefore the GC-MS analysis has been used. In this section both the results of the GC-FID and the GC-MS ($m/z=85$) will be presented. The GC-MS traces do not show the light hydrocarbon range, because the detection does not start until they have passed the column. Because of this the main aim is to use the GC-MS chromatogram $m/z = 85$ to compare the heavy n-alkanes, pristane, phytane, n- C_{17} and n- C_{18} . All the chromatograms (both from GC-FID and GC-MS) are found in figure 4.8.-4.32., and in the appendix, the exact values of the calculated parameters are found in table 4.2.

To get a more accurate calculation of response factors for n-alkanes and isoprenoids, a North Sea standard oil (NSO-1, from NPD) have been analysed on both the GC-FID and GC-MS apparatus. The GC-FID trace of the NSO oil has then been used as a standard and the GC-MS values have been multiplied by a calculated number to allow a direct comparison between GC-FID and GC-MS data. Then the same conversion factors have been applied to the rest of the GC-MS chromatogram showing $m/z=85$ data.

Before quantification of all reported compounds the baseline setting was controlled and manually corrected. The exact values for the different parameters are found in table 4.2.

Lavrans discovery (samples L1, L2: inclusion extracts)

The fluid inclusions in the two sandstone samples from the Lavrans Field both have n-C₁₈ as their highest peak (see GC-MS chromatogram $m/z = 85$ in figure 4.8. and 4.9.), the peaks decrease rapidly down to n-C₂₂ and from there and beyond the decrease is moderate. The pristane and phytane peaks are short relative to the n-alkane peaks.

The carbon preference index (CPI) is calculated over the range n-C₂₁ to n-C₂₆, CPI 1 and n-C₃₀ to n-C₃₂, CPI 2 (see chapter 3.5.2.). The inclusion samples from Lavrans have the highest odd predominance in CPI 1 in the sample set and no predominance at all in CPI 2, see table 4.2 for exact values. Pristane/n-C₁₇ and phytane/n-C₁₈ ratios are among the lowest in the dataset indicating high thermal maturity.

Njord Field (samples N1: oil, N2: inclusion extract)

The oil sample has a distribution of n-alkanes with a maximum peak at n-C₁₅, and a high amount of light hydrocarbons detectable down to n-C₇. The apparent loss of the lighter compounds can be caused either by evaporation or biodegradation. If the n-alkane peaks are disregarded, pristane is the dominant peak (see GC-FID trace in figure 4.10.).

The fluid inclusion sample has n-C₁₆ as its highest peak and peak highs decrease rapidly down to n-C₁₉. Peaks n-C₂₀ to n-C₂₂ are constant, remaining peaks decrease moderately until the last detectable peak n-C₃₅ (see figure 4.11.). Calculated CPIs show no to odd predominance in both oil and inclusion extract. Plotted against the pr/ph values it can give information about maturity and facies (figure 4.5.)

Smørbukk Field (samples S1, S3, S5, S8: core extracts, S2, S4, S6, S7, S9: inclusion extracts)

All extract samples from the Smørbukk Field show a normal n-alkane distribution, and worth noticing is the increasingly visible bell shape of the chromatograms with depth (figure 4.12. – 4.15.). The three shallowest samples have n-C₁₈ as the highest n-alkane peak while the sample at 4751.3 m (S8) has n-C₂₁ as the dominating n-alkane peak. There are no detectable peaks below n-C₁₄ in the light hydrocarbon range. In S8 the phytane peak is higher than the pristane peak; this is the only sample in the whole sample set where this is the case.

The five inclusion samples have a variety of different n-alkane patterns. The two shallowest samples (S2, S4) show irregular peak intensities up to n-C₂₃ and from there the n-alkanes decrease down to the last detectable peak. Samples S6 and S7 show a modest decrease in n-

alkanes, following the highest peak at n-C₁₇ and n-C₁₈, down to the last detectable peak. In the S7 sample the peaks representing compounds heavier than n-C₂₅ do not separate distinctly from the background noise. The deepest inclusion sample (S9) has its maximum peak towards the heavier compounds compared to the other samples. The highest peak is n-C₂₉, and the following peaks drop rapid in intensity down to n-C₃₉.

The CPI values show a variance from odd to even with no specific pattern. Pr/n-C₁₇ and ph/n-C₁₈ ratios show a difference between the core and inclusion extracts. The core extracts have values between 0.78 - 0.86 and 0.54 – 0.62 respectively, the inclusions have values between 0.24 – 0.46 and 0.22 to 0.4 for the same parameters. The three shallowest Smørbukk core samples have the highest values in the dataset for the pr/n-C₁₇. Pr/ph values are highest for the three shallowest formations, and the samples from Tilje have the lowest value (see figure 4.6.).

Smørbukk South Field (samples SS1, SS2: oils, SS3, SS4: inclusion extracts)

In well 6506/12-3 the two oil samples both have light end biased n-alkane distributions and show very similar appearances. Both samples show a nearly constant decrease in peak intensity. The intensity of the lightest hydrocarbons was so high that the peak signals were too high for the selected range and attenuations of the GC-FID (see figure 4.17. – 4.19.).

The two inclusion samples also have very similar appearances with peak maxima between n-C₂₀ and n-C₂₂. There are no detectable peaks before n-C₁₇, and up to the maxima there is a rapid increase in the intensity of the peaks. From the maximum and beyond there is a moderate decrease in peak intensity.

CPI values calculated show no to odd predominance for the samples. The pr/n-C₁₇ values are 0.66 (SS1) and 0.7 (SS2) for the oils, and 0.45 (SS3) and 0.43 (SS4) for the fluid inclusions. Ph/n-C₁₈ ratios have values 0.57, 0.5, 0.37 and 0.34 respectively. The pr/ph ratio range from 0.29 – 1.61, with the two inclusion samples having the lowest values in the sample set (see table 4.2. for exact values and illustrated in figure 4.6.).

Tyrihans Field (samples TN1: oil, TN2, TN3, TS1: inclusion extracts)

The single oil sample from well 6407/1-3 show an n-alkane distribution with compounds detectable down to n-C₇, and the highest peak is n-C₁₅ (figure 4.20.). The sample shows a reduction of the peak highs in the light hydrocarbon range which can have been caused by biodegradation or phase fractionation.

In the Tyrihans North inclusion samples the dominant peak is n-C₁₇ (figure 4.21. and 4.22.), while in the Tyrihans South sample the maximum is shifted towards n-C₁₉ (figure 4.23.).

Like for the other samples, the oil sample show higher pr/n-C₁₇ and ph/n-C₁₈ ratios than the inclusion samples (see table 4.2. for exact values). The CPI 1 value shows an odd predominance for all samples, while the CPI 2 show no, or even predominance.

Trestakk discovery (samples TR1: oil, TR2, TR3, TR4: inclusion extracts)

The oil sample from the Trestakk Field show a light end biased n-alkane distribution. The peaks decrease uniformly down to peak n-C₁₄, and from peak n-C₁₇ the n-alkanes decrease in steps down to the last identifiable n-alkane peak at n-C₃₆ (figure 4.24.).

The inclusion samples have their highest peaks in the range from n-C₁₇ to n-C₂₀. In the two samples TR2 and TR3 the phytane peak is dominant when the n-alkanes are disregarded (see figures 4.25. – 4.27.).

Pr/n-C₁₇ ratios range between 0.32 and 0.45, and ph/n-C₁₈ ratios range from 0.29 to 0.35 for the inclusion samples. The oil sample has 0.78 and 0.74 for the same parameters. CPI 1 values show no to odd predominance for the Trestakk samples. CPI 2 show even predominance for the oil and the deepest inclusion extract, and odd predominance for the two samples at 3932 m (TR2 and TR3).

Sample	Sample type	Analyse	Pr/n-C17	Ph/n-C18	Pr/Ph	CPI 1	CPI 2	(Pr/n-C17)/(Ph/n-C18)
N1	oil	GC-FID	0,78	0,46	1,83	1,05	1,00	1,71
SS1	oil	GC-FID	0,66	0,57	1,29	1,05	1,00	1,16
SS2	oil	GC-FID	0,70	0,50	1,61	1,05	1,00	1,41
TN1	oil	GC-FID	0,77	0,70	1,18	1,04	0,99	1,10
TR1	oil	GC-FID	0,78	0,74	1,22	1,04	0,98	1,05
X1	oil	GC-FID	0,80	0,50	1,80	1,10	1,02	1,58
S1	core ext	GC-FID	0,86	0,62	1,41	1,03	1,00	1,39
S3	core ext	GC-FID	0,82	0,60	1,21	1,08	1,00	1,37
S5	core ext	GC-FID	0,80	0,57	1,40	1,12	0,92	1,41
S8	core ext	GC-FID	0,78	0,54	0,98	1,04	1,02	1,44
L1	incl ext	GC-MS	0,20	0,16	1,37	1,28	1,00	1,30
L2	incl ext	GC-MS	0,26	0,19	1,25	1,35	1,00	1,38
N2	incl ext	GC-MS	0,35	0,32	2,57	1,11	1,00	1,08
SS3	incl ext	GC-MS	0,45	0,37	0,29	1,04	1,02	1,21
SS4	incl ext	GC-MS	0,43	0,34	0,38	1,06	1,03	1,27
TN2	incl ext	GC-MS	0,31	0,30	1,50	1,04	0,90	1,03
TN3	incl ext	GC-MS	0,45	0,49	1,56	1,04	1,00	0,91
TS1	incl ext	GC-MS	0,46	0,33	1,35	1,03	0,95	1,41
TR2	incl ext	GC-MS	0,32	0,29	0,88	1,00	1,01	1,10
TR3	incl ext	GC-MS	0,36	0,35	1,22	1,07	1,04	1,03
TR4	incl ext	GC-MS	0,45	0,33	1,75	1,04	0,88	1,39
X2	incl ext	GC-MS	0,56	0,20	2,74	1,10	0,98	2,78
X3	incl ext	GC-MS	0,24	0,17	2,33	1,10	1,10	1,39
X4	incl ext	GC-MS	0,55	0,27	1,66	1,09	1,00	2,01
Y1	incl ext	GC-MS	0,41	0,47	2,79	0,96	1,08	0,87
S2	incl ext	GC-MS	0,24	0,22	1,26	0,74	1,00	1,06
S4	incl ext	GC-MS	0,42	0,33	1,41	1,19	0,78	1,27
S6	incl ext	GC-MS	0,46	0,25	1,67	1,16	0,90	1,80
S7	incl ext	GC-MS	0,41	0,40	1,91	1,55	n.m.	1,03
S9	incl ext	GC-MS	0,43	0,34	0,77	0,91	1,10	1,26

Table 4.2. Data from the GC-FID and GC-MS chromatogram m/z = 85.

The well 6407/4-1 discovery (samples X1: oil, X2, X3, X4: inclusion extracts)

In well 6407/4-1 the oil sample shows a light end biased n-alkane distribution. The n-alkanes decrease evenly down to n-C₁₄ and then there is a modest decrease from n-C₁₅ and beyond.

The inclusion samples all show similar n-alkane distributions with the highest peaks in the n-C₁₇ to n-C₂₂ range. The n-alkane peaks decrease evenly from the highest peak down to n-C₃₆.

Sample X2 and X3 both display a “step-down” in peak intensity after the dominant peaks (see figures 4.28. – 4.31.).

The CPI values change from a CPI 1 with odd predominance to even predominance in CPI 2 for sample X2, the rest of the CPI values show odd predominance. Pr/ph values range from 1.66 to 2.74 for the inclusion samples, and the oil sample have pr/ph value at 1.8.

Well 6407/10-1 (Y1: inclusion extract)

Sample Y1 have n-C₁₇ as the highest peak and show a rapid decrease in peak intensity down to n-C₁₉. Then the peaks increase towards a second top at n-C₂₂ and then decrease moderately outwards (figure 4.32.).

The pr/ph value is the highest in the data set with 2.79, and the CPI changes from even to odd predominance from CPI 1 to CPI 2.

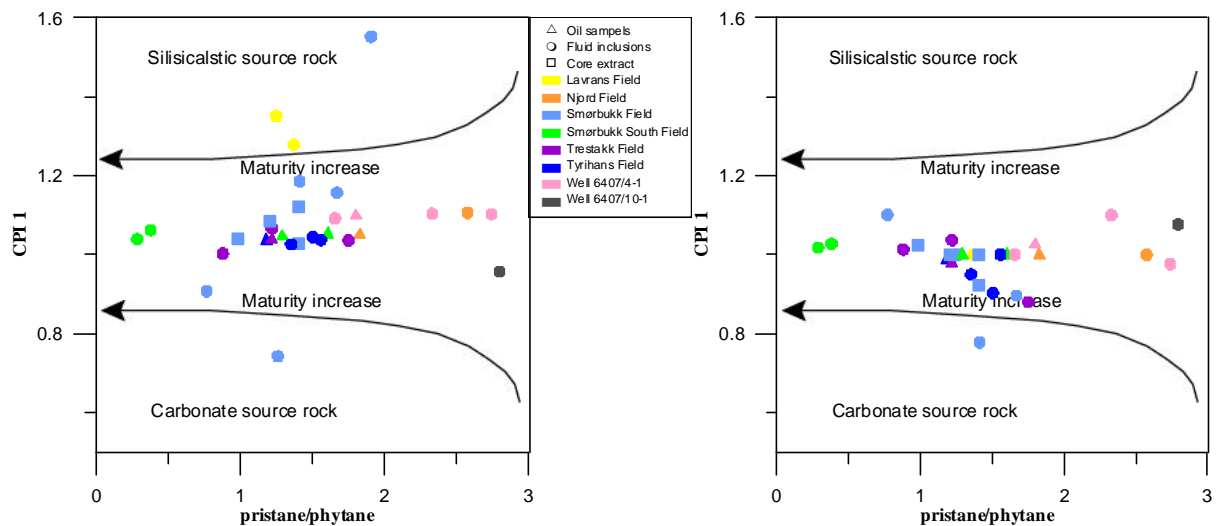


Figure 4.5. The pristane/phytane ratio plotted against both CPI1 and CPI2. Note that the CPI 1 values show a wider range than the CPI 2 values, and the oil samples are less scattered than the inclusion samples.

4. Results

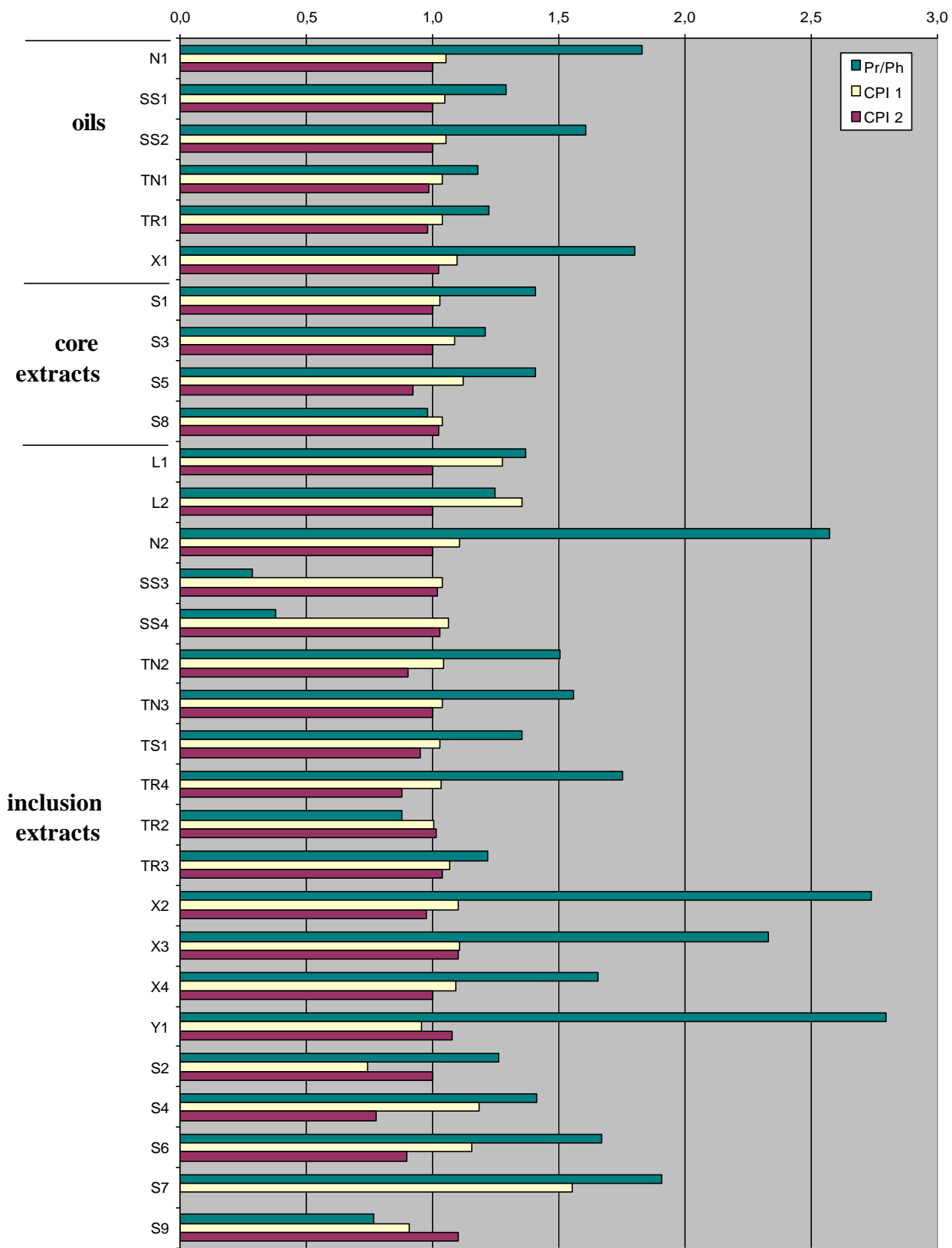


Figure 4. 6. The CPI and pristane/phytane ratios calculated from the GC-FID trace and the GC-MS $m/z = 85$ chromatogram.

4.3. GC-MS oils and extracts

All the samples were analysed on the GC-MS instrument, see chapter 3.3 for further details. The GC-MS technique makes it possible to study compounds present in only small concentrations in the petroleum. The compounds of main interest in this study are generally referred to as “biomarkers” (Waples and Machihara, 1991). These compounds will retain their carbon skeleton through diagenesis and thermal maturation, and only minor changes take place like isomerisation at chiral centra, aromatisation of ring structures or cracking of side chains. These reactions will occur with increased maturity and by calculating the ratio between reactants and products in biomarker transformations it is possible to obtain information about thermal maturity and in general about facies of the source kerogen. More information about biomarkers and their application is found in Peters and Moldowan (1993). Note that also methyl dibenzothiophenes and phenantrenes compounds which are not biomarkers, were studied by GC-MS.

A presentation of each field/discovery and some key numbers are given in the following section. All the biomarker values are given in table 4.3 and the different chromatograms are found in figure 4.7. – 4.31. The parameters and identification of peaks are described in detail in chapter 3.5.3.

The chromatograms $m/z=231$ and $m/z=253$ have in many of the samples a low signal to noise ratio and are very difficult to interpret. Therefore these results will not be discussed, but the values are given in table 4.3.

Lavrans Field (samples L1, L2: inclusion extracts)

Inclusion samples from the Lavrans field have $Ts/(Ts+Tm)$ values at 0.75 (L1) and 0.73 (L2). For L1 the hopane/sterane ratio is 0.78 and the $29Ts/(29Ts + \text{norhopane})$ ratio is 0.36, the L2 sample show 1.07 and 0.24 for the same parameters. The L2 sample has a higher amount (1.48) of C_{24} tetracyclic terpanes than L1 (0.44), and it also presents a high concentration of C_{27} steranes (parameter 13), $\%C_{27} = 41$, $\%C_{28} = 30$ and $\%C_{29} = 29$. See table 4.3 for comparison with the rest of the data set. There is also a big difference between the samples in the MDR ratio, L1 have a ratio of 2.06, while L2 have 7.13. The methylphenantrene ratios (MPR) are the highest in the sample set, 1.5 (L1) and 1.74 (L2). Vitrinite reflectance calculated from the MPR also shows the highest values in the sample set with 1.14 and 1.21 respectively.

Njord Field (samples N1: oil, N2: inclusion extract)

Few peaks was possible to identify from the $m/z = 191$ chromatogram obtained from the inclusion sample N2 (see chromatogram in figure 4.10.). However, the $Ts/(Ts+Tm)$ ratio is found to be 0.71 (N1) and 0.53 (N2), the $29Ts/(29Ts + \text{norhopane})$ ratio is 0.39 and 0.24 respectively. N1 have the highest hopane/sterane ratio in the dataset with 2.58, N2 have 1.84 for the same ratio. The calculated vitrinite reflectance value (R_m) is 0.87 for N1 and 0.89 for N2. Sample N2 has a higher concentration of tricyclic terpanes relative to the C_{30} hopane,

(parameter 7 = 1.64) compared to N1 (0.63), but N1 has a higher metyldibenzothiophene ratio (MDR) with a value of 4.35 compared to L2s value of 3.0. Values for the other molecular parameters from the GC-MS chromatogram is listed in table 4.3 below.

Smørbukk Field (samples S3, S8: core extract, S9: inclusion extract)

Two Smørbukk extracts and 5 inclusion samples were analysed on the GC-MS (figures 4.11. – 4.14.), but 4 of the inclusion samples did not contain sufficient amounts of organic material to get good signals on the chromatogram (see chapter 4.4. for microscopy examination of the samples). These samples will therefore not be described in this section.

The two core extract samples have hopane/sterane ratios at 0.74 and 0.52, Ts/(Ts+Tm) ratios at 0.74 and 0.67, and 29Ts/(29Ts + norhopane) ratios at 0.47 and 0.53 which are among the highest observed. The bisnorhopane/(bisnorhopane + norhopane) ratio for the two samples S3 and S8 are 0.32 and 0.34 respectively. The amount of tricyclic and tetracyclic terpanes is highest in sample S8 with values of 11.74 (parameter 7) and 1.87 (parameter 8), S3 has 2.71 and 0.33 for the same parameters. The two extracts (S3 and S8) have the highest MDR value in the sample set, and they also have high calculated vitrinite reflectance values (parameter 22-25), see table 4.3. for the exact values of the parameters.

The inclusion sample S9 has the highest bisnorhopane/(bisnorhopane + norhopane) ratio with 0.45, and has relative high amounts of tricyclic and tetracyclic terpanes indicated by parameter 7 = 7.51 and parameter 8 which is 0.81. S9 has a MDR value at 1.92, which is low compared to the two core extracts, and show calculated vitrinite reflectance values between 0.65 and 0.88 (see table 4.3. for the specific values)

Smørbukk South Field (samples SS1, SS2: oils, SS3, SS4: inclusion extracts)

The oil samples have hopane/sterane ratios at 1.17 (SS1) and 1.57 (SS2) respectively, and the diahopane/(diahopane + normoretane) ratio is 0.8 and 0.91 for the two samples. Parameter 1, Ts/(Ts + Tm) and 29Ts/(29Ts + norhopane) both show the highest observed values for sample SS1, respectively 0.74 and 0.56. The other oil sample has values of 0.67 and 0.44 for the same parameters. SS1 has the lowest vitrinite reflectivity calculated from MPR (R_m) in the dataset with 0.5, the SS2 shows R_m values at 0.92%, but SS1 shows high vitrinite reflectivity calculated with the MDR value ($R_{m(2)}=0.98\%$). The parameters calculated from the methylphenantrenes (parameter 18-20) all have low values for sample SS1 compared to the other Smørbukk South samples (see table 4.3 for specific values). Inclusion samples SS3 and SS4 from Smørbukk South have hopane/sterane ratios at 1.5 and 1.46, and both have diahopane/(diahopane + normoretane) ratios at 0.86. The two samples have values at 0.66 and 0.67 for Ts/(Ts + Tm), 0.41 and 0.43 for 29Ts/(29Ts + norhopane) and R_m values at 0.83% and 0.89% respectively.

Trestakk Field (samples TR1: oil, TR2, TR3, TR4: inclusion samples)

Several of the parameters from the Trestakk Field show similar values for the oil sample and the three inclusion samples (see table 4.3). The inclusion samples have 29Ts/(29Ts+ norhopane) values between 0.42 and 0.47, the diahopane/(diahopane + normoretane) ratio

Sample	Sample type	1	2	3	4	5	6	7	8	9	10	11	12
L1	incl ext	0,75	1,00	0,63	0,81	0,36	0,24	5,24	0,44	0,78	0,58	0,48	0,79
L2	incl ext	0,73	0,67	0,58	0,92	0,24	0,09	7,70	1,48	1,07	0,59	0,53	0,74
N1	DST	0,71	0,87	0,60	0,91	0,39	0,40	0,63	0,08	2,58	0,66	0,48	0,64
N2	incl ext	0,53	1,00	0,49	1,00	0,24	0,33	1,64	n.m.	1,84	0,56	0,38	0,52
S3	core ext	0,74	1,00	0,52	1,00	0,47	0,32	2,71	0,33	0,74	0,65	0,62	0,62
S8	core ext	0,67	1,00	0,55	1,00	0,53	0,34	11,71	1,87	0,52	0,62	0,46	0,72
S9	incl ext	0,78	1,00	0,44	1,00	0,59	0,45	7,51	0,81	0,37	0,55	0,51	0,68
SS1	DST	0,74	0,91	0,57	0,88	0,56	0,28	1,48	0,27	1,17	0,61	0,50	0,70
SS2	DST	0,66	0,80	0,69	0,88	0,44	0,36	1,13	0,12	1,57	0,58	0,52	0,67
SS3	incl ext	0,66	0,86	0,57	0,92	0,41	0,32	1,28	0,18	1,50	0,62	0,52	0,62
SS4	incl ext	0,67	0,86	0,58	0,92	0,43	0,31	1,35	0,19	1,46	0,61	0,51	0,62
TN1	DST	0,63	0,82	0,61	0,93	0,41	0,27	0,95	0,15	2,22	0,68	0,55	0,69
TN2	incl ext	0,73	1,00	0,58	0,89	0,40	0,28	2,45	0,24	2,36	0,55	0,49	0,72
TN3	incl ext	0,67	n.m.	0,48	1,00	0,43	0,00	2,15	0,22	1,86	0,46	0,44	0,63
TS1	incl ext	0,73	1,00	0,59	0,91	0,41	0,20	1,45	0,18	2,50	0,59	0,49	0,67
TR1	DST	0,61	0,91	0,59	0,92	0,49	0,33	0,91	0,18	1,78	0,63	0,56	0,69
TR2	incl ext	0,68	0,87	0,58	0,91	0,46	0,29	0,87	0,13	2,13	0,60	0,52	0,66
TR3	incl ext	0,66	0,92	0,60	0,93	0,47	0,28	0,74	0,13	2,20	0,63	0,50	0,66
TR4	incl ext	0,73	1,00	0,56	0,89	0,42	0,26	0,91	0,13	2,36	0,61	0,48	0,67
X1	DST	0,75	1,00	0,58	1,00	0,54	0,32	4,71	0,67	1,01	0,66	0,46	0,86
X2	incl ext	0,74	1,00	0,55	0,83	0,57	0,27	3,27	0,51	0,99	0,60	0,52	0,76
X3	incl ext	0,86	1,00	0,55	1,00	0,55	0,27	2,60	0,41	1,01	0,56	0,51	0,72
X4	incl ext	0,75	1,00	0,57	0,81	0,45	0,27	3,17	0,44	1,09	0,53	0,49	0,68
Y1	incl ext	n.m.	n.m.	0,32	1,00	n.m.	0,41	1,18	0,00	2,13	0,64	0,65	0,56

Table 4.3. Parameters calculated from the GC-MS chromatograms.

Sample	Sample type	13	14	15	16	17	18	19	20	21	22	23	24	25	26	MDBTs/MPs
L1	incl ext	35	35	30	0,59	0,60	1,50	0,62	0,53	2,06	1,14	0,77	1,03	0,66	2,49	0,28
L2	incl ext	41	30	29	0,64	0,59	1,74	0,52	0,58	7,13	1,21	0,71	1,15	1,03	0,93	0,61
N1	DST	32	33	35	0,55	0,63	0,84	0,58	0,43	4,35	0,87	0,75	0,79	0,83	5,32	0,09
N2	incl ext	35	34	31	0,45	0,91	0,89	0,39	0,42	3,00	0,89	0,64	0,78	0,73	3,88	0,13
S3	core ext	32	31	37	0,89	0,12	1,30	0,85	0,51	8,22	1,07	0,91	0,98	1,11	3,43	0,15
S8	core ext	35	34	31	0,97	0,03	1,06	1,02	0,51	9,38	0,98	1,01	0,97	1,19	3,84	0,14
S9	incl ext	31	36	33	n.m.	n.m.	0,86	0,60	0,40	1,92	0,88	0,76	0,73	0,65	4,18	0,12
SS1	DST	34	34	32	0,90	0,33	0,39	0,40	0,32	6,45	0,50	0,64	0,55	0,98	2,53	0,17
SS2	DST	34	33	33	0,79	0,29	0,94	0,68	0,47	5,29	0,92	0,81	0,90	0,90	4,70	0,12
SS3	incl ext	32	35	33	0,28	0,58	0,77	0,62	0,42	4,67	0,83	0,77	0,77	0,85	3,68	0,13
SS4	incl ext	32	35	33	0,43	0,59	0,88	0,71	0,43	1,93	0,89	0,83	0,80	0,65	2,00	0,29
TN1	DST	40	31	29	0,73	0,42	0,91	0,58	0,43	4,22	0,90	0,75	0,79	0,82	1,21	0,39
TN2	incl ext	36	33	31	0,81	0,61	0,79	0,39	0,39	2,05	0,84	0,63	0,71	0,66	0,96	0,52
TN3	incl ext	34	39	27	n.m.	n.m.	0,72	0,45	0,36	2,20	0,80	0,67	0,65	0,67	2,81	0,16
TS1	incl ext	33	36	31	0,69	0,67	0,88	0,58	0,44	3,58	0,89	0,75	0,82	0,77	3,89	0,14
TR1	DST	35	33	32	0,89	0,31	0,93	0,65	0,42	4,73	0,91	0,79	0,78	0,86	1,52	0,29
TR2	incl ext	33	34	33	0,38	0,59	0,94	0,60	0,46	4,30	0,92	0,76	0,86	0,82	2,33	0,22
TR3	incl ext	33	35	32	0,60	0,42	0,83	0,65	0,43	7,50	0,86	0,79	0,80	1,06	1,16	0,39
TR4	incl ext	32	34	33	0,70	0,61	0,66	0,37	0,35	2,13	0,75	0,62	0,62	0,67	1,57	0,29
X1	DST	40	34	25	0,96	0,19	0,78	0,55	0,36	5,00	0,83	0,73	0,65	0,88	2,33	0,16
X2	incl ext	30	35	35	0,66	0,40	1,08	0,57	0,48	3,33	0,99	0,74	0,91	0,75	3,18	0,18
X3	incl ext	29	36	35	0,51	0,75	0,75	0,47	0,42	3,33	0,81	0,68	0,78	0,75	7,03	0,08
X4	incl ext	29	35	36	0,57	0,58	0,74	0,43	0,43	3,00	0,81	0,66	0,79	0,73	3,61	0,16
Y1	incl ext	46	28	27	n.m.	n.m.	0,77	0,39	0,39	1,75	0,83	0,63	0,71	0,64	4,10	0,13

Table 4.3. (cont.) Parameters calculated from the GC-MS chromatograms.

vary from 0.87 to 1.0, and the $\beta\beta/(\beta\beta + \alpha\alpha)$ of C_{29} parameter has values from 0.6 to 0.63, R_m range between 0.75 and 0.92%. For the oil sample the respective values are 0.49, 0.91, 0.63 and 0.91%. The three calculated vitrinite reflectivities (parameter 23 – 25) varies between 0.62 and 1.06% for the inclusion samples and the oil indicate by these parameters a maturity between 0.78 and 0.86%. The hopane/sterane ratio for the inclusion samples show values from 2.13 to 2.36 and the MDR ratio range from 2.13 to 7.5. The oil sample has hopane/sterane ratio at 1.78 and MDR ratio at 4.73.

Tyrihans Field (samples TN1: oil, TN2, TN3, TS1: inclusion samples)

All four samples have a high hopane/sterane ratio, compared to the other samples in the dataset, with values ranging from 1.86 to 2.5 (the oil sample have 2.22). The $T_s/(T_s + T_m)$ ratio for the oil sample is 0.63, $29T_s/(29T_s + \text{norhopane})$ 0.41 and MPI 1 has a value at 0.58. $\%C_{27}$ is relatively high in the TN1 sample with $\%C_{27} = 40$ while $\%C_{28} = 31$ and $\%C_{29} = 29$. The calculated vitrinite reflectivities (parameter 22-25) lie in the range 0.75-0.9% vitrinite reflectance.

The inclusion samples have $T_s/(T_s+T_m)$ values between 0.67 and 0.73, $29T_s/(29T_s + \text{norhopane})$ range from 0.4 to 0.43 and MPI 1 show values between 0.39-0.58%. In the oil sample TN1 the C_{27} was the dominating sterane, while $\%C_{28}$ is dominating in the inclusion sample from Garn (TN3), $\%C_{28} = 39$, see table 4.3. for the other values. Calculated vitrinite reflectivities (parameter 22-25) vary within the range 0.63-0.89%. Sample TN2 has the lowest 3-methylphenantrene/4-methyldibenzotiofene ratio in the dataset being 0.96, the other Tyrihans inclusion samples have ratios between 2.81 and 3.89, and the oil sample has a value of 1.21 for this parameter.

Well 6407/4-1 (samples X1: oil, X2, X3, X4: inclusion samples)

Peak identification was made more difficult on the samples from well 6407/4-1 because of a lower signal/noise ratio compared to many of the other samples in the dataset (see figures 4.27. – 4.30.), but despite of that, most of the parameters could be calculated. The oil sample has hopane/sterane ratio at 1.01 and C_{23} - C_{29} tricyclic terpanes/ C_{30} hopane ratios have higher values than in many of the other samples with values up to 4.71. The $29T_s/(29T_s + \text{norhopane})$ ratio is 0.54. Oil sample X1 has a high content of C_{27} steranes ($\%C_{27}=40$, $\%C_{28}=34$ and $\%C_{29}=25$), while the three inclusion samples have C_{28} and C_{29} steranes as the main components (exact numbers are given in table 4.3).

The inclusion sample X3 has the highest $T_s/(T_s + T_m)$ ratio in the dataset with a value of 0.86 and the two other inclusion samples have values of 0.74 and 0.75 respectively. Hopane/sterane ratios vary between 0.99 and 1.09, and the C_{23} - C_{29} tricyclic terpanes/ C_{30} hopane ratios show values with a range of 2.6-3.27. The $29T_s/(29T_s + \text{norhopane})$ ratio range between 0.45 and 0.57. Two of the inclusions (X2 and X3) and the oil sample have values between 0.54 and 0.57 which are higher than for most of the samples in this study.

Well 6407/10-1 (sample Y1: inclusion sample)

This sample will be used for comparison purposes only and because of the low signal to noise ratio in the chromatogram, it will only receive a short presentation of its results (see table 4.3 for further information on the parameter values). The sample has generally low calculated vitrinite reflectivities (parameter 22-25) ranging between 0.63 and 0.83%. %C₂₇ steranes is the highest in the dataset (%C₂₇=46, %C₂₈=28 and %C₂₉=27) and the hopane/sterane ratio is 2.13. The diasterane/(diasterane + regular sterane) has the lowest ratio in the data set with a value of 0.56,

4.4. Microscopy

The methodology behind identifying hydrocarbon inclusions in sand grains is described in detail in chapter 3.4.

Because of poor results from the GC-MS analysis on some of the inclusion samples, the sands were examined in the microscope to determine the amount of inclusions. This optical examination is central to all serious petroleum inclusion work. The six samples in question were the S2, S4, S6 and S7 from the Smørbukk Field, TN3 from the Trestakk North field and Y1 from well 6407/10-1. For comparison purposes the samples SS4 and TR3 were also examined.

In general, the inclusion samples examined have light blue fluorescence colour (see figure 4.7.) except Y1 which show yellow fluorescence colour. The light blue colour indicate a light oil (Bodnar, 1990) with API values between circa 40 and 50 (Sellwood et al., 1993).

Based on subjective observations, a scale from 1 to 5 has been used to describe the amount of fluorescing inclusions in the sample, 1 reflects a low number and 5 a high amount of inclusions. Both sample SS4 and TR3 score 2-3. If the inclusions in sample TR3 occur evenly spread among the grains, every grain will contain one inclusion (value 3-4). The samples Y1, S2 and S6 have 1 on the scale. Sample TN3 contain slightly more inclusions, while S2 and S7 contain few to nil inclusions respectively (~0) (see table 4.4. for more detailed information).

Sample	Observed amount of fluorescing inclusions
S2	1
S4	0-1
S6	1
S7	0
SS4	2-3
TN3	1-2
TR3	3
Y1	1

Table 4.4. The observed amount of fluorescing petroleum inclusions in different sand samples from the sample set. 0 means nil observed petroleum inclusions – whilst 5 corresponds to the highest number of inclusions we have observed.

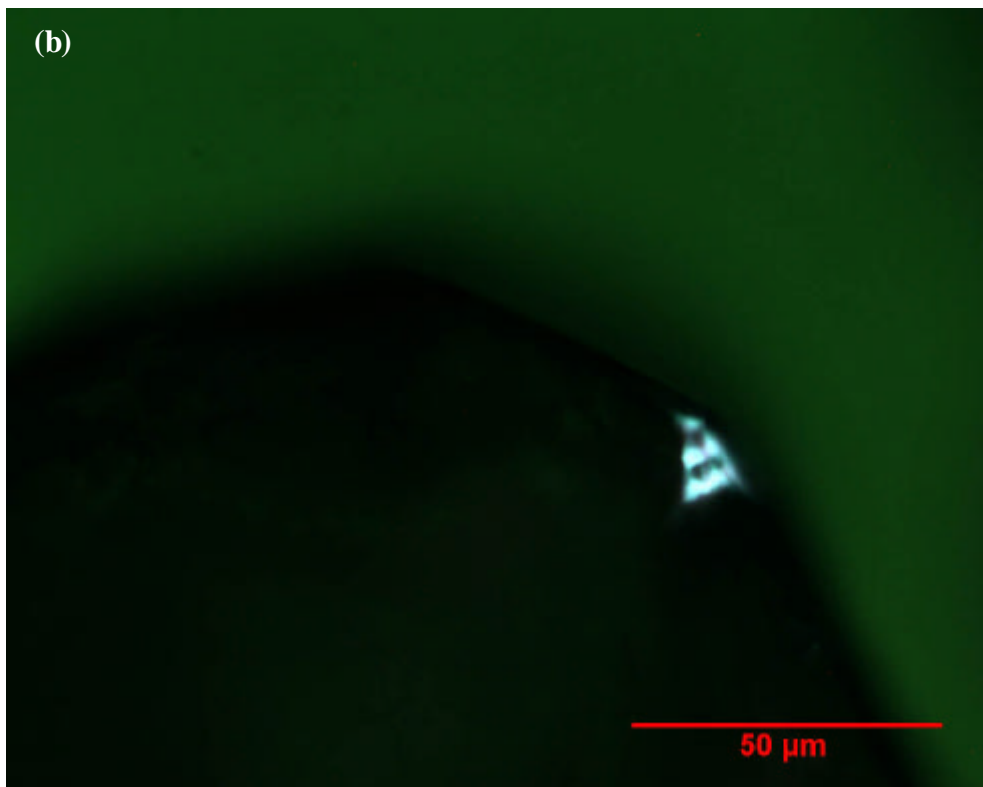


Figure 4.7. Fluorescing fluid inclusion in authigenic mineral phases from two fields in the Haltenbanken area. The photograph is taken under ordinary optical microscopical conditions, but with UV light for identification of petroleum inclusions. (a) One of the few petroleum inclusions in the S6 sample from the Smørbukk field. (b) Three overlapping fluid inclusions are seen in the SS4 sample from the Smørbukk South field.

4. Results

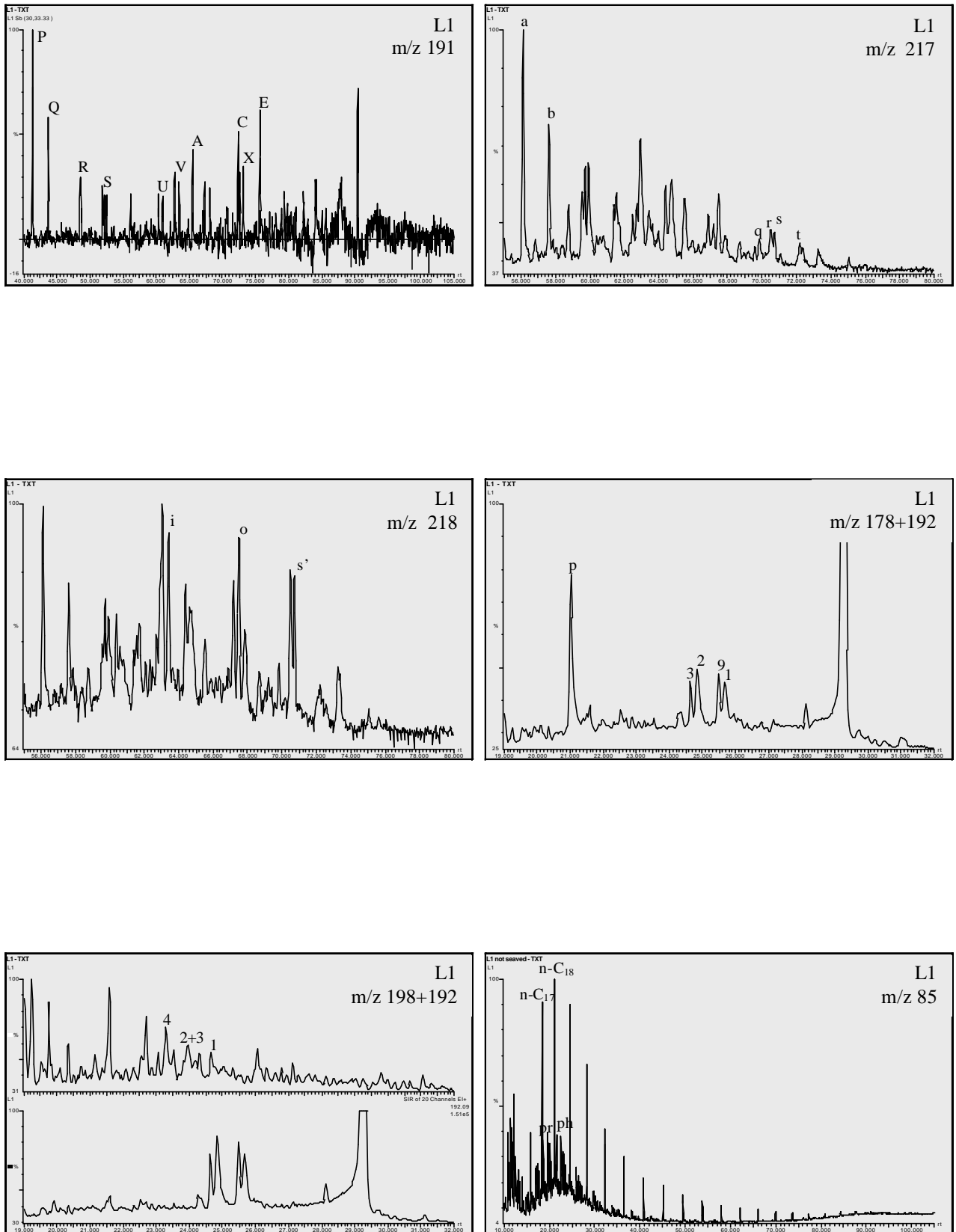


Figure 4.8. The GC-MS results for DST sample L1 from the Lavrans Field.

4. Results

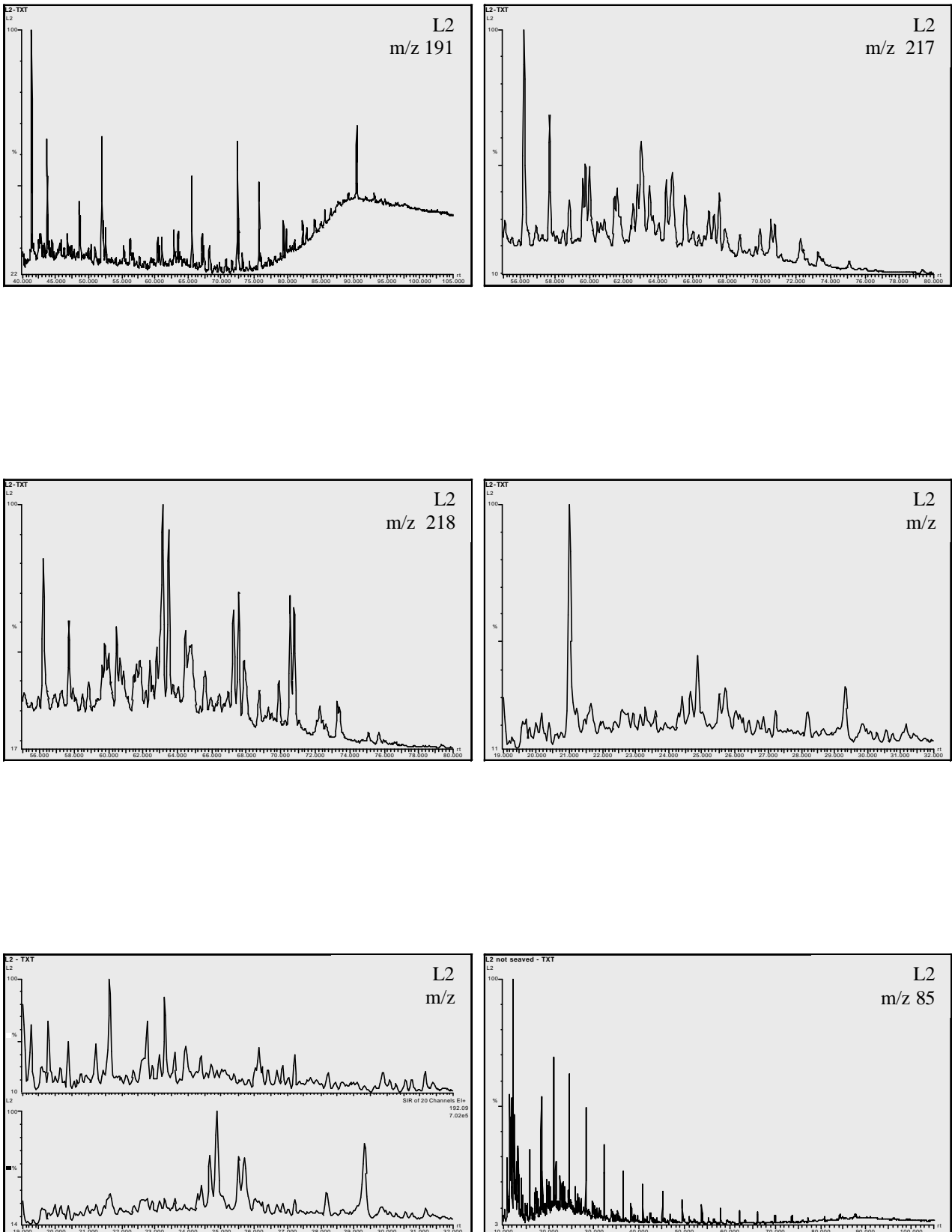


Figure 4.9. The GC-MS results for inclusion extract sample L2 from the Lavrans Field.

4. Results

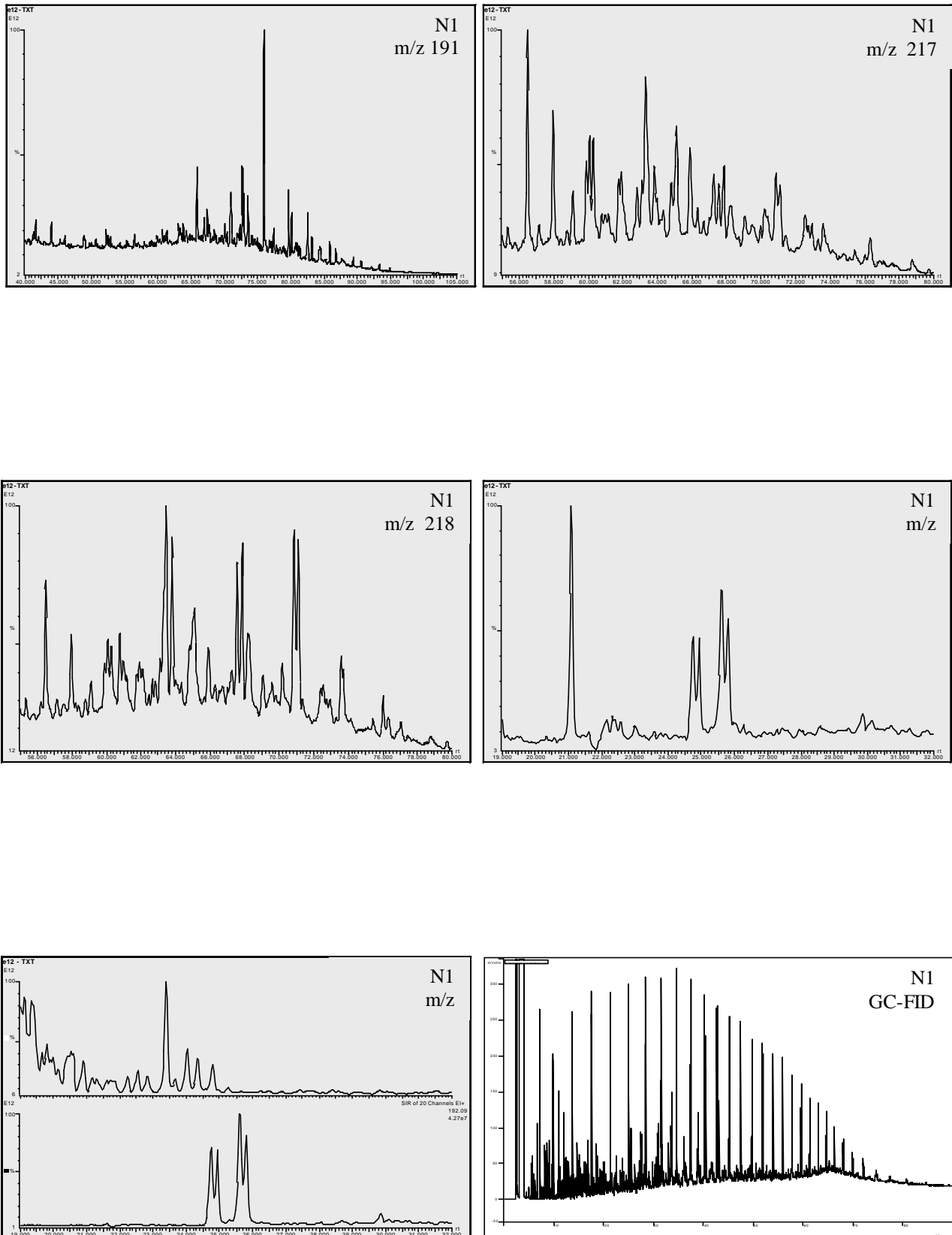


Figure 4.10. The GC-FID and GC-MS results for DST sample N1 from the Njord Field.

4. Results

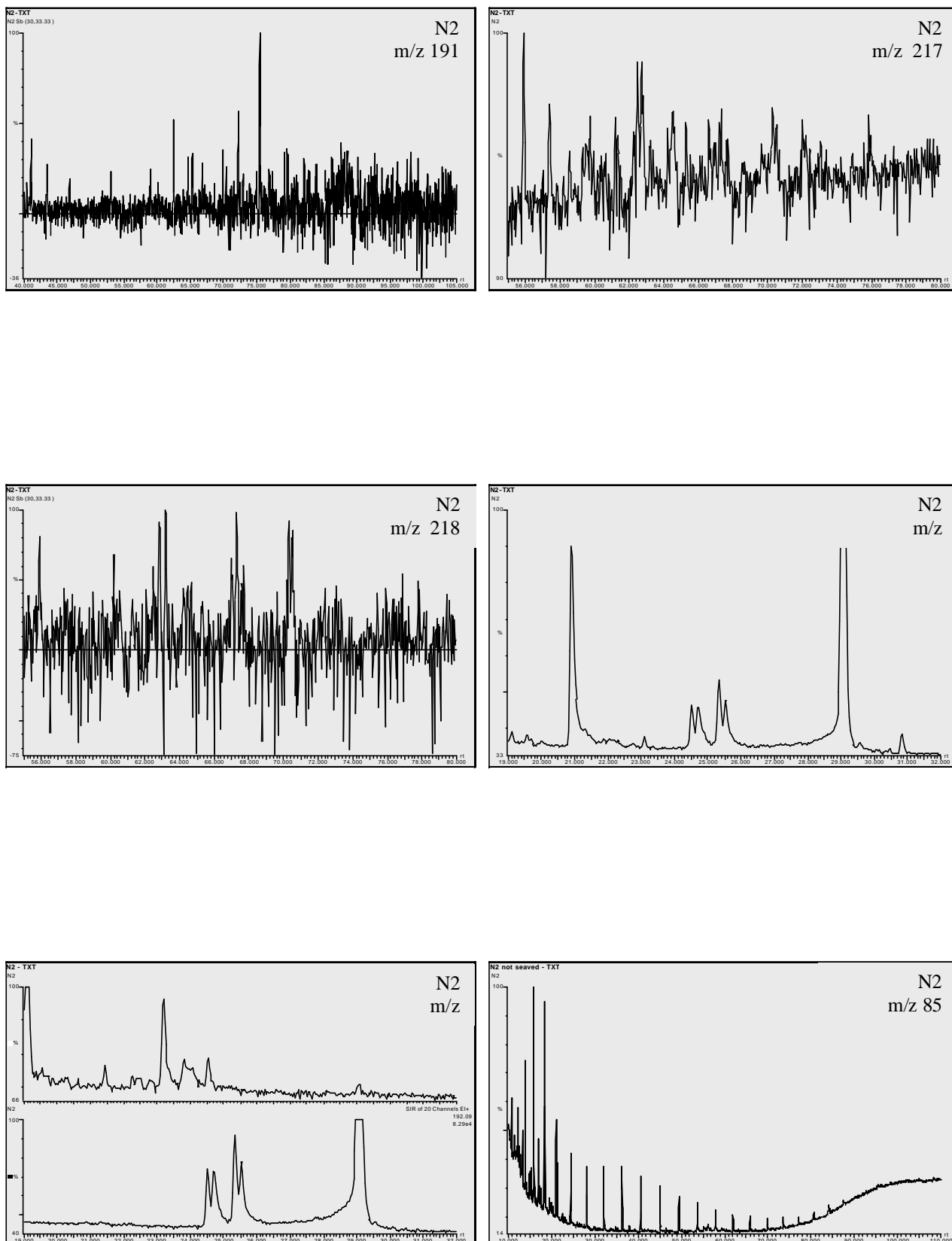


Figure 4.11. The GC-MS results for inclusion extract sample N2 from the Njord Field.

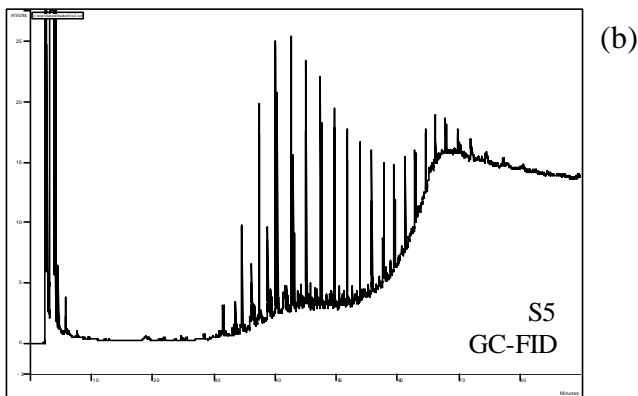
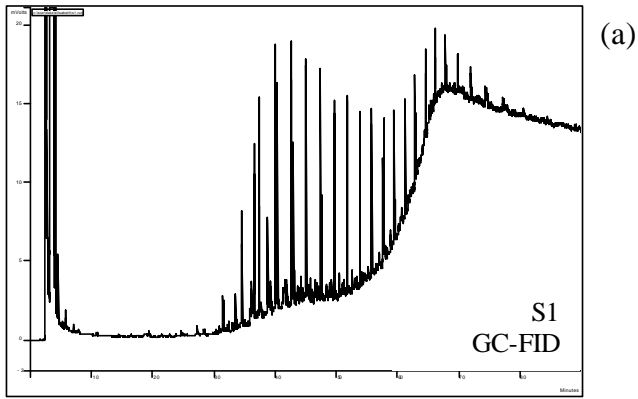


Figure 4.12. (a) GC-FID trace for the core extract sample S1 from the Garn formation in the Smørbukk field. (b) The GC-FID trace for S5, core extract from the Tofte formation. The two samples illustrate the fact made in the text, with depth the bell shape become more evident (S5 being the deepest sample).

4. Results

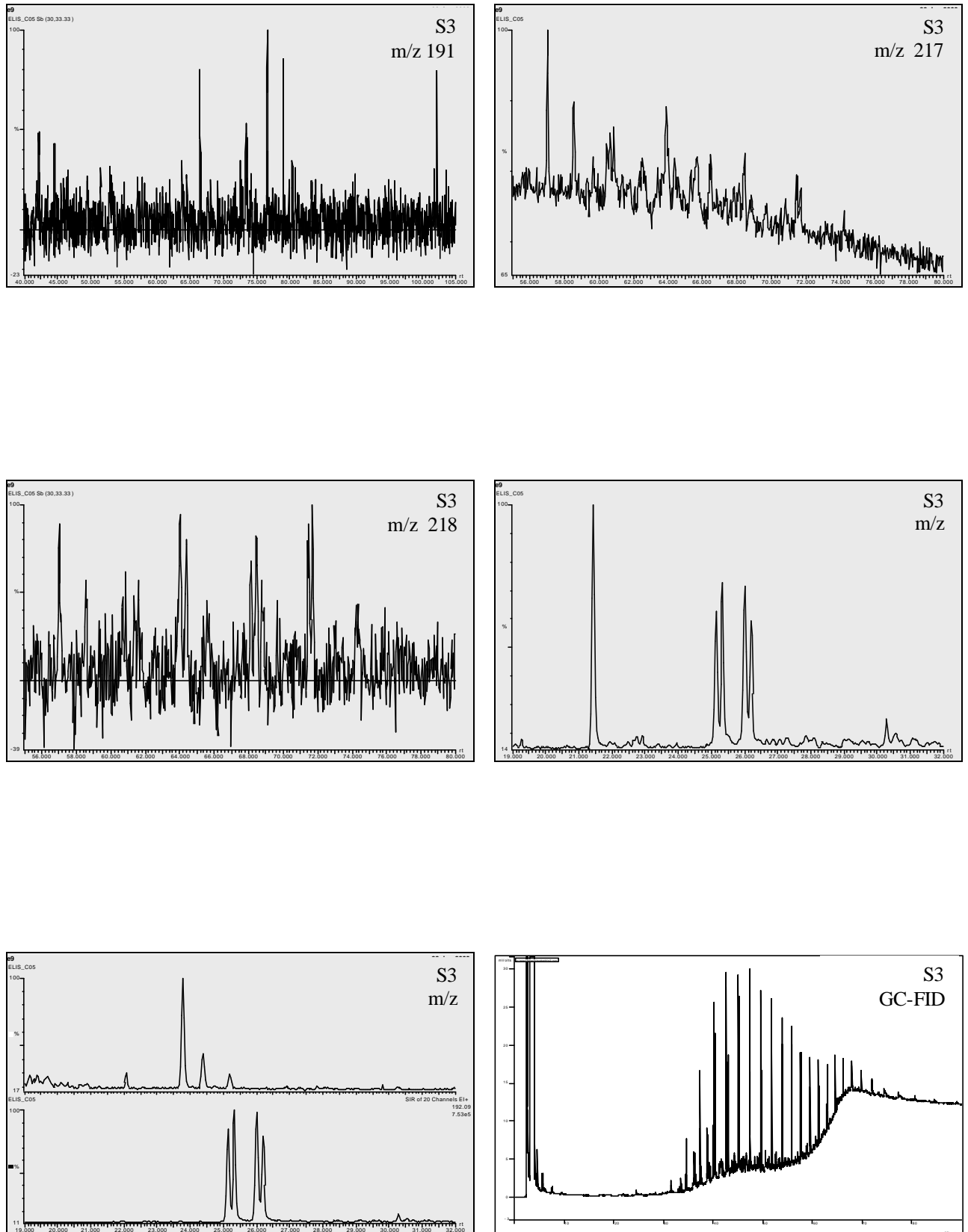


Figure 4.13. The GC-MS and GC-FID results for core extract sample S3 from the Smørbukk Field, Not formation.

4. Results

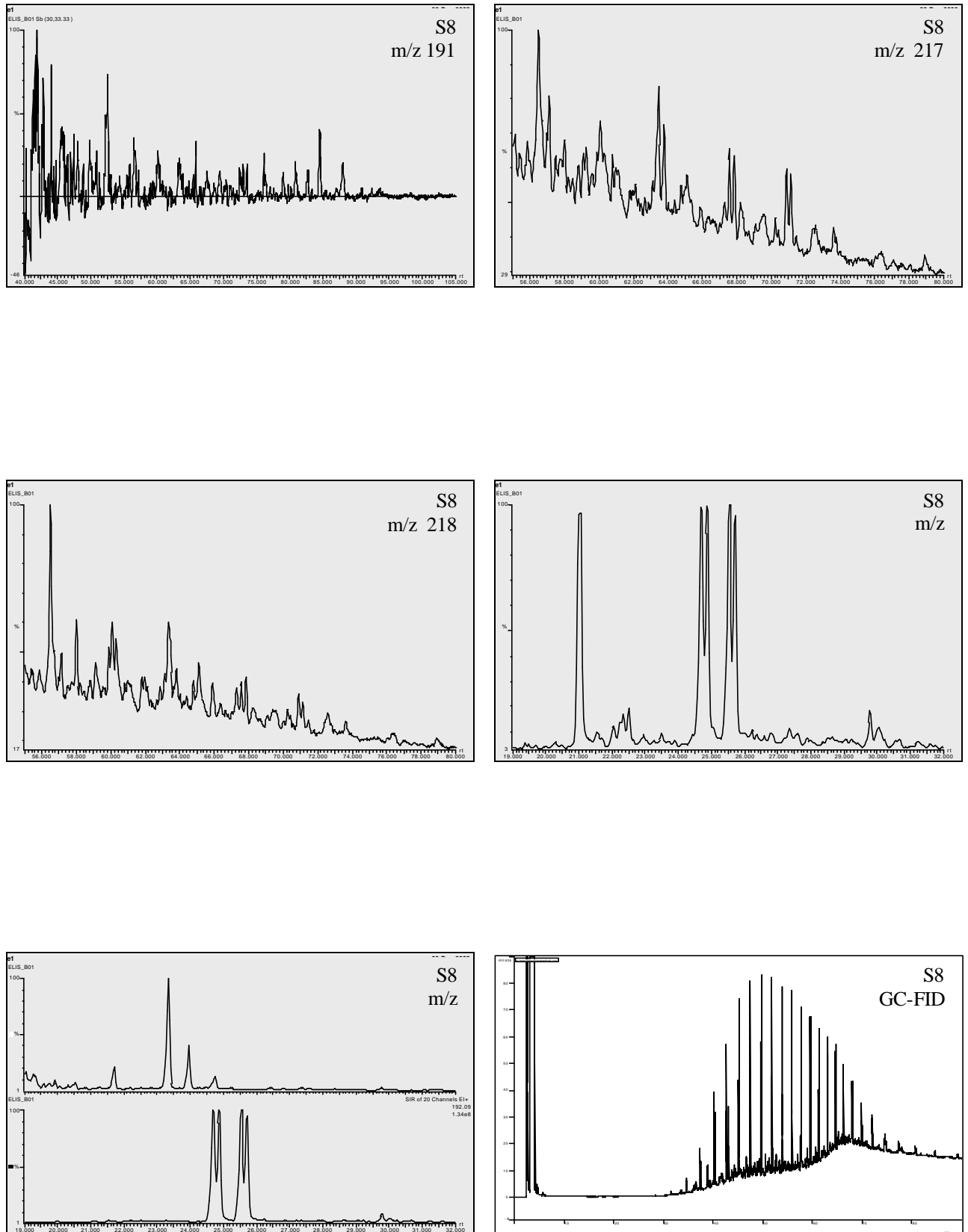


Figure 4.14. The GC-MS and GC-FID results for the core extract sample S8 from the Tilje formation, Smørbukk Field.

4. Results

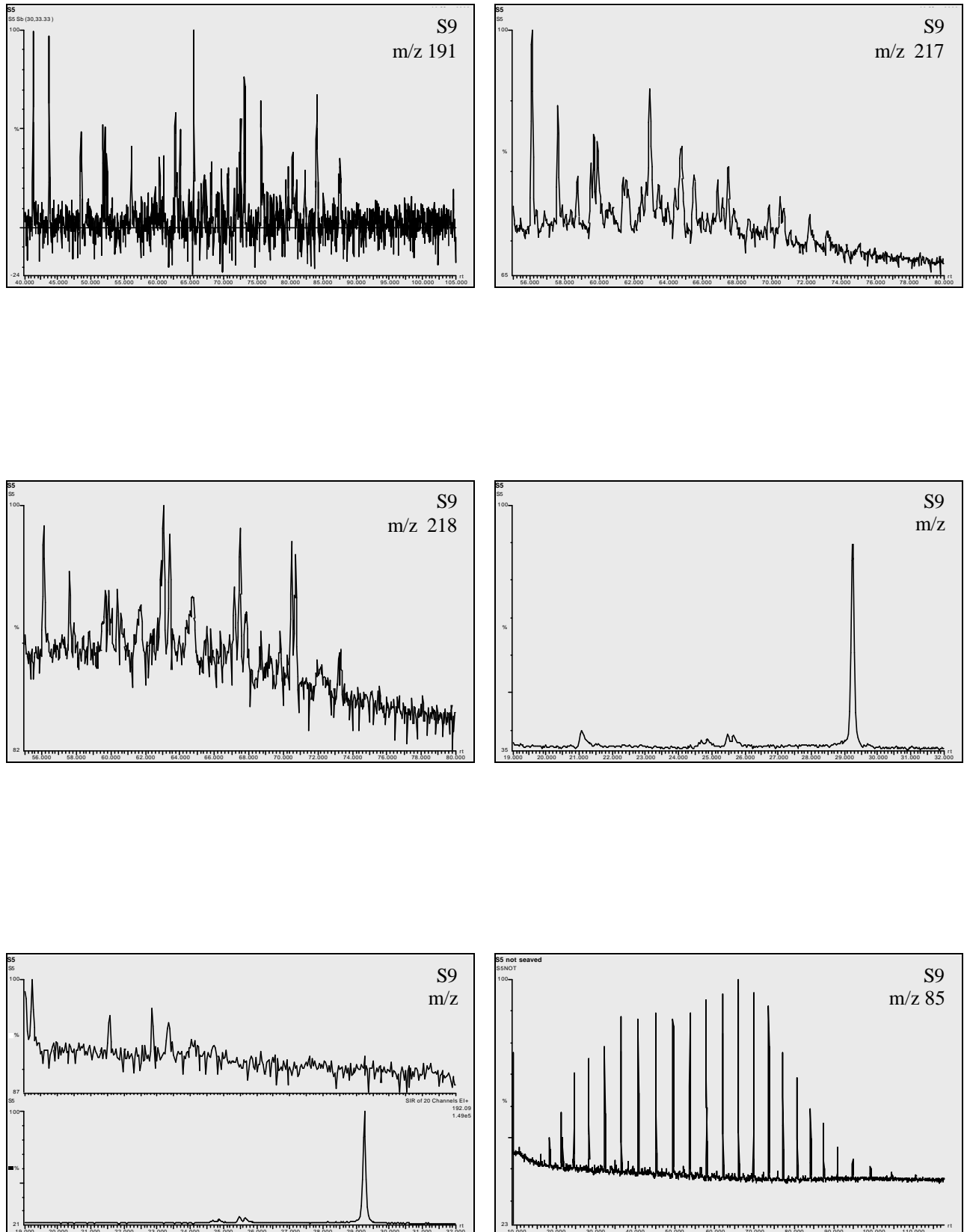


Figure 4.15. The GC-MS results for sample S9, inclusion extract from the Tilje formation, Smørbukk Field.

4. Results

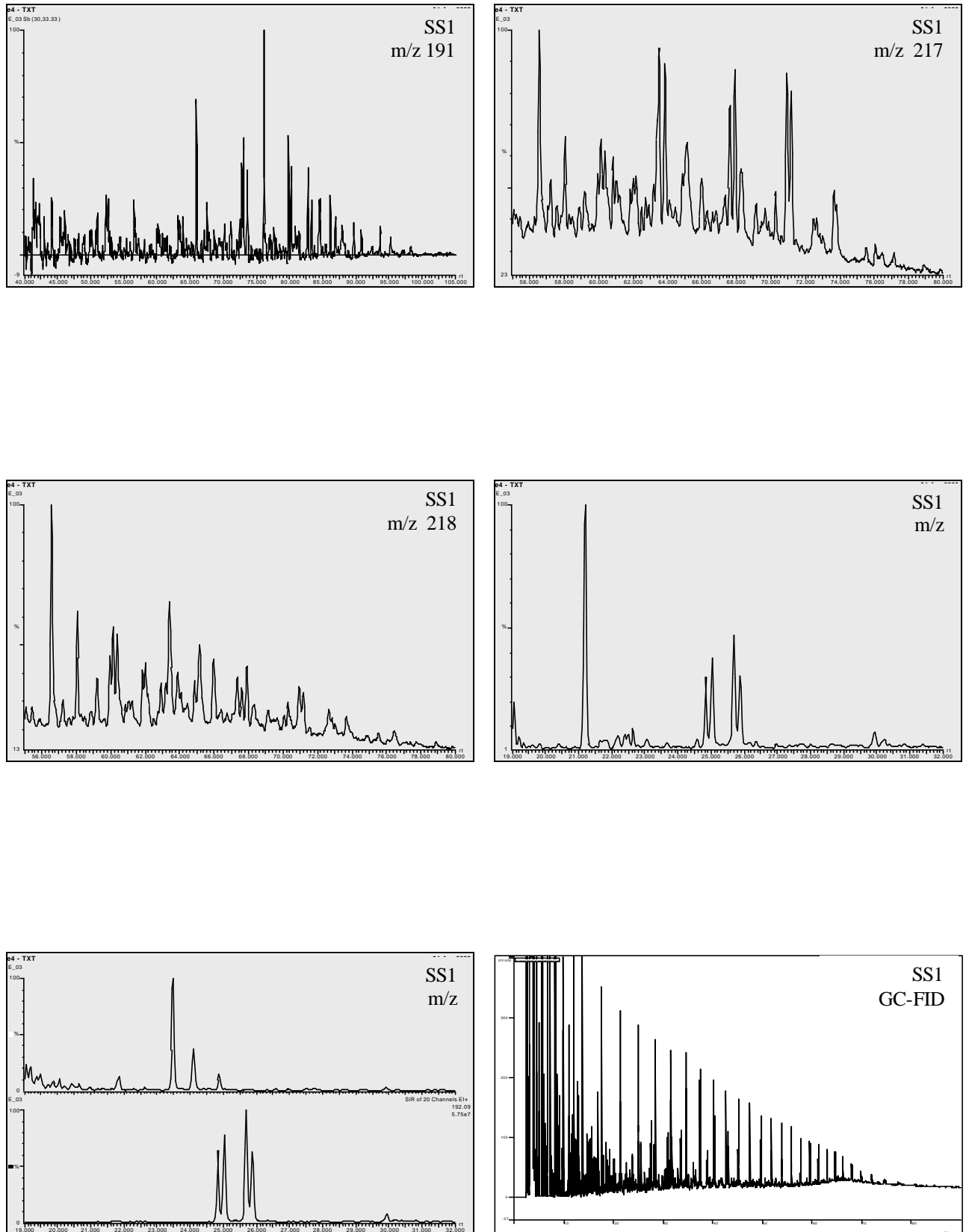


Figure 4.16. The GC-MS and GC-FID results for DST sample SS1 from the Smørbukk South Field.

4. Results

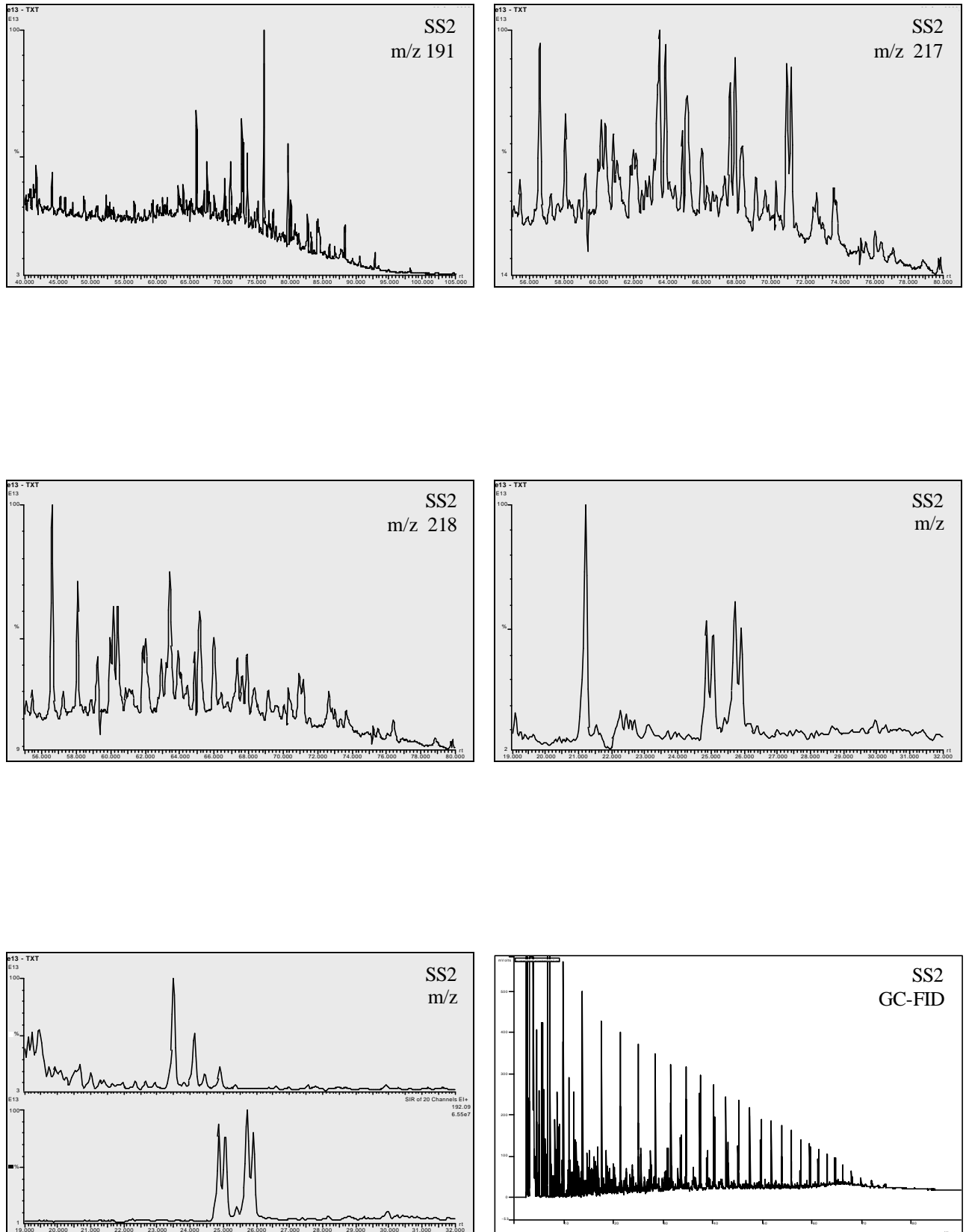


Figure 4.17. The GC-MS and GC-FID results for DST sample SS2 from the Smørbukk South Field.

4. Results

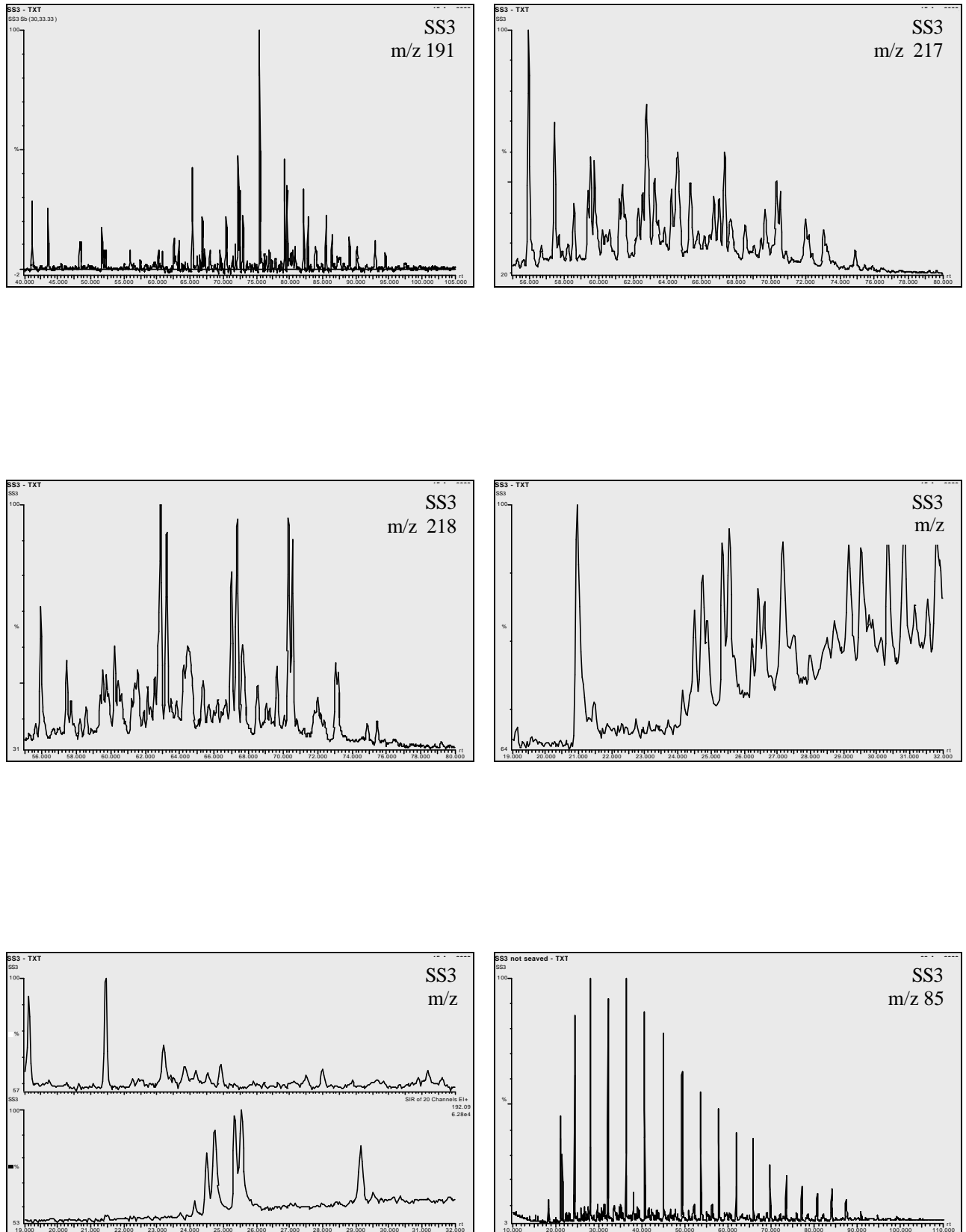


Figure 4.18. The GC-MS results for inclusion extract sample SS3 from the Smørbukk South Field.

4. Results

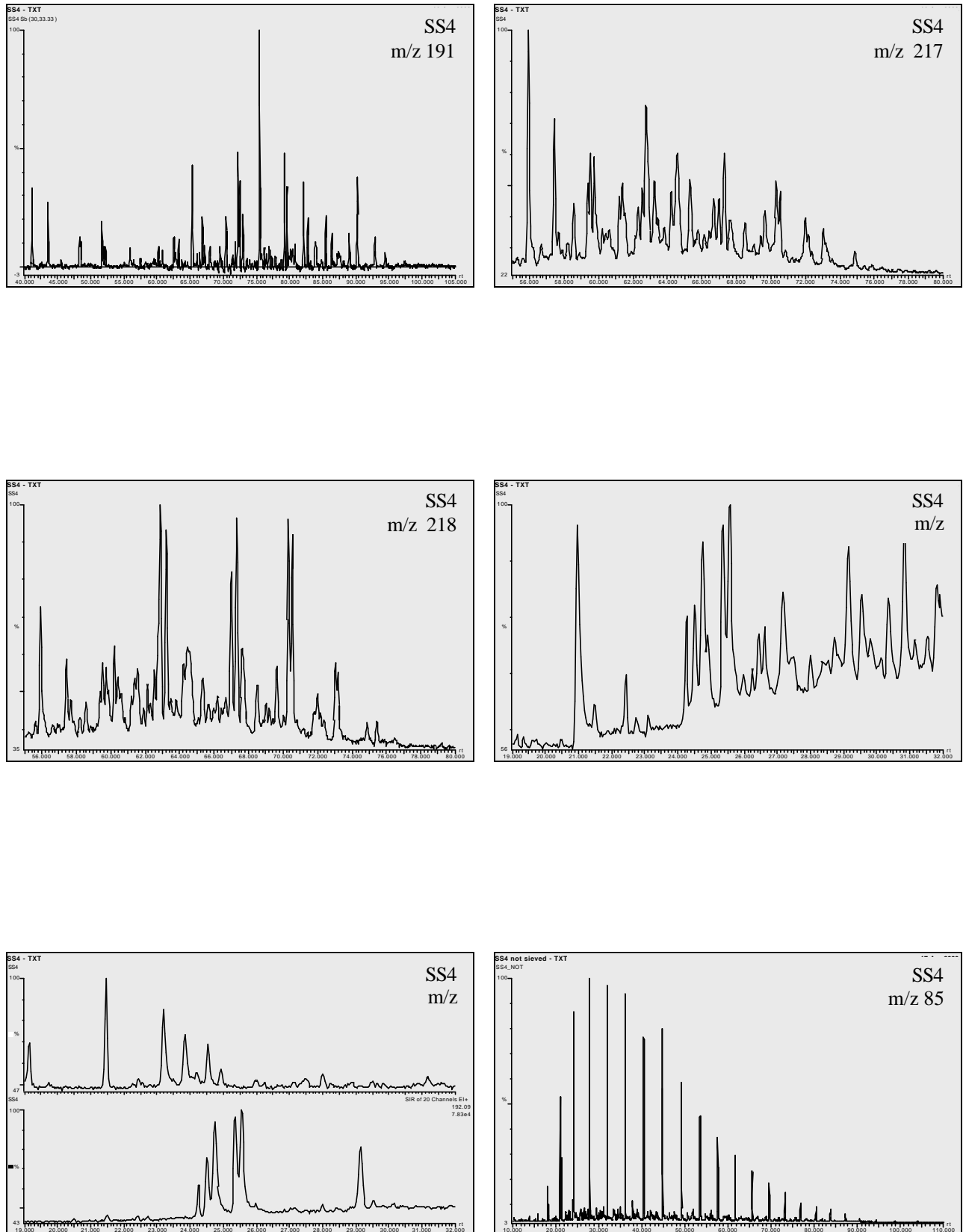


Figure 4.19. The GC-MS results for inclusion extract sample SS4 from the Smørbukk South Field.

4. Results

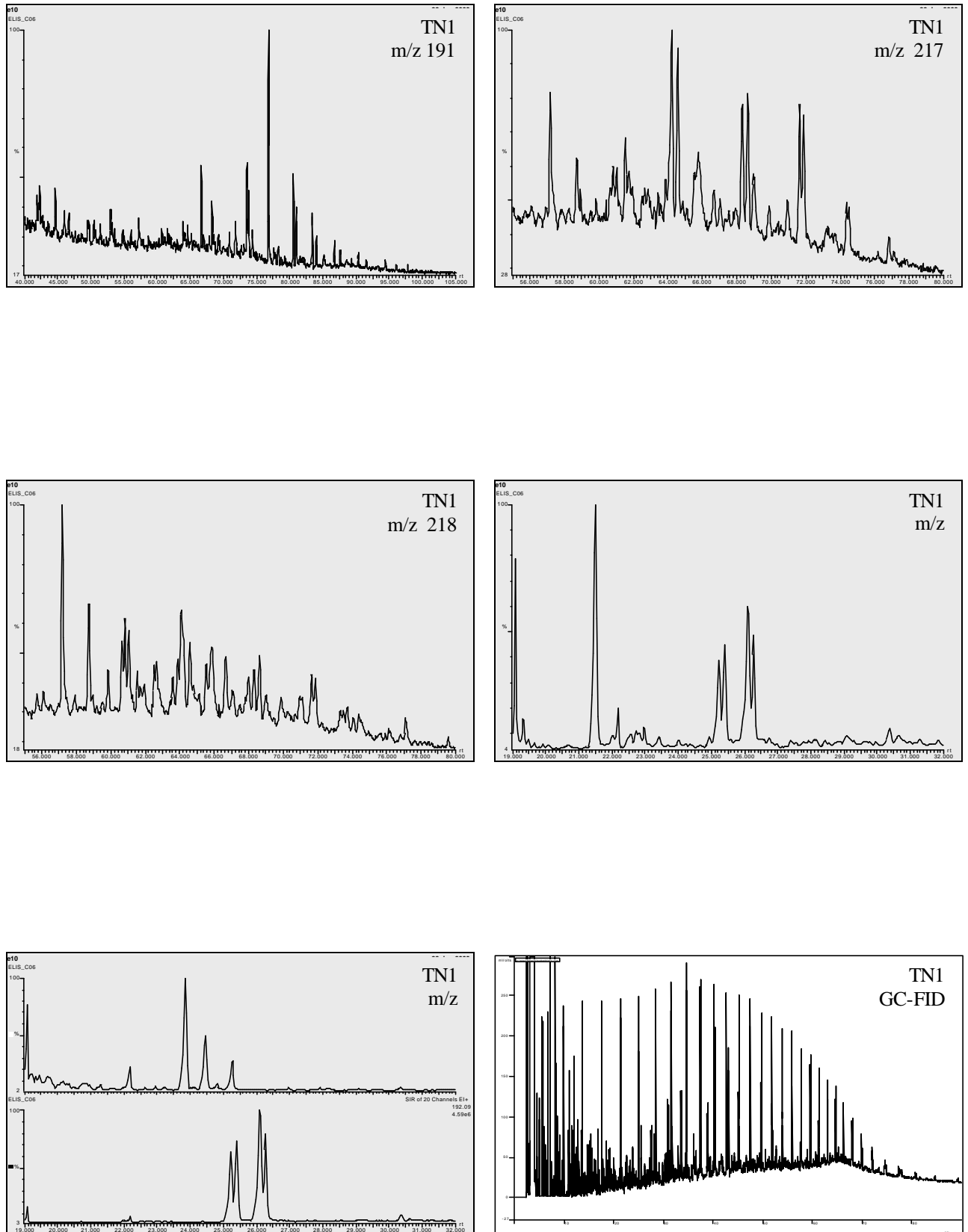


Figure 4.20. The GC-MS and GC-FID results for DST sample TN1 from the Tyrihans Field.

4. Results

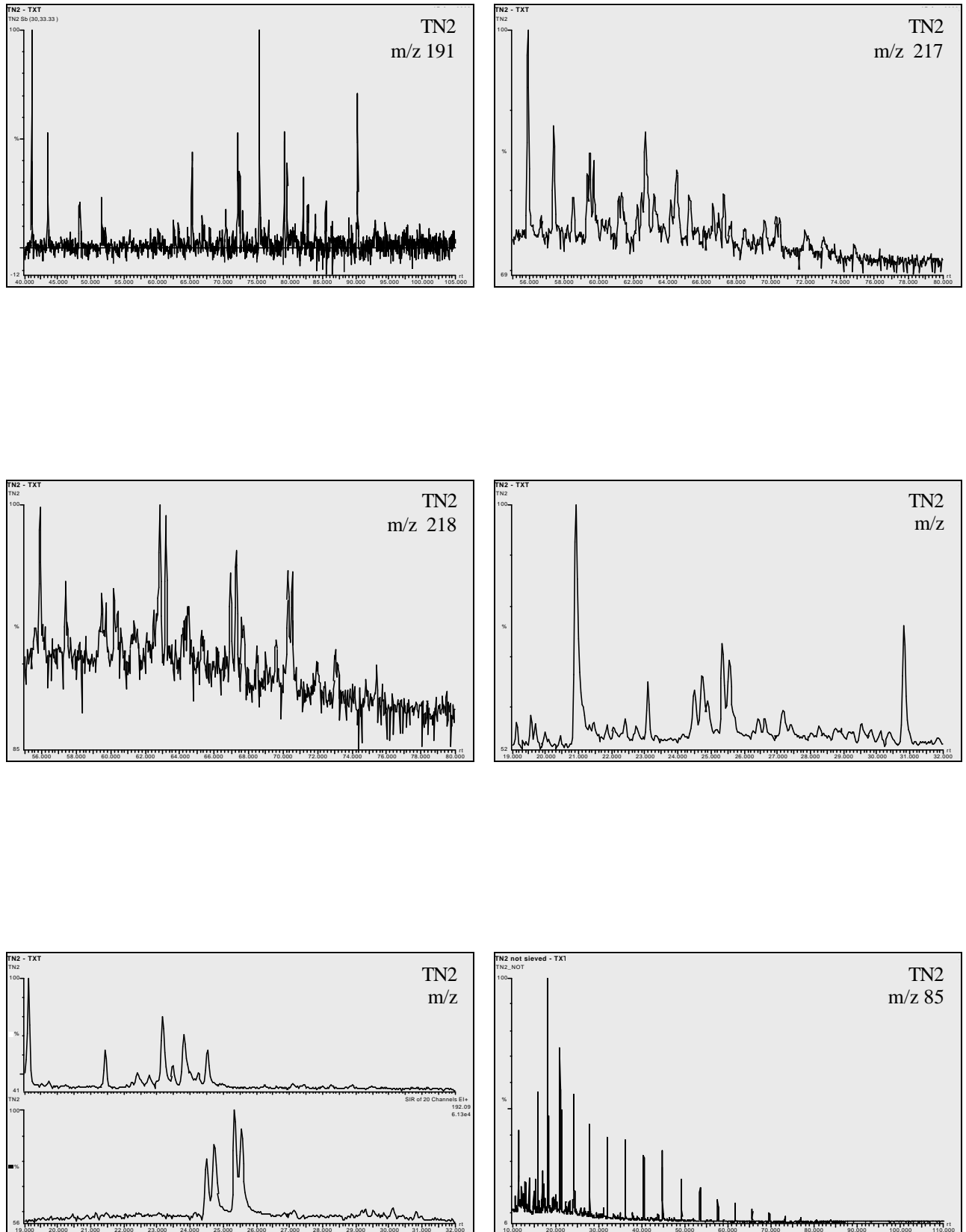


Figure 4.21. The GC-MS results for inclusion extract sample TN2 from the Tyrihans Field.

4. Results

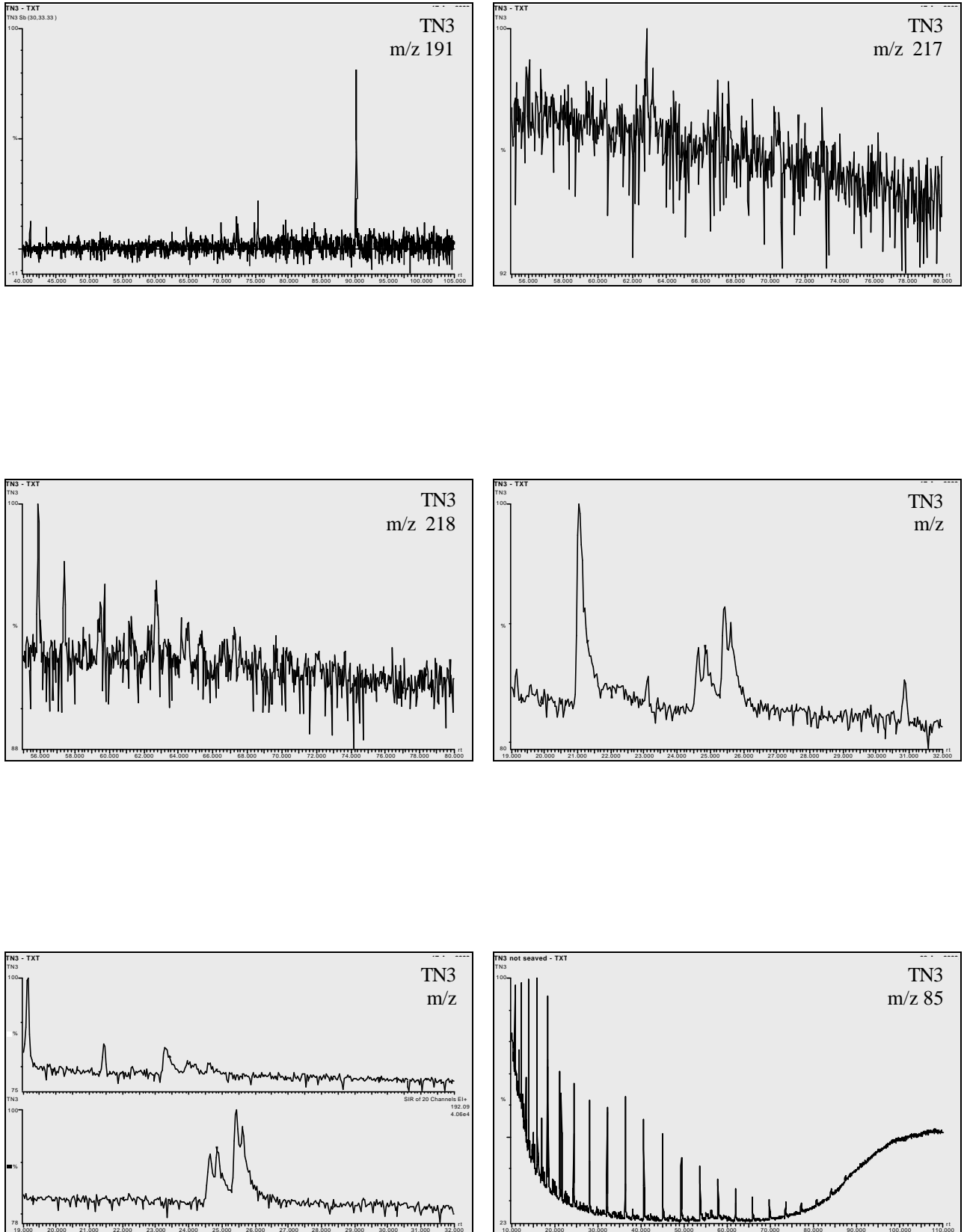


Figure 4.22. The GC-MS results for inclusion extract sample TN3 from the Tyrihans North Field.

4. Results

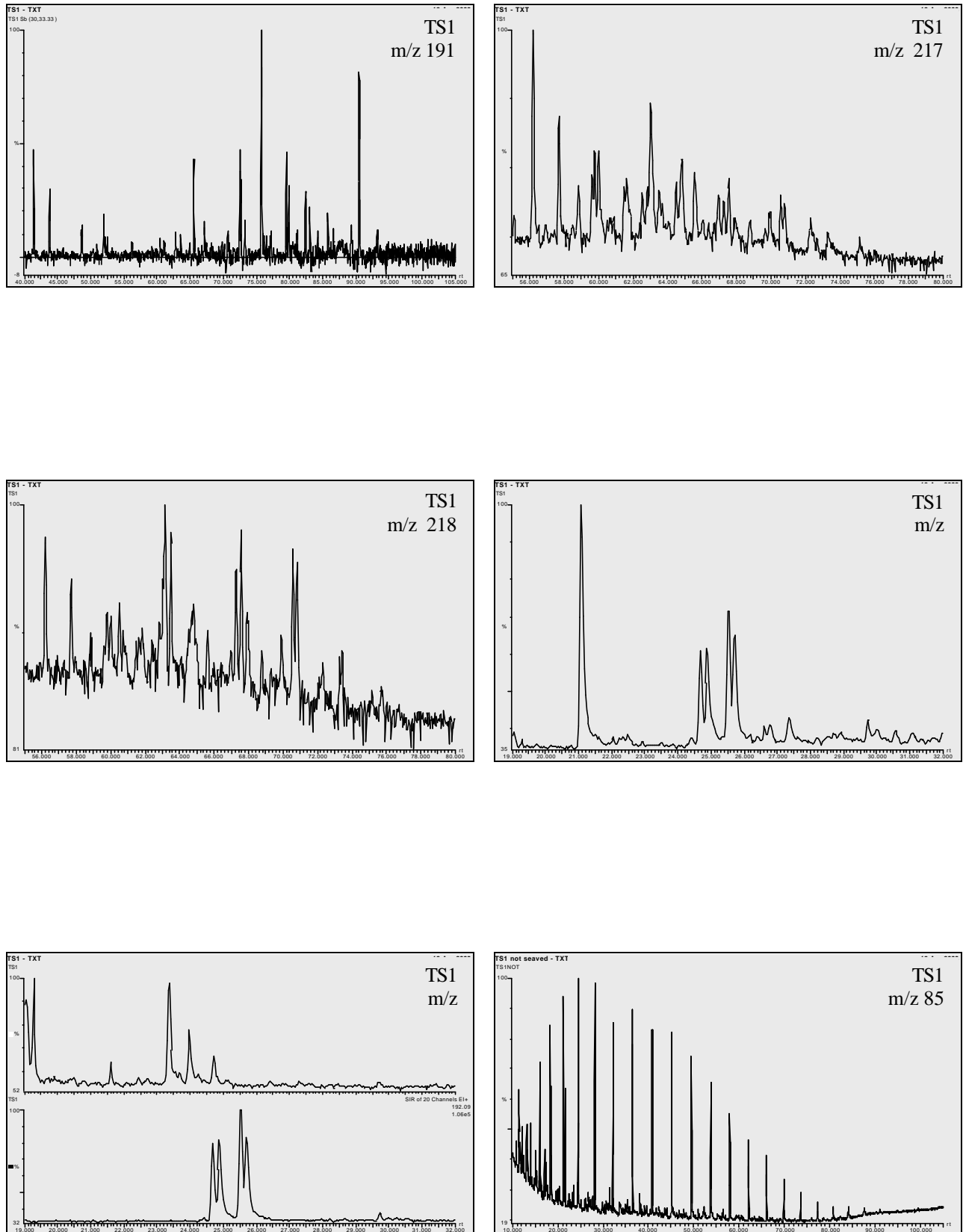


Figure 4.23. The GC-MS results for the inclusion extract sample TS1 from the Trestakk South Field.

4. Results

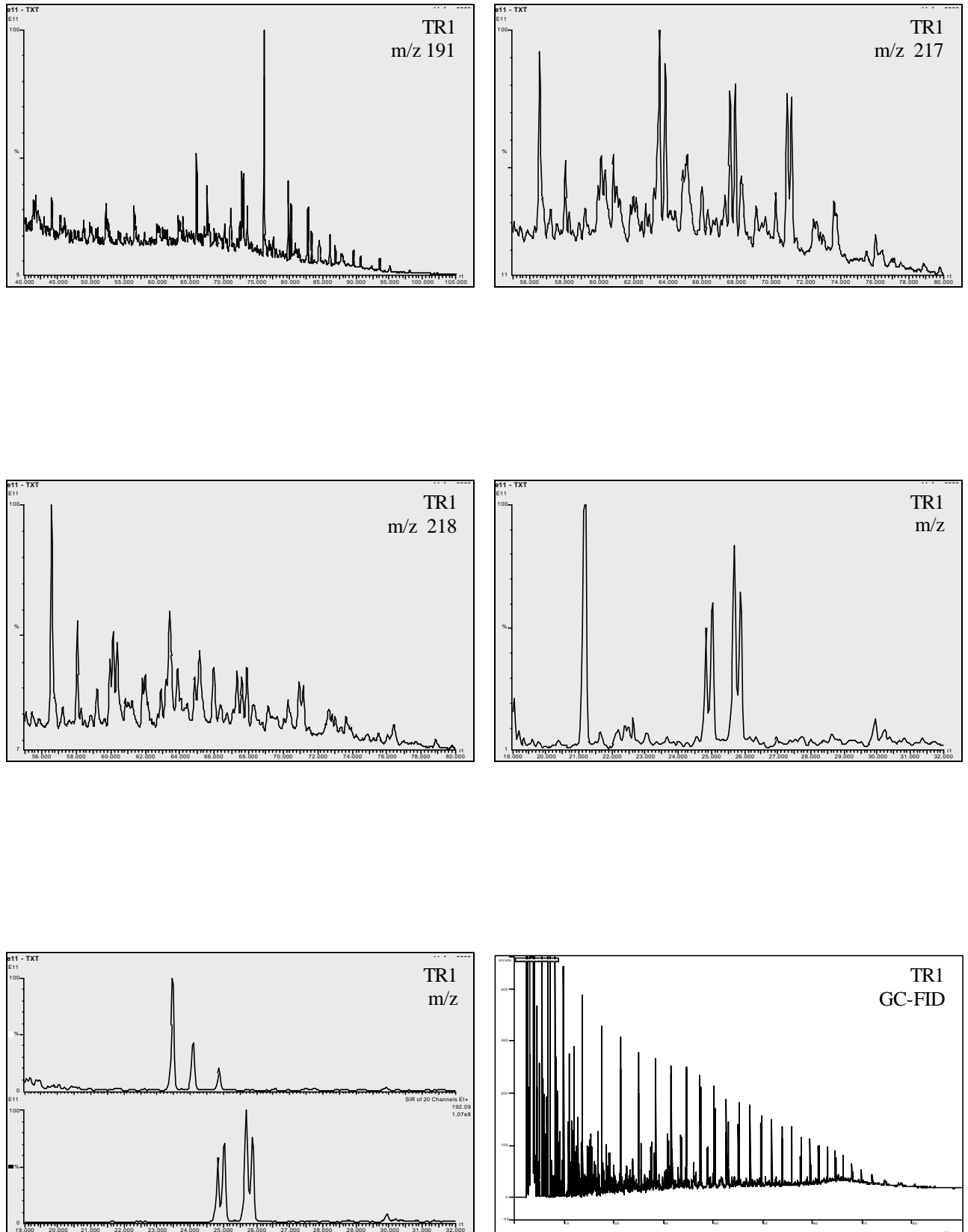


Figure 4.24. The GC-MS and GC-FID results for DST sample TR1 from the Trestakk North Field.

4. Results

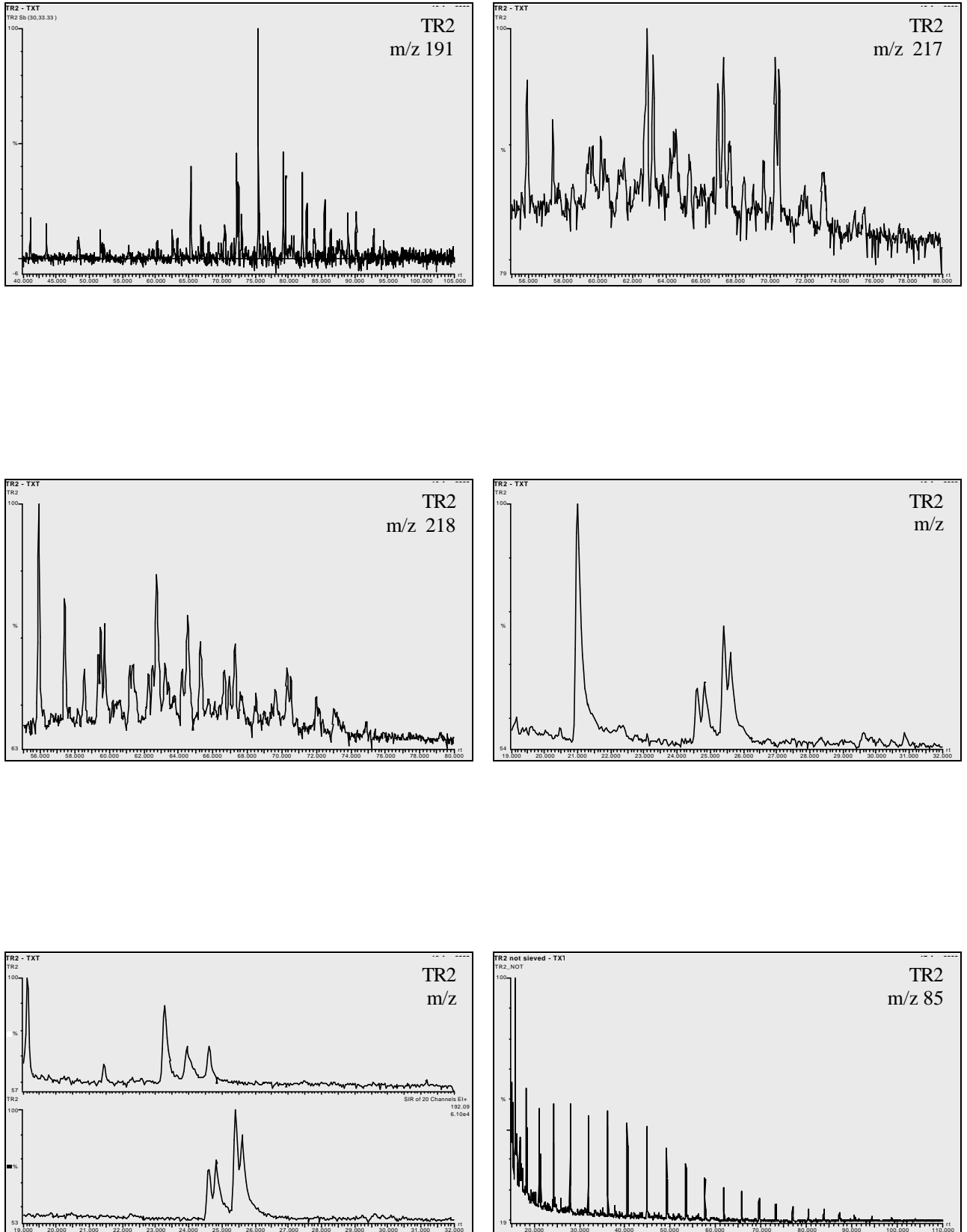


Figure 4.25. The GC-MS results for inclusion extract sample TR2 from the Trestakk North Field.

4. Results

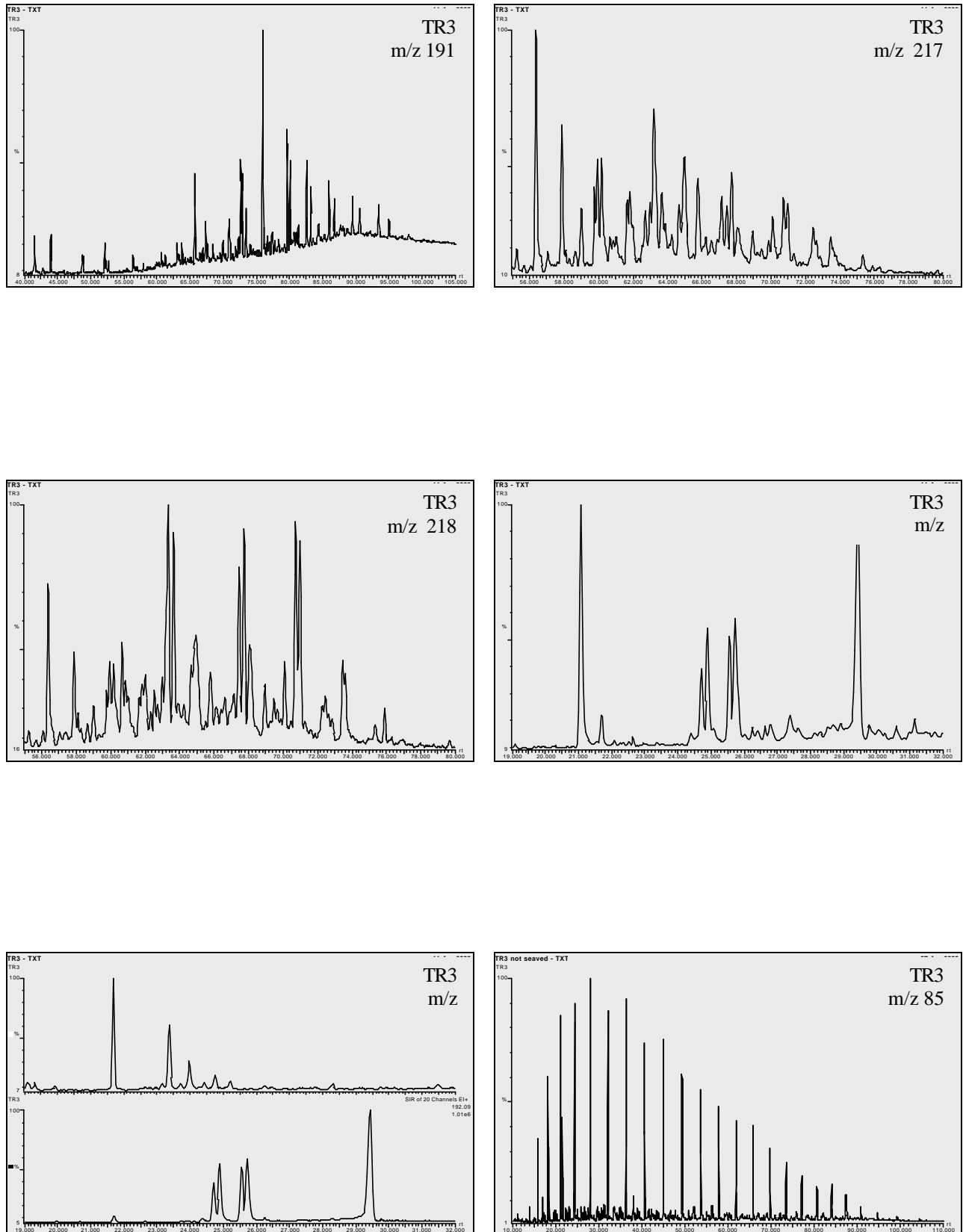


Figure 4.26. The GC-MS results for inclusion extract sample TR3 from the Trestakk North Field.

4. Results

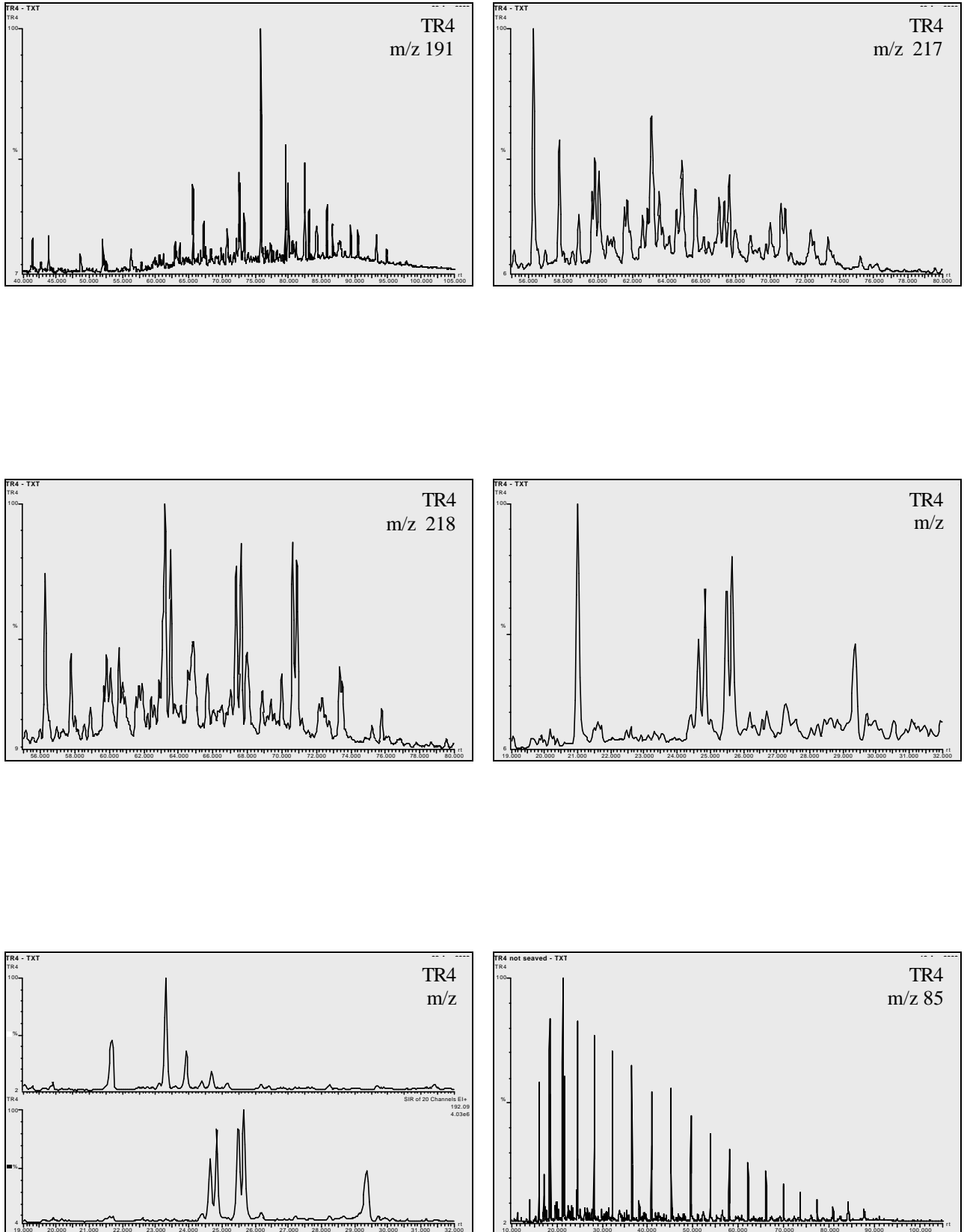


Figure 4.27. The GC-MS results for inclusion extract sample TR4 from the Trestakk North Field.

4. Results

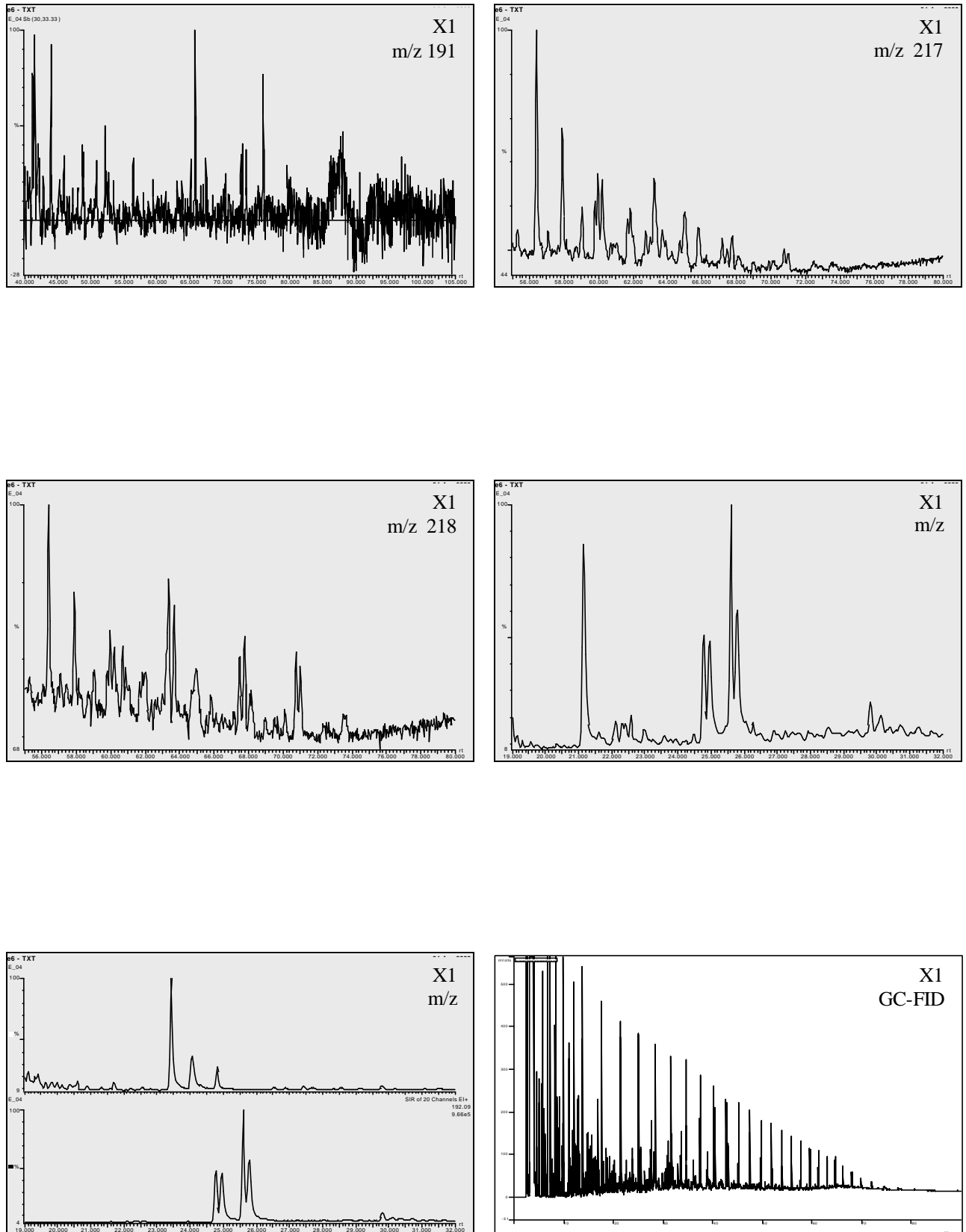


Figure 4.28. The GC-MS and GC-FID results for DST sample X1 from the well 6407/4-1.

4. Results

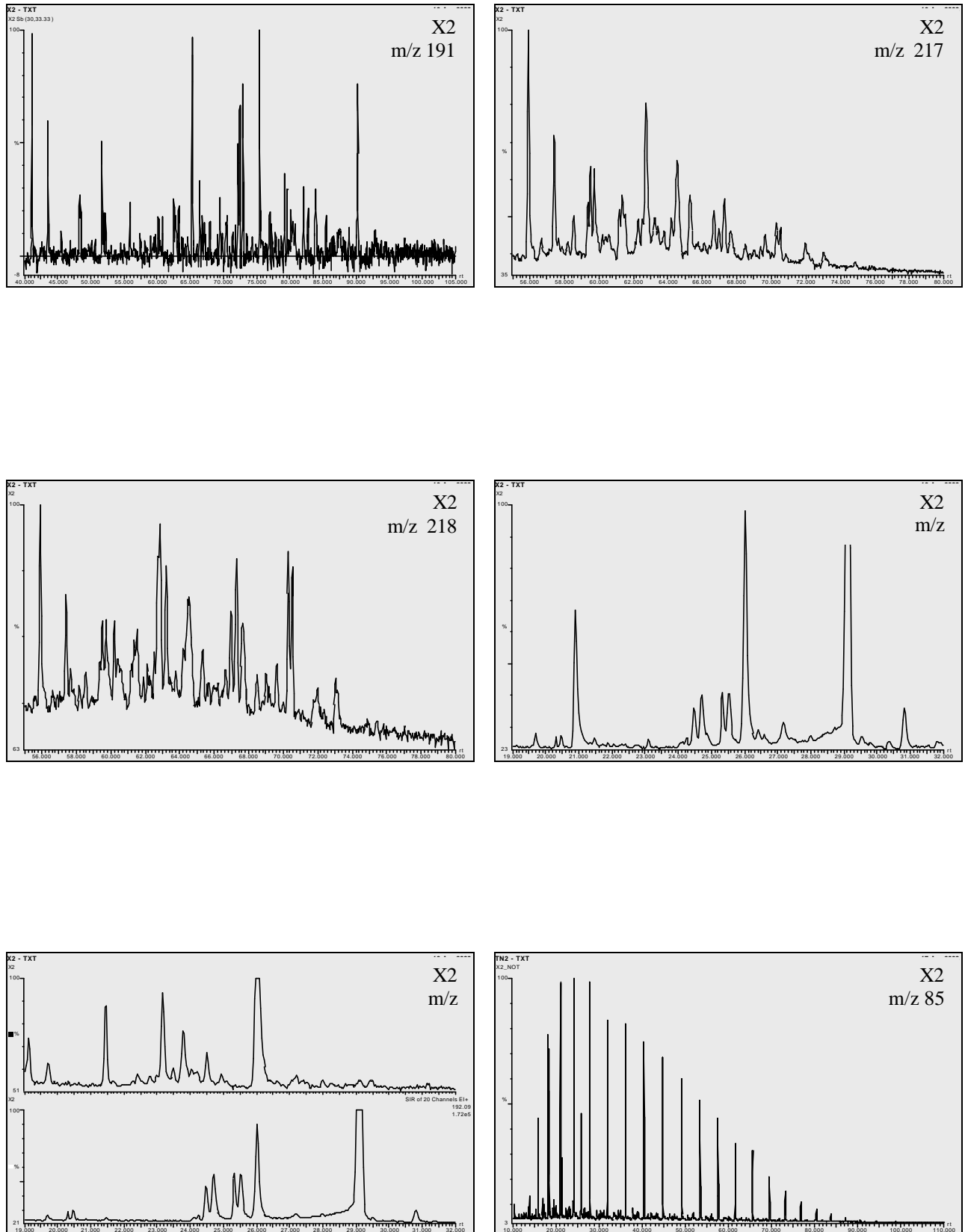


Figure 4.29. The GC-MS results for inclusion extract sample X2 from the well 6407/4-1.

4. Results

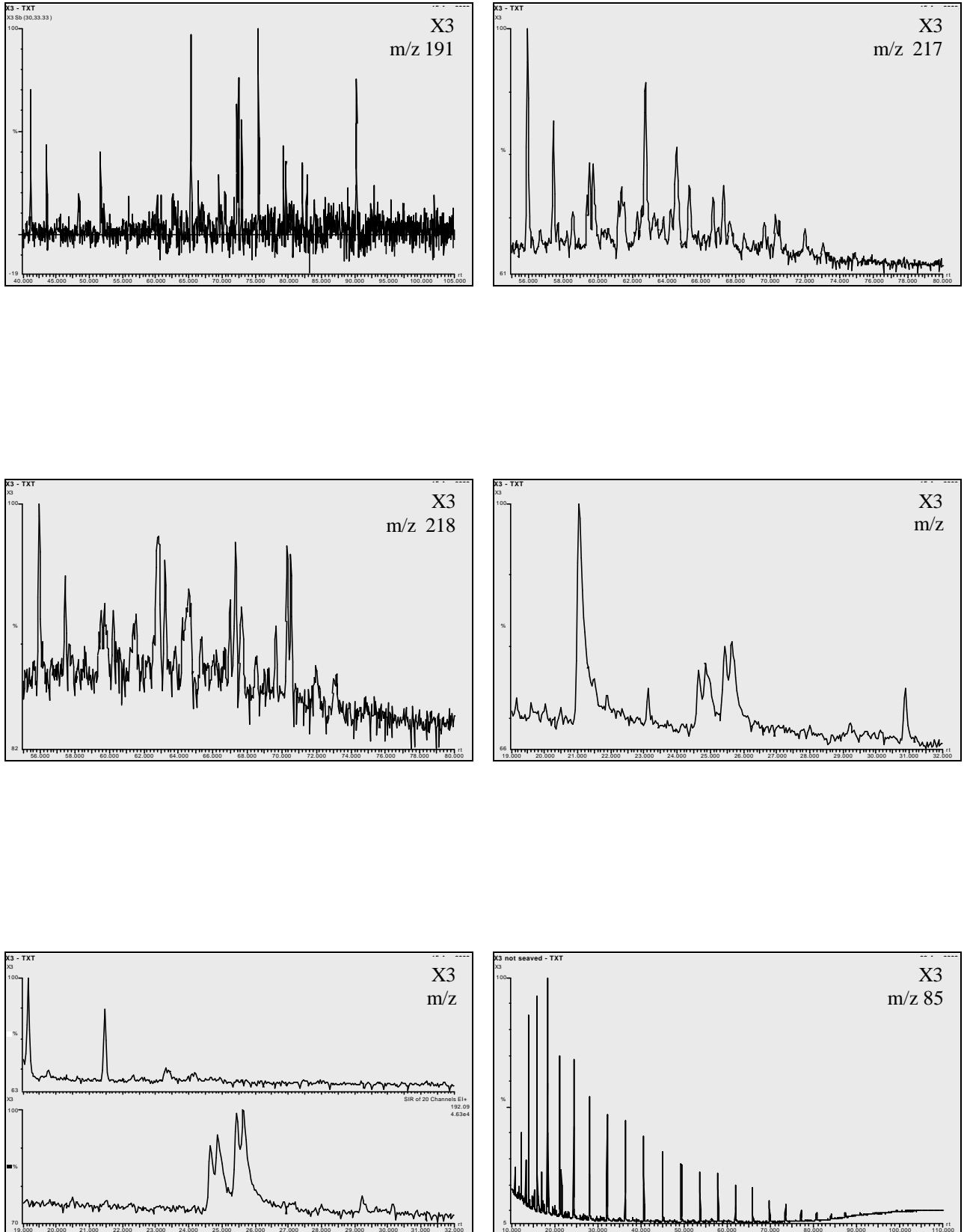


Figure 4.30. The GC-MS results for inclusion extract sample X3 from the well 6407/4-1.

4. Results

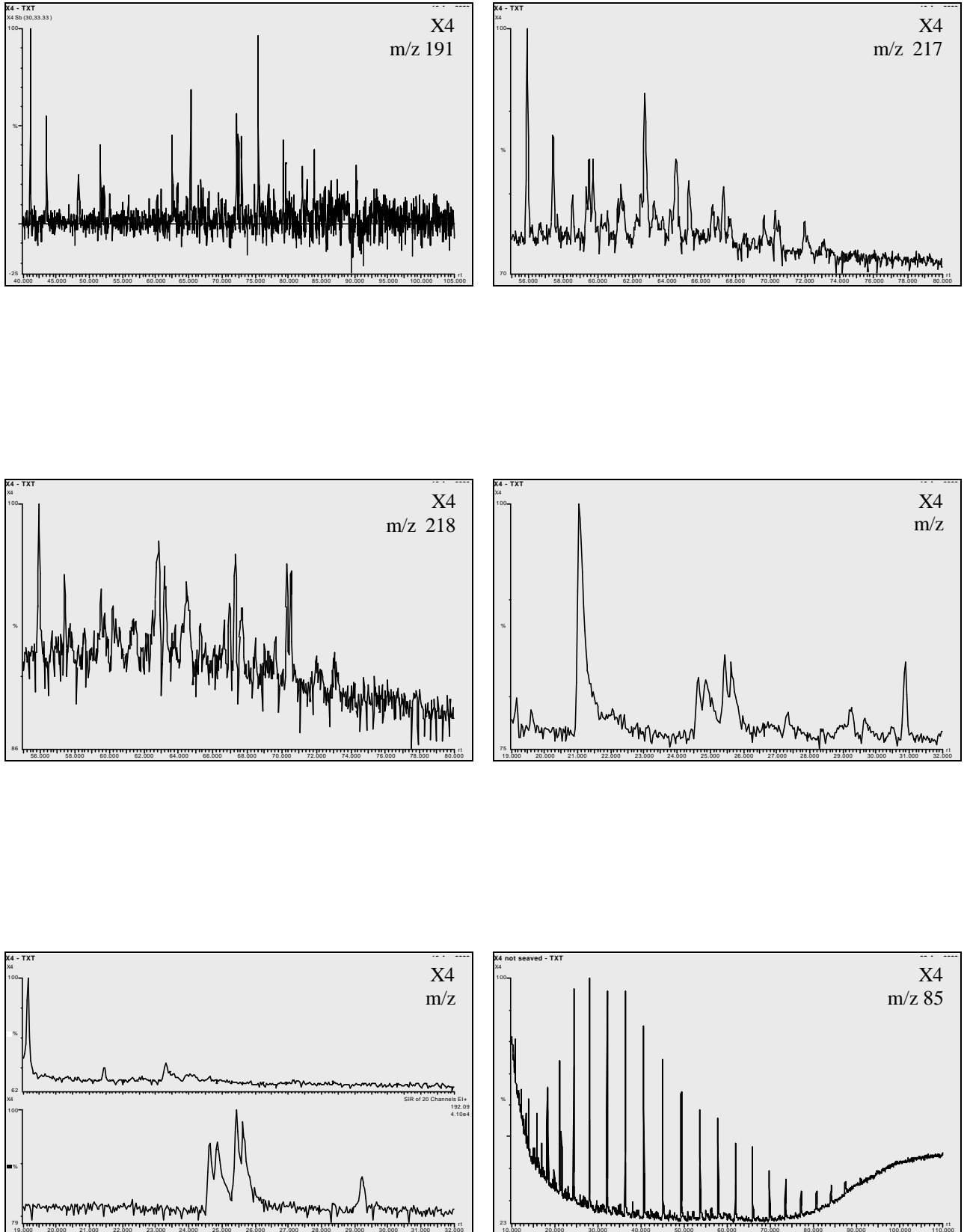


Figure 4.31. The GC-MS results for inclusion extract sample X4 from the well 6407/4-1.

4. Results

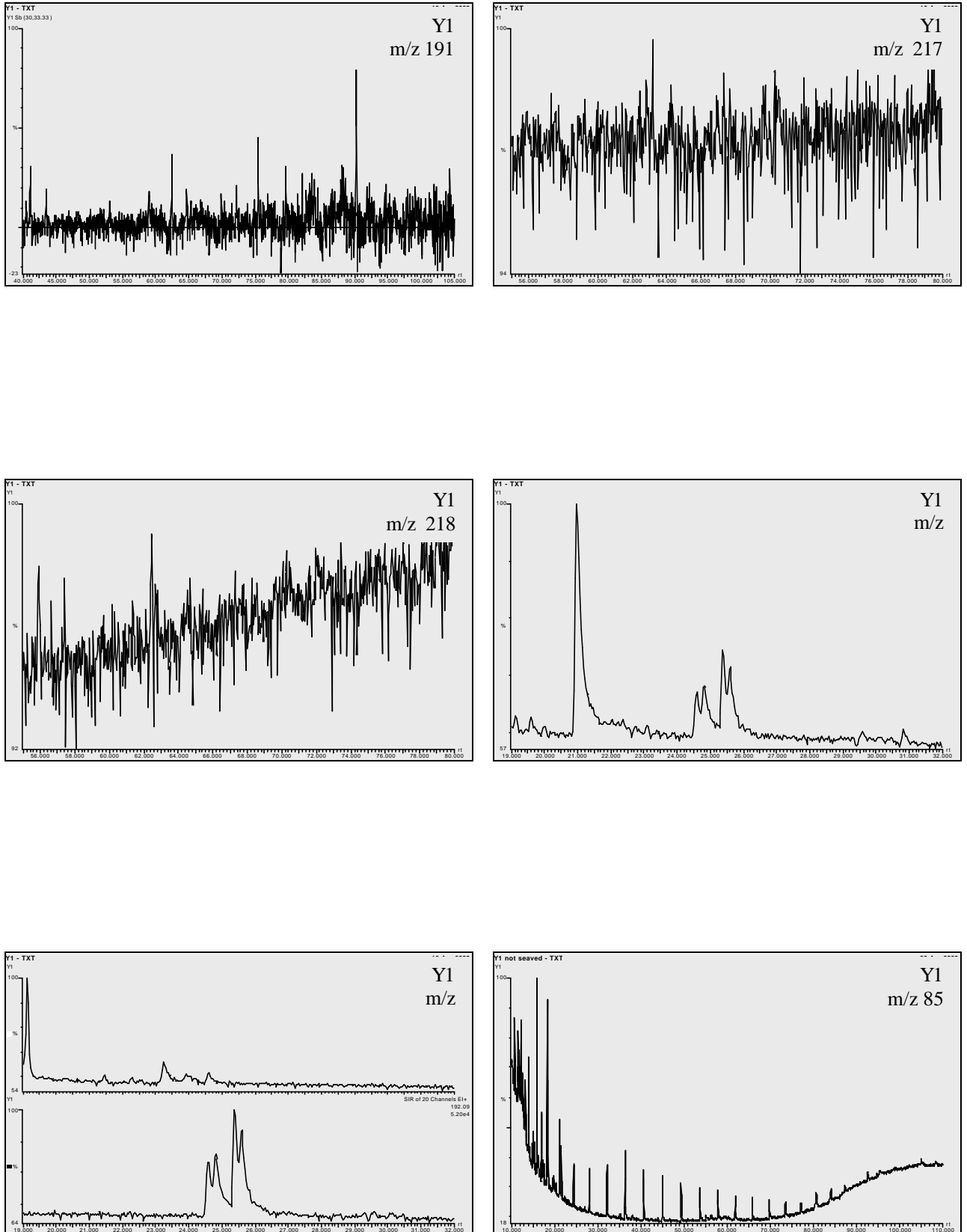


Figure 4.32. The GC-MS results for inclusion extract sample Y1 from the well 6407/10-1.

5. Discussion and conclusions

In the first section the limitations and problems within the sample set will be discussed. Then follows a short comparison between the oils/extracts and the inclusions based on results from the GC-MS analysis, finally all the fields are compared and the general trends within the Haltenbanken area is discussed.

- 5.1. Problems and limitations in the sample set
- 5.2. Biomarker parameters: inclusions versus oil/extract
- 5.3. Comparison between the fields in the Haltenbanken Area

5.1. Problems and limitations in the sample set

Comparing GC-MS and GC-FID traces, is it possible?

The GC-MS chromatogram $m/z = 85$ was used together with the GC-FID trace for comparing the pristane, phytane and n-alkane distribution between the oil/extract and inclusion samples. As the concentrations of alkanes are low in the inclusions extracts, the CPI, pr/ph, pr/n-C₁₇ and ph/n-C₁₈ ratios were determined from the GC-MS analysis due to the higher sensitivity of this technique. An increase in thermal maturity will create more n-alkanes due to cracking in the kerogen and the pristane/n-C₁₇ and phytane/n-C₁₈ ratios decrease (Tissot et al., 1971). However, isoprenoids have different response factors from n-alkanes on the GC-MS compared to GC-FID, and for this reason were correction factors applied. Even if the NSO standard was used to “calibrate” the difference between the two instruments, the samples from the GC-MS chromatogram consistently show higher maturities compared to the GC-FID trace (see figure 5.1 and 5.11.). For this reason these results will not be used to compare oil/core extracts and inclusions, but rather as a supplement when comparing oil-oil samples from the different fields.

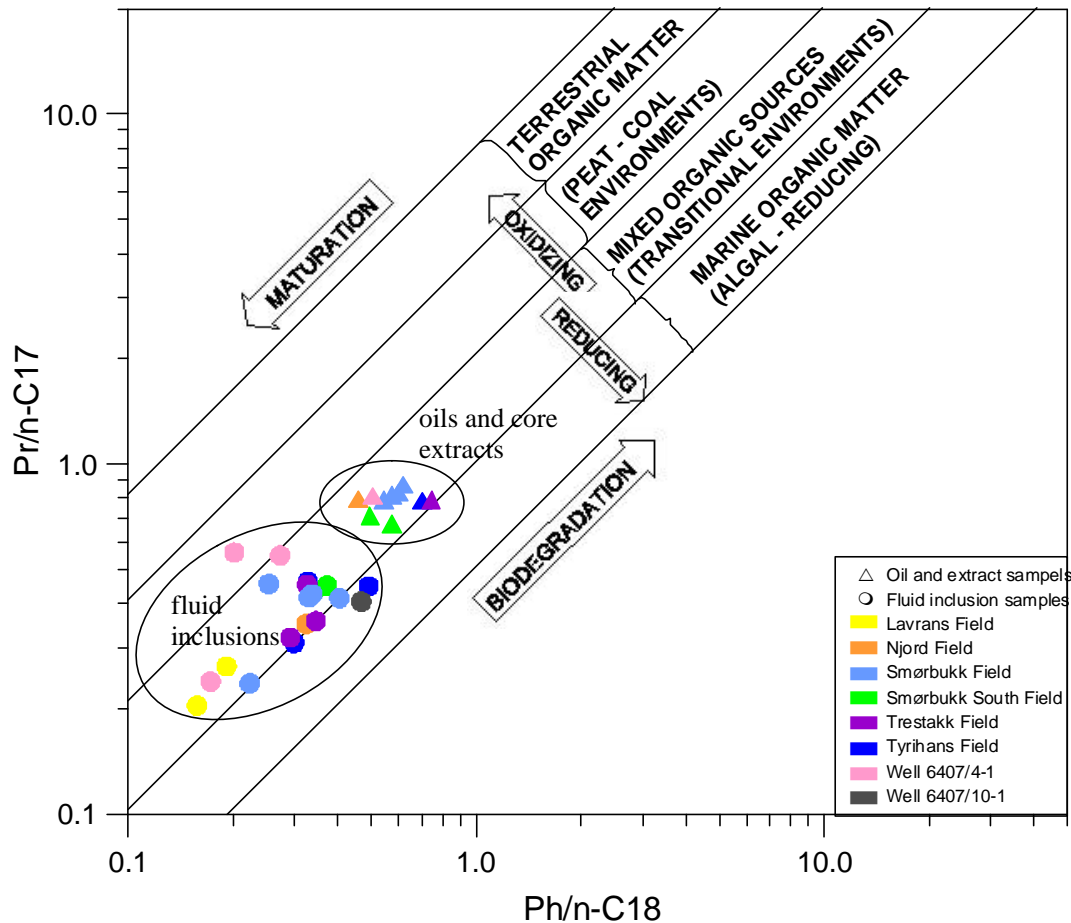


Figure 5.1. The pristane/n-C₁₇ versus phytane/n-C₁₈ ratios for the sample set (modified from Shanmugam, 1984). Note the higher maturity of the inclusion samples compared to the oil/core extract samples.

Low signal-to-noise ratios

Low biomarker concentrations lead on several occasions to low signal-to-noise ratios, precluding detailed biomarker analysis. The reason for a low biomarker concentration can be small amounts of petroleum inclusions or high maturities causing the transformation of biomarkers to have reached equilibrium. Peters and Moldowan (1993) stated that very low biomarker concentrations are typical of highly mature rock extracts, oils or condensates, where nearly all biomarkers have been destroyed.

In this sample set, inclusion samples from Njord (N2), Smørbukk (S2, S4, S6 and S7), Tyrihans North (TN3), Lavrans (L1) and well 6407/10-1 (Y1) have low signal-to-noise ratios or no signal at all. By examination in the microscope the poor signal can be explained by very small amounts of petroleum inclusions in the samples. The amount of inclusions in the samples range from 0 to 1-2 on a scale from 0-5 and such small amounts of inclusions can not readily be analysed for biomarkers. Another reason for the low signal-to-noise ratio may be the fact that some of the fields contain mature condensates. Other deep condensate traps have also been reported to contain small amounts of inclusions which is interesting since inclusion entrapment at 120°C is a relatively fast process (Walderhaug, 1994).

It is generally difficult to analyse aromatic hydrocarbons in inclusions because their concentration is always less than that of saturated hydrocarbons. Such was the case also in this study, and the chromatogram of $m/z = 231$ and $m/z = 253$ generally have much lower signal to noise ratios than did the steranes and hopanes in the same samples. These data are therefore omitted from the samples.

A question that also arises is how real the peaks are if the noise is high, can a noise peak interfere with a biomarker peak and generate an abnormal high value? An example is the tricyclic terpane peak V (chromatogram $m/z = 191$) in sample N2 (figure 4.9.), one of the peaks is extremely high compared to the other and this is very likely due to contamination.

5.2. Biomarker parameters: Inclusions versus reservoir oil/extract (south-north)**Njord field**

During catagenesis, the C_{27} 17a (H)-trisorhopane (Tm) show a lower relative stability than the C_{27} 18a (H)-trisorhopane (Ts) (Seifert and Moldowan, 1978) and thus the $Ts/(Ts + Tm)$ ratio will increase with increasing maturity. Used together with the $29Ts/(29Ts + \text{norhopane})$, where 29Ts will increase relative to norhopane during thermal maturation (Moldowan et al., 1991), and parameter 16 ($C_{20}/(C_{20} + C_{28})$) triaromatic steroids the results indicate the N1, oil sample to have a higher maturity than the N2, inclusion sample (see figure 5.2.). This is also illustrated in the chromatogram with an increase in the 29Ts peak compared to the norhopane peak from sample N2 to N1.

Medium range maturity parameters give information about the maturity of the petroleum in the range $C_{13} - C_{19}$. The amount of medium range molecules in petroleum vary from black oils, with moderate relative concentrations, to condensates, with high relative concentrations. The use of both biomarker and medium range maturity parameters give a better understanding of the maturity and history of the oil/condensate. Maturities calculated from the medium-range maturity parameters support that the oil sample has the highest maturity of the two samples, except from the MPR ratio and the related calculated vitrinite reflectance. These parameters do, however, not function well with type II derived petroleum at low to medium maturity.

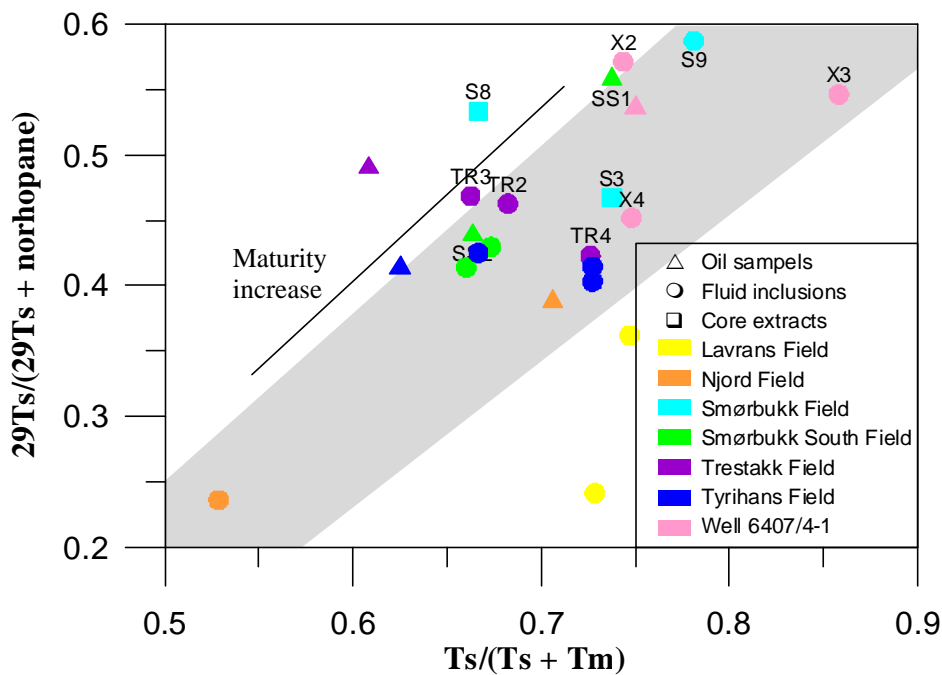


Figure 5.2. Maturity parameters $Ts/(Ts+Tm)$ and $29Ts/(29Ts + \text{norhopane})$ plotted together reflecting maturity differences within the sample set, there is an increase in maturity towards the top right. The grey field is the general trend displayed in Karlsen (2000).

A high amount of 28, 30 bisnorhopane in the samples, especially in the oil sample N1, is an indicator of anoxic conditions during deposition of the source rock (Peters and Moldowan, 1993). There have been several studies confirming this conclusion (Dahl and Speers, 1985: Horstad, 1989), but anoxic source rocks have also been reported containing no bisnorhopane and Waples and Machihara (1991) suggested its occurrence to be dependent upon a particular bacterial population or algal bloom. As seen in the ternary diagram in figure 5.3. the two samples plot close together in the estuarine area. But the validity of the ternary diagram from Shanmugan (1984) is debated, and interpretation of source rock and its facies based entirely on sterane distributions alone is not recommended (Moldowan et al., 1985: Horstad, 1989).

If the Njord samples are compared to the sample from the dry well 6407/10-1 (Y1) located just south of the actual field, the few biomarker maturity parameters calculated for Y1 show a closer resemblance to the oil than the inclusion sample. The medium range maturity

parameters indicate the inclusions in the dry well to be generated from a less mature source rock, with calculated vitrinite reflectance's ranging from 0.63 to 0.83 indicating that the oil has been expelled in the early stage of oil generation. The distribution of %C₂₇, %C₂₈ and %C₂₉ differ between the Njord samples and the sample from the dry well, the 6407/10-1 sample plots closer to open marine depositional environment (see figure 5.3.).

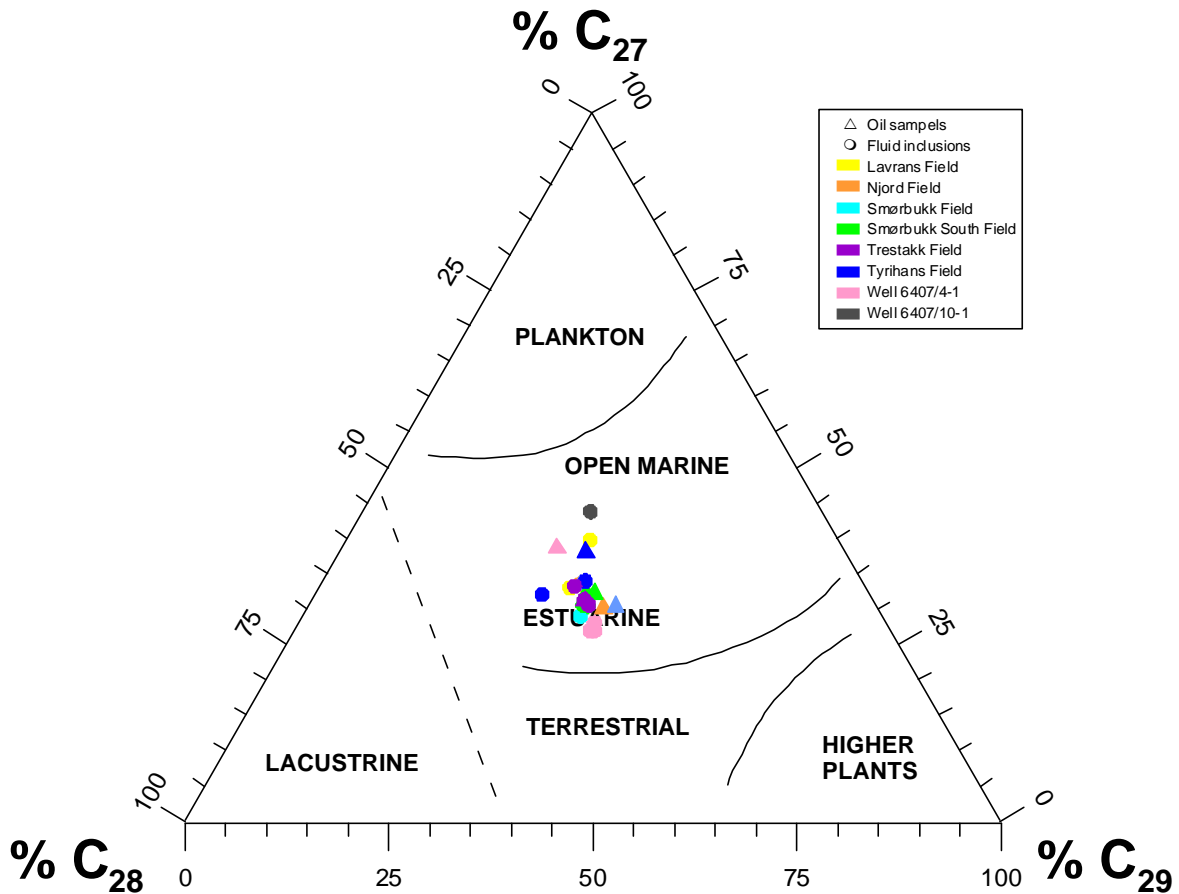


Figure 5.3. Ternary diagram after Shanmugan (1984), showing the relationship between the C₂₇, C₂₈ and C₂₉ $\beta\beta$ steranes from the Haltenbanken area, showing variation in depositional environment (facies). It is indicated that both inclusions and free petroleum in the traps was sourced from mainly the same source rock facies but at variable maturities.

The differences both within the field and with respect to the sample from the dry well are not sufficient enough to conclude concerning the possibility for different sources for the samples, but are more a result of the changes in facies within the source rock, maturity and different expulsion time. The results indicate anoxic type II shale as the source for the petroleum both in the trap and the inclusions.

Well 6407/4-1

Vitrinite reflectance calculated from methylphenantrenes and methyl dibenzothiophenes (table 4.3.) show that the petroleum in the petroleum inclusions in the three sand samples and the DST sample from well 6407/4-1 are close to peak oil generation as defined by Peters and Moldowan (1993). Inclusion sample X2 show a slightly higher biomarker maturity than the other samples, this maturity difference is also evident for the medium range maturity parameters. The biomarker maturity parameters show in general high maturity for all the samples, but vary with respect to which sample show the highest maturity. In the $m/z = 191$ chromatogram the 29Ts peak is in three of the samples (X1-X3) higher than the norhopane peak, a sign of high maturities (Moldowan et al., 1991). Also, the diahopane (hopane x) is much higher than the normoretane peak (D), which in some cases are difficult to separate from the background noise.

The fact that not all the maturity parameters conform with each other may be explained by different responses of the parameters to thermal stress or maturity in the source rock (Hughes et al., 1985), as well as mixing effects e.g., mixing a low maturity petroleum with higher biomarker concentrations (cf. Requejo, 1992) with a high maturity petroleum with lower biomarker concentrations (Karlsen et al., 1993).

The hopane/sterane and the bisnorhopane/(bisnorhopane + norhopane) parameters both have similar values for the four samples (figure 5.4.), and when the C_{27} , C_{28} and C_{29} steranes are plotted in a ternary diagram (figure 5.3.) the source rock facies is indicated to be estuarine to open marine. The inclusion samples plot towards the terrestrial area, while the oil is more towards the open marine depositional environment, indicating different facies.

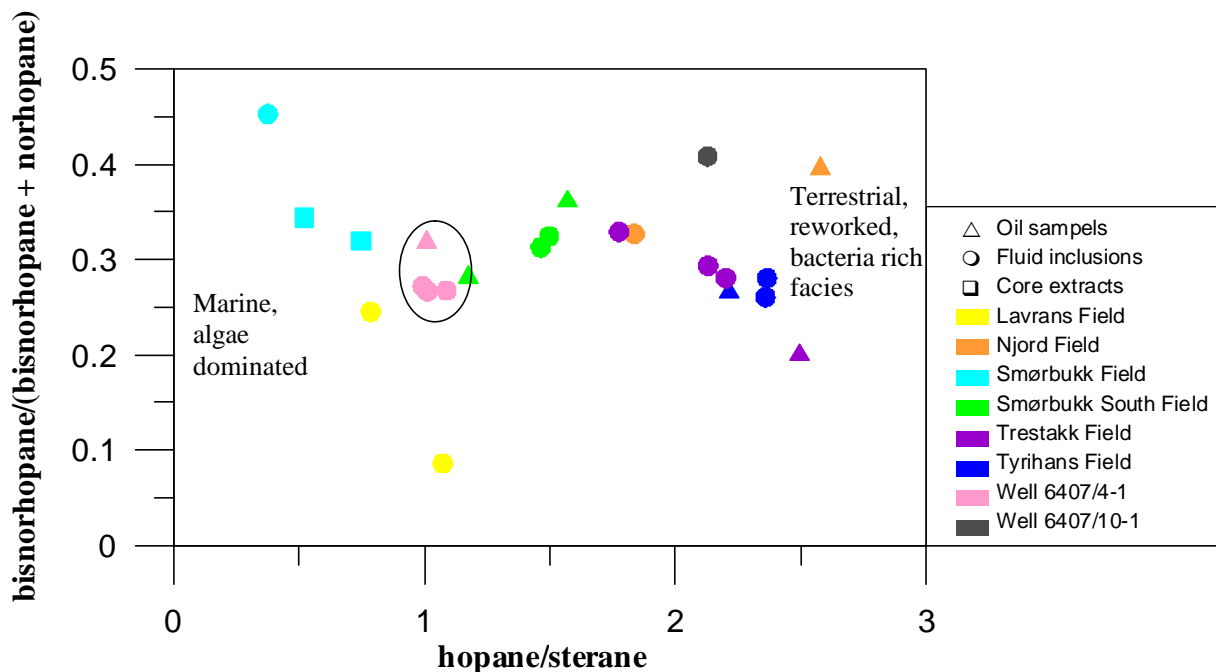


Figure 5.4. Cross plot of the facies parameters hopane/sterane versus bisnorhopane/(bisnorhopane+norhopane). Low hopane/sterane ratios indicate marine, algae dominated organic matter, while higher ratios point to other bacteria rich facies, bacterially reworked organic matter or a terrestrial input (Peters and Moldowan, 1993). The sample set shows a scattered pattern, but note that samples from the same field is grouped together, e.g. the samples from well 6407/4-1.

The slight difference in facies, but uniform maturity may be explained with petroleum being generated from a more distal part of the source rock. Occurring both with vertical and lateral movement of the source rock, causing another part of the source rock to reach the oil window, or oil is generated from a different source rock. In this case because of indications of genetic relationship it is most likely that the generated petroleum originates from the same source rock but there has been a shift to a more distal facies because of the subsidence in the Haltenbanken area (figure 5.5).

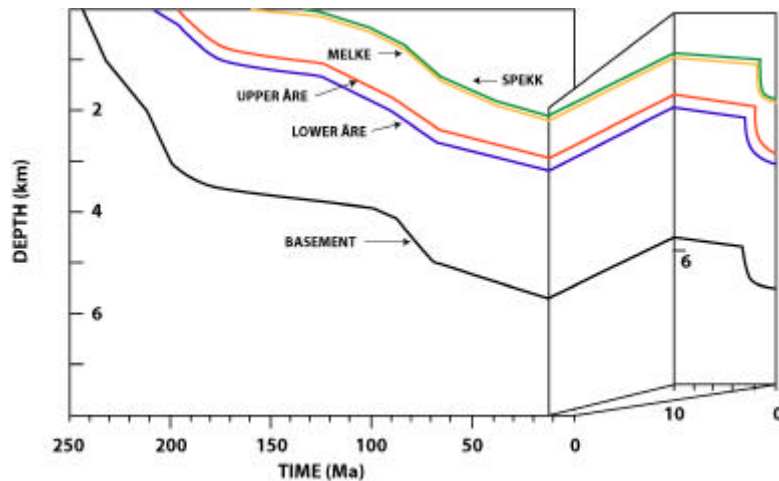


Figure 5.5. The subsidence rate calculated from well 6507/7-5 showing the higher rate of subsidence the last 2 Ma. There has been a progressively deeper burial towards the west in the Haltenbanken Area (Conoco Norway, 1986).

Tyrihans field

Sample TN2 and TN3 are from the same depth in the borehole and because of the small amount of inclusions (1-2 as seen in the microscope) in TN3, only sample TN2, which contain more inclusions will be used in the comparison with the other samples.

The Tyrihans North oil is the least mature in the sample set and the biomarker maturity parameters vary in which is the most mature, the inclusions or the oil (in figure 5.2. the inclusion samples are the most mature and in 5.6. the oil is the most mature of the samples).

However the calculated vitrinite reflectivities and the medium range maturity parameters indicate the oil sample to have a higher maturity than the inclusion samples. The higher amount of the more thermally stable 4-methyldibenzothiophene relative to 1-methyldibenzothiophene is also an indication of higher maturity in the oil sample. The inclusion sample from Tyrihans South (TS1) shows almost the same maturity as the oil, while the inclusion samples from the Garn formation in Tyrihans North show lower maturities.

The methyldibenzothiophene/phenanthrene ratio is by Radke et al. (2001) described as an excellent indicator of source rock lithology, shales have ratios < 1 and carbonates have ratios > 1 . This parameter also assesses the availability of reduced sulfur in the source rock, and

plotted together with the pristane/phytane ratio (figure 5.7.) can give valuable information about the different Eh-pH regimes of the sediments when deposited (paleodepositional environment). The MDBTs/MPs ratio for the samples in the Tyrihans North show relatively high values up to 0.52. This is well within the area of shaley facies, as are all the samples, but the Tyrihans samples contain a considerably higher amount of sulfur than the rest of the sample set. Compared to the Tyrihans South inclusion sample where the amount of sulfur is low (0.14) it is likely that the two traps received petroleum from slightly different organic facies within the shale source rock. The Tyrihans North petroleum being derived from a more sulfur rich facies, indicating less clay because this will generate the petroleum with the highest sulphur content (Welte et al., 1997).

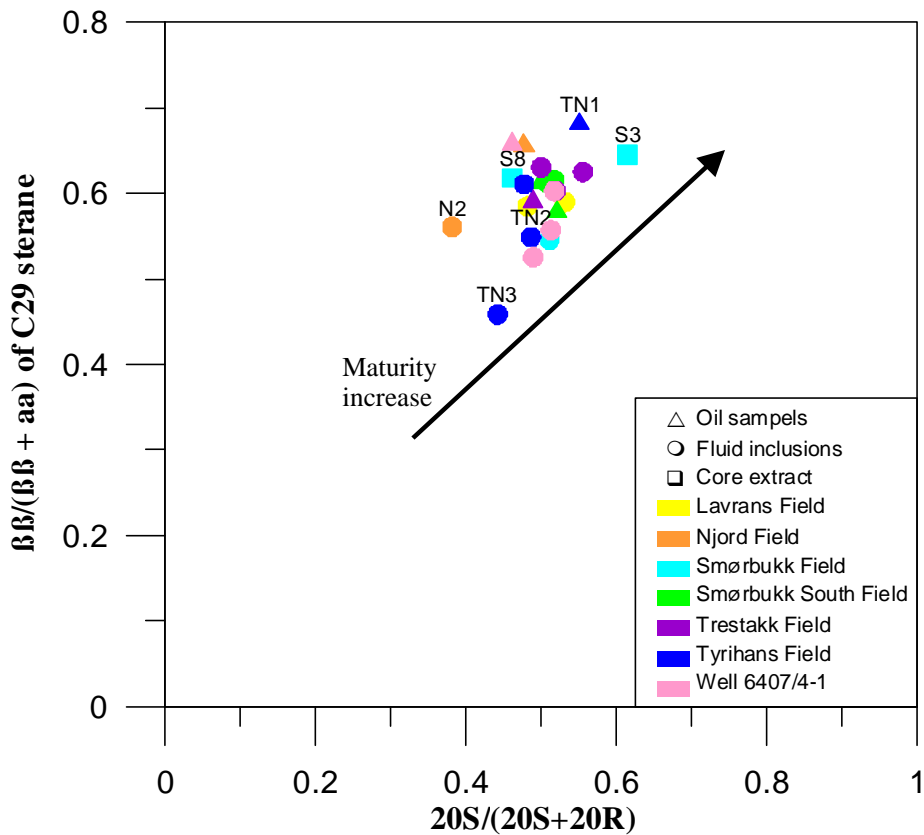


Figure 5.6. Both parameters plotted reflect maturity, the higher value – the higher maturity. The Tyrihans North inclusion sample, TN3, together with the inclusion sample from Njord show lower maturities than the other samples. The Tyrihans oil and the core extract from Smørbukk, Not formation show the highest maturities.

It is likely that the Tyrihans North structure received early generated petroleum with low maturity and that this is the petroleum observed in the inclusions. Later, both the Tyrihans North and South structure received a more mature petroleum (derived from slightly different facies), now found in the Tyrihans North reservoir and in the petroleum inclusions in the gas filled reservoir in the South structure.

Trestakk field

Genetic relationship between hydrocarbons can be indicated from different biomarker parameters. If the two biomarker parameter 10, $20S/(20S + 20R)$ of C_{29} $\alpha\alpha$ -sterane isomers and parameter 11, $\beta\beta/(\beta\beta+aa)$ of the C_{29} (20R + 20S) sterane isomer (Mackenzie et al., 1980), together with parameter 4, C_{30} -hopane/(C_{30} -hopane + C_{30} -moretane) show little variation, this is an indication of genetic related samples. The samples from Trestakk show uniform values between the oil and the inclusions. The oil sample show a slightly higher maturity than the

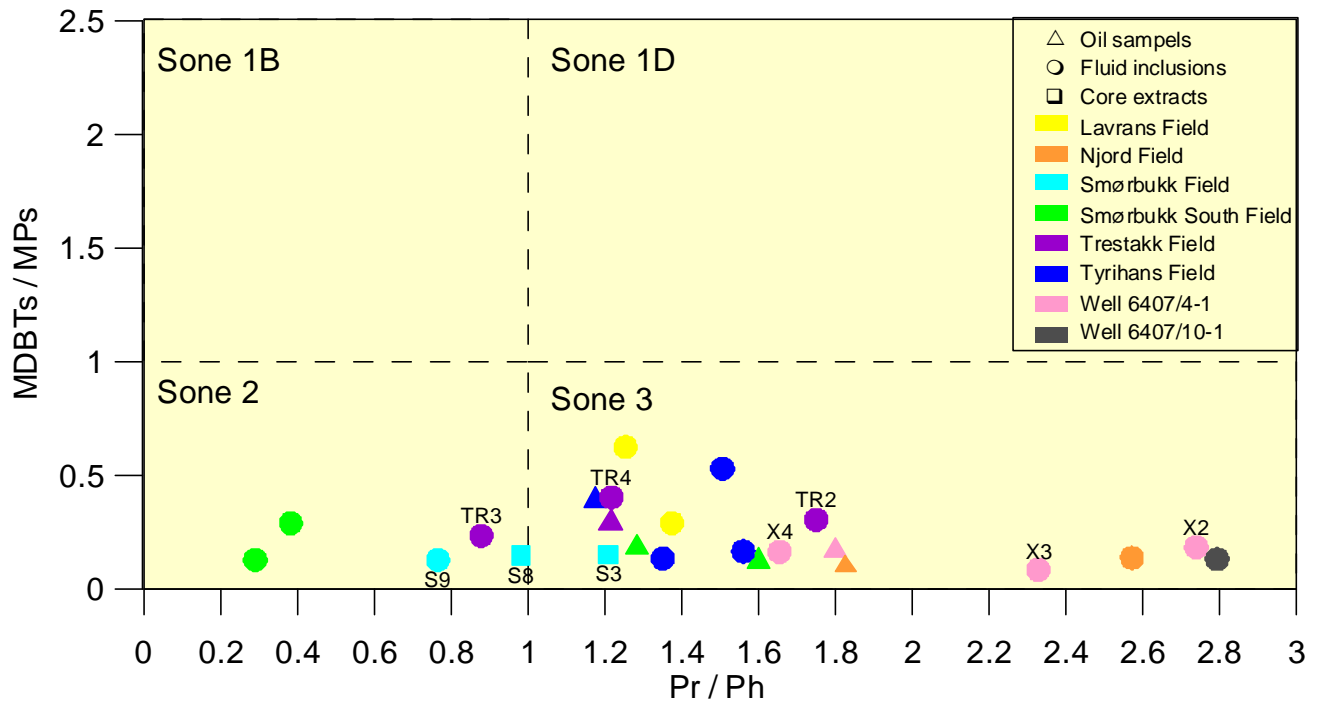


Figure 5.7. Cross-plot between methyl dibenzothiophene and methylphenanthrene against the pristane/phytane relationship indicating source rock facies (modified from Radke et al, 2001). Note that most of the samples are from a source rock deposited in marine and lacustrine environments.

Sone 1B - lacustrine sulphur-rich and marine deposits with different lithology, including marls.

Sone 1D - immature marine marls

Sone 2 - lacustrine sulphur-poor deposits with different lithology

Sone 3 - Marine and lacustrine deposits

inclusion samples in the biomarkers with a high 29Ts relative to norhopane, and several of the biomarker parameters show higher values for the oil sample than for the inclusion samples. The calculated vitrinite reflectivities and the medium range maturity parameters have a wider range with the deepest inclusion sample showing considerable lower maturities than the rest of the samples.

The facies parameters show small variations in the Trestakk samples and results indicate the petroleum to have been generated from a shaley deposit tentatively in an estuarine environment (see figure 5.3.).

From the results it is most likely to believe that the majority of the inclusions have been formed when the petroleum found today was present in the trap, but at an earlier stage. During

burial of the source rock a more mature petroleum is expelled and mixed with the oil already in the reservoir, causing the oil to have a slightly higher maturity than the inclusions.

Smørbukk South Field

The samples from the Smørbukk South field are taken from three different formations, but despite this the parameters describing genetic relationship is uniform, indicating the same source rock for the petroleum in the Lysing, Garn and Tilje formations. Furthermore, the biomarker maturity parameters show little variation between the samples. But the calculated vitrinite reflectivity and the medium range maturity parameters show a more diverse picture. The oil trapped in the Tilje formation (SS1) show lower maturities than the rest of the samples with vitrinite reflectivities from 0.5 to 0.98. According to Peters and Moldowan (1993) the oil generated before the vitrinite reflectivity reaches 0.6 is immature, but the other results indicate the petroleum in Tilje (SS1) to be more mature than the other samples (see figure 5.2. and 5.9.).

The facies parameters show little variation in value between the samples, the presence of 28, 30 bisnorhopane and hopane/sterane ratios between 1.17 and 1.57 (normal Kimmeridge Clay, the North Sea equivalent to Spekk, have hopane/sterane values at typically ~2), together with the ternary plot (figure 5.3.) imply the petroleum to be generated from a marine shale.

Smørbukk field

Because of poor results from the GC-MS analysis on several of the extract and inclusion samples from the Smørbukk field, only three samples (two extracts and one inclusion) are discussed here concerning biomarker parameters. However, since all the extracts have been analysed on the Iatroscan instrument these results will be more thoroughly discussed.

Generation of extractable hydrocarbons during burial produces more saturated hydrocarbons than aromatic hydrocarbons. This results in an increase in the saturated versus aromatic hydrocarbons ratio (S/A) with higher maturities (Philippi, 1965: Tissot et al., 1971: Albrecht et al., 1976). The four core extracts, derived from four different sandstone formations show large variations in the S/A ratio. The deepest sample from the main reservoir unit the Tilje formation shows the highest ratio, while the sample from the above lying Tofte formation has the lowest ratio. This large difference would imply a much higher maturity in the Tilje sample, this is substantiated by the GC-FID results. Figure 4.1. illustrates the increase in maturity from Garn → Not → Tofte → Tilje.

The samples analysed on the GC-MS are from Tilje (S8, core and S9, inclusion) and Garn (S3, core). The 29Ts/(29Ts+norhopane) ratio and the diasteranes/(diasteranes + regular steranes) ratio have working ranges up to 1.0 VRE% (van Graas, 1990) and can reveal maturity differences between the samples. From the cross-plot in figure 5.8. it is given that the core and inclusion sample from Tilje show generally a higher maturity than the core extract from Not. Also the much higher content of tri- and tetracyclic terpanes to hopanes in the Tilje samples indicates higher maturities. Because the tri- and tetracyclic terpanes are more resistant to maturity than the C₃₀ hopane (Peters and Moldowan, 1993) it is thought that a more extensive degradation of the C₃₀-hopane due to high maturities will cause large variation

in the tricyclic terpanes/C₃₀-hopanes and tetracyclic terpanes/C₃₀-hopanes ratios seen in the Smørbukk samples.

There are little variations between the facies parameters, but the Not sample is indicated to be derived from a slightly more sulphur rich source (figure 5.7.), but all samples are generated from a marine source rock.

From the data it is given that the petroleum trapped in the Tilje formation has a higher maturity than the others. There are only small variations between the inclusion and the core extract and it is likely to believe that the fluid inclusions was formed when the sandstone was filled with the petroleum now extracted from the core.

The Lavrans field south of Smørbukk show considerably lower biomarker maturities in the two inclusion samples taken from the Garn formation than Smørbukk and the rest of the sample set. This can in general be explained by the diagenetic history (Bang, 1998) which involved early concentric quartz overgrowth followed by oil migration and chlorite overgrowth before the last phase of hydrocarbon migration. The result is lack of inclusions containing the latest and most mature petroleum.

5.3. Comparing the fields

5.3.1. Maturity

Medium range maturity parameters

The n-alkane distribution changes as a result of the maturity of the source rock, and this is often reflected by the CPI ratio (Philippi, 1965; Peters and Moldowan, 1993) in particular for low to medium maturity oils. The GC-FID traces of the samples show a light-end-biased to “normal North Sea extract” pattern. Because of the difficulties comparing GC-FID and GC-MS chromatogram m/z = 85 traces (described in chapter 5.1.) oil and extract samples will be discussed separate from the inclusion samples concerning the medium range parameters.

Based on the pr/n-C₁₇ and ph/n-C₁₈ ratios (cross-plotted in figure 5.1. and 5.11.) the oil and extract samples can be arranged into a sequence based on maturity. The highest maturity in the oils is found in the Njord and Smørbukk South samples, followed by the sample X1 from 6407/4-1, Smørbukk core extracts and the least mature samples are found in Tyrihans and Trestakk.

Maturities in the inclusion samples show a slightly different pattern. Lavrans has the highest maturity (no oil sample in this study) → 6407/4-1 → Smørbukk → Njord, Trestakk and to the least mature samples in Tyrihans and Smørbukk South.

The pristane/phytane ratio can be used as a maturity indicator, with increasing thermal maturity the ratio will increase (Alexander et al., 1981). But caution should be taken when

applying this ratio because both diagenetic processes and facies may affect it. For the oil and core extract samples the pr/ph ratio indicate high values in Njord and 6407/4-1, followed by the rest of the samples (see figure 5.1., 5.11. and table 4.2.). The samples from the dry well 6407/10-1, together with 6407/4-1 and Njord show the highest values for the inclusions. Because of the effect the depositional environment has on the pr/ph ratio, the high values may also indicate a different source rock or facies.

CPI values for the sample set mainly vary between 0.88 and 1.2 indicating high maturities (Bray and Evans, 1965). Five of the samples differ from the rest of the sample set. The two Lavrans inclusion samples and the inclusion sample from Tilje (S7) in the Smørbukk field have an odd predominance with values between 1.28 and 1.55, while the Smørbukk inclusion samples from Garn and Not have values at 0.74 and 0.78 respectively, indicating even predominance.

Biomarker maturity parameters

Long chained biomarkers constitute the heavier part of the petroleum. These maturity indicators can in some cases show contrasting maturities compared to the medium range parameters.

The $20S/(20s+20R)$ ratio of steranes reaches equilibrium at 0.5-0.55 (Seifert and Moldowan, 1986), corresponding to a vitrinite reflectance value of about 0.8%. At these maturities peak oil generation have been reached or surpassed. All the samples, except the inclusion sample from Njord have reached this equilibrium. The maturity parameter $22S/(22S+22R)$ for hopanes is valid for maturities ranging up to early oil generation ($R_o=0.6\%$), and the ratio has an equilibrium ranging from 0.57 to 0.62 (Seifert and Moldowan, 1986). The values of the samples in the data set are close to equilibrium, except for the Smørbukk core sample from Not (S3) and the inclusion sample from Tilje (S9), and the inclusion sample from Njord (N1). Both these two parameters indicate maturities at peak oil generation for the whole sample set (see figure 5.8.), except for the inclusion samples from Njord and Smørbukk (S9), which have a lower maturity because of trapping of a less mature oil.

$22S/(22S+22R) < 0.6$ is mainly due to in-situ generated material, typically non migrated.

The maturity difference within the data set is illustrated by the cross-plot of the ratios $29Ts/(29Ts+norhopane)$ and $diasterane/(diasterane+regular\ sterane)$ in figure 5.9. As seen from the figure the oil samples from each field is more mature than the inclusion samples. The maturity trend from the oils indicate 6407/4-1 to be the most mature, followed by Smørbukk South, Smørbukk and Trestakk → Tyrihans North, and the least mature sample is from Njord. Maturity in the inclusion samples show a wider variety with a trend from the most mature to the least mature; 6407/4-1, Smørbukk → Trestakk → Tyrihans, Smørbukk South → Lavrans → Njord.

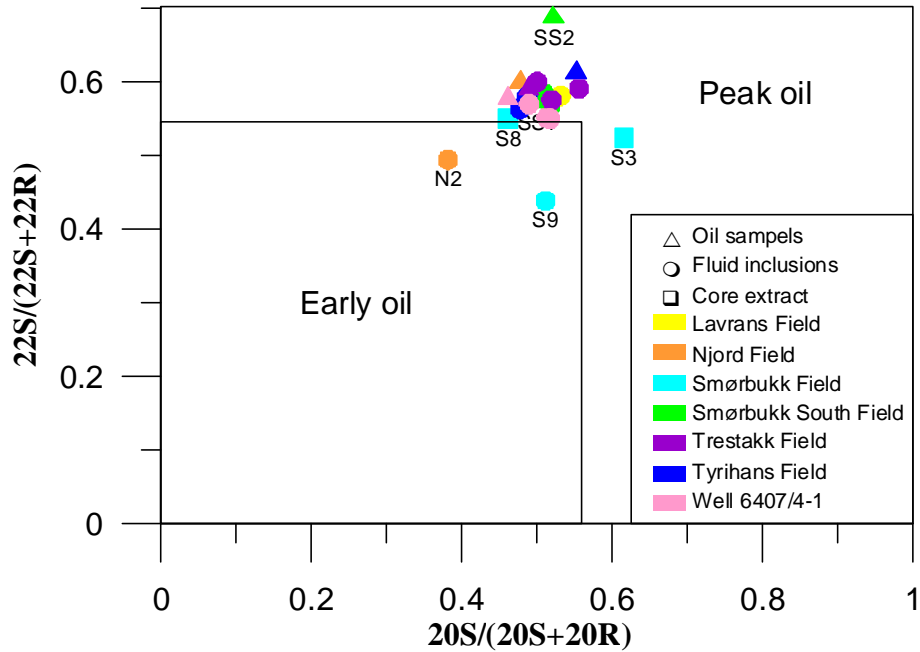


Figure 5.8. A cross-plot of two parameters describing maturity increases. Both parameters are described in chapter 3.5.3. The figure illustrates that all except two samples have reached peak oil generation; the two samples are the fluid inclusion samples from Njord (N1) and from the Tilje formation in Smørbukkk (S9). The 22S/(22s+22R) ratio indicate the samples to have been generated in-situ, meaning they have short migration paths.

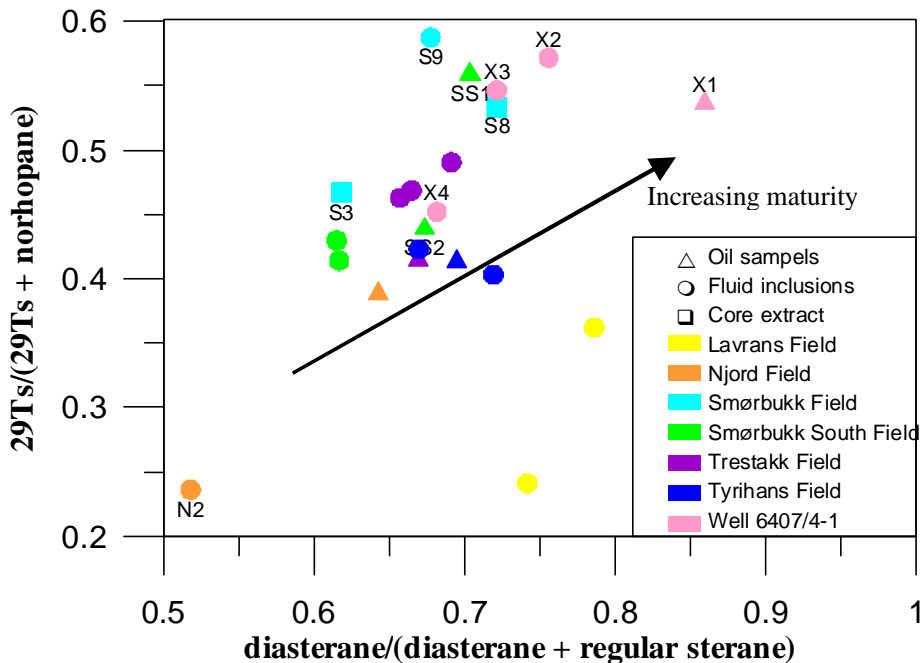


Figure 5.9. Both parameters indicate maturity differences within the data set, and plotted together the maturity trend between the fields appear. The maturity increases with an increase in the parameter value. Worth noticing is the oil sample from Njord, which was indicated to be among the most mature by the medium range maturity parameters, while the opposite trend is observed in the biomarker parameters. This suggests that the Njord oil sample is a mix between e.g. low maturity oil and a more mature condensate.

The two maturity parameters C_{23} - C_{29} tricyclic terpanes/ C_{30} $\alpha\beta$ -hopane and C_{24} tetracyclic terpanes / C_{30} $\alpha\beta$ -hopane (Mello et al., 1988) increase with increasing thermal maturities. Figure 5.10. illustrate the maturity differences between the petroleum in the dataset, the suggested trend from the least mature to the most mature is; Njord \rightarrow Trestakk and Smørbukk South \rightarrow Tyrihans \rightarrow 6407/4-1 \rightarrow Smørbukk and Lavrans. Note the contrasting maturities in the Njord oil sample from high maturities in the medium range parameters to low maturities in the biomarker parameters. This indicates the oil to be a mixture of i.e. a low maturity oil and a higher maturity condensate.

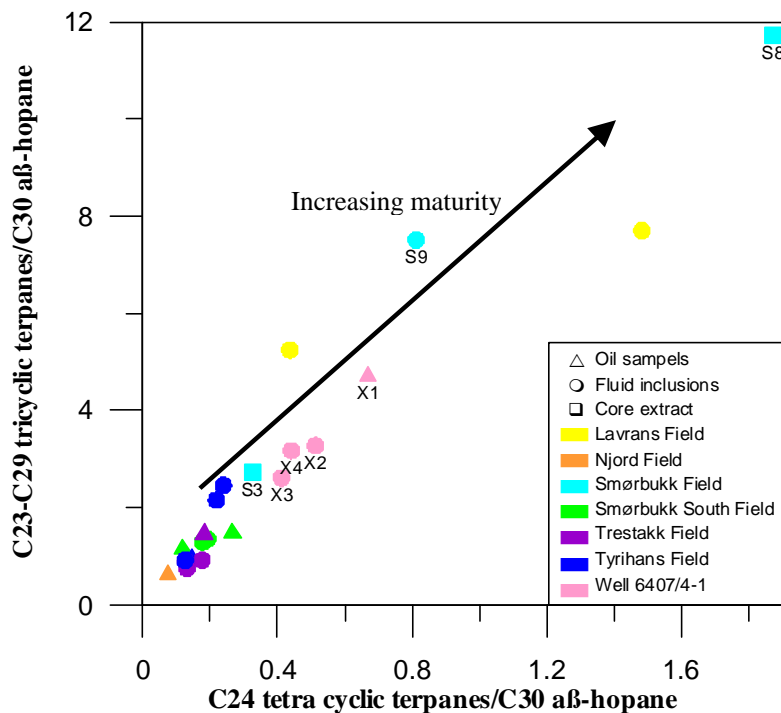


Figure 5.10. The two maturity parameters increase with increasing maturities meaning the highest maturity samples plot in the upper right corner. Note the low maturity of the Njord oil sample, which is a contrast to the high maturities found in the medium range maturity parameters. This indicates a mixing between a low maturity oil (biomarker parameters) and a more mature condensate (medium range parameters).

Summary of maturity

A general trend within the dataset is that the oils show higher maturities than the inclusion samples from the same field, indicating the inclusion to have been trapped before the arrival of the latest and most mature petroleum found in the DST samples. But be aware of the general inhibiting effect petroleum have on cementation, and because of that it is likely that fluid inclusions are most actively trapped during filling of the reservoir than at an later time, when most of the water has been displaced (Munz et al., 1999).

The Njord samples show high maturities in the medium range parameters, while the biomarker parameters show low maturities. This can be caused by mixing of a low maturity oil and high maturity condensate, indicating several pulses of petroleum.

The maturity trend from the petroleum in the inclusions is roughly from south-east to north-west, with Njord having the least mature petroleum, and Smørbukk the most mature. The exception is the 6407/4-1 well located north of Njord which is showing high maturities in both medium range and biomarker maturity parameters for the inclusion samples.

Also the oil sample from 6407/4-1 show high maturities, together with Smørbukk South and core samples from the Smørbukk field. The least mature oil samples are from Trestakk and Tyrihans. As indicated above the Njord oil is a mixture of two or more petroleum pulses and is most mature in the medium range, but least mature for the biomarkers.

The Spekk formation is deeper buried towards the centre of the basins than on the flanks, see the picture on the front of the paper showing top Spekk and how it deepens towards the north-west. Because deeper burial of the source rock will generate more mature petroleum, this supports the results found in this study. Njord, on the rim of the basin having the least mature petroleum, and the most mature petroleum found in Smørbukk, more towards the centre of the basin. The 6407/4-1 well may have received its petroleum from a local sub-basin that subsided more than other sub-basins in the area. This is possible because of the deposition of the source rock in the depressions between the rotated fault blocks, and differential subsidence of each block.

5.2.2. Organic facies of the samples

The Haltenbanken area has two recognized source rocks, one being the late Jurassic Spekk formation and the other is the early Jurassic Åre formation. The two formations were deposited in two different environments. The shales in the Spekk formation was deposited in a marine environment and contain type II/III kerogen (Whitley, 1992), whilst Åre is a type III and IV (coal) source rock with mostly deltaic terrestrial organic matter (e.g. Odden et al., 1998).

Medium range facies parameters

Pr/ph ratios typical for type II marine shales are 0.6-1.6 (Elvsborg et al., 1985; Cohen and Dunn, 1987), the samples in the dataset mainly fall into this category, except samples from Njord, 6407/10-1 and 6407/4-1. These samples have higher values indicating a more terrestrial input. But when pr/ph values are plotted towards hopane/sterane values the figure indicate most of the samples to be derived from a marine source rock (figure 5.12.).

The conclusion from figure 5.1. and 5.11. is that the depositional environment for the source rock that generated the petroleum in the samples are transitional, meaning it is marine with terrestrial input. This is by Shanmugan (1984) described to be typical for a proximal type II source rock. From the figures a proximal to distal sequence can be found for both oils and inclusions. The Njord and 6407/4-1 oil samples are the oils with the highest terrestrial input, followed by Smørbukk and Smørbukk South, and the Trestakk and Tyrihans North oils show the least terrestrial input. The petroleum in the inclusion samples are wider spread, indicating higher diversity. 6407/4-1 samples show the highest input of terrestrial organic matter →

Smørbukk, Smørbukk South, Lavrans → Trestakk, Tyrihans, Njord → 6407/10-1 are deposited in the most marine, reducing environment.

Inclusion samples from Smørbukk South (SS3 and SS4), Smørbukk (S9) and Trestakk (TR2), together with the core extract sample S8 from Smørbukk have pr/ph values below 1.0, indicated by figure 5.7. to be generated from a lacustrine, sulphur-poor deposit. This may be an indication of more proximal depositional environments for the source rock.

Biomarker facies parameters

The presence of 28, 30 bisnorhopane in all the samples, both inclusions and oils/extracts, indicate the hydrocarbons to have been generated from generally the same source rock facies. A plot of the hopane/sterane ratio towards the bisnorhopane/(bisnorhopane+norhopane) ratio give a scattered impression. But note the inclusions and the oils from the same field plot close together in most cases, indicating the inclusion and trapped petroleum to have been generated from mainly the same facies (see figure 5.4.). A high hopane/sterane ratio can indicate terrestrial input, while low ratios are typical for marine derived petroleum. Based on this it is possible to suggest a sequence from proximal (most terrestrial input) to distal; Njord, Tyrihans, Trestakk → Smørbukk South → 6407/4-1, Lavrans → Smørbukk.

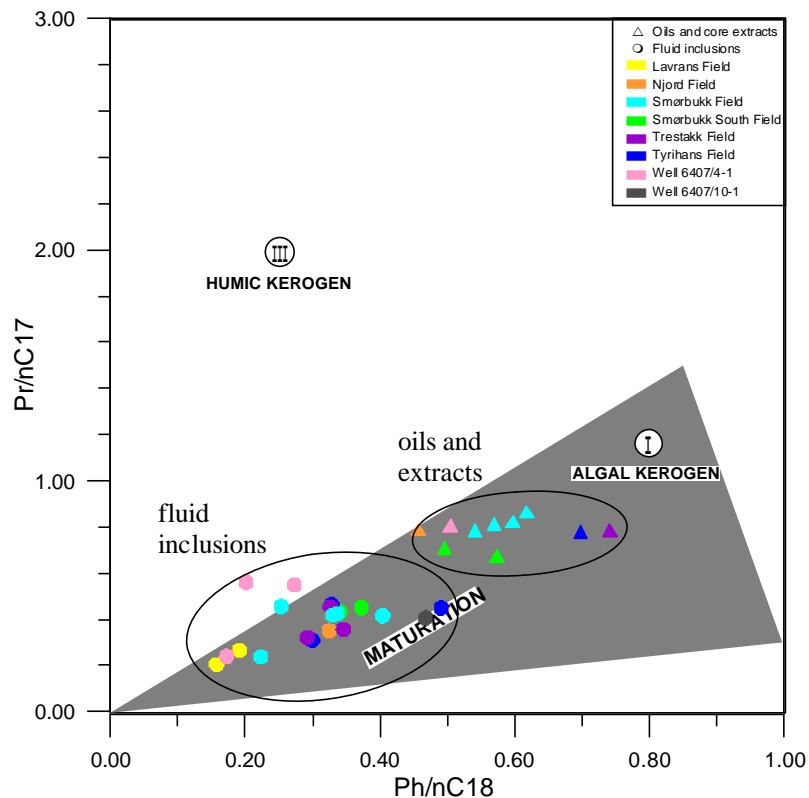


Figure 5.11. A plot of the Ph/n-C₁₈ ratio versus the Pr/n-C₁₇ ratio (modified from Connan and Cassou, 1980) indicating the maturity as well as the type of kerogen present in the source rock from where the petroleum originated.

The relationship between C_{27} , C_{28} , and C_{29} $\beta\beta$ steranes have been used to distinguish source rock facies of petroleum. The ternary plot in figure 5.3. are divided into sub-areas where the individual areas are assigned to specific depositional environments (Shanmugam, 1984). Most of the samples plot in the estuarine area, indicating a terrestrial input. But the oil sample from Tyrihans North and 6407/4-1, together with inclusion samples from Lavrans and 6407/10-1 plot closer to the open marine area. This may either indicate a shift towards more distal facies in the source rock or petroleum being derived from local sub basins.

Summary of organic facies

In this study none of the samples show evidence of being derived from the terrestrial Åre formation with type III kerogen. It is important to note that the petroleum expected from this formation is composed of ~80% gas/condensate (Heum et al., 1986). The high temperature needed to expel gas/condensate would to a large extent destroy the biological markers (Peters and Moldowan, 1993), however, recent results from Patience (2003) based on isotopical models conclude that the gases on Mid-Norway are most likely to have been generated from a marine source, not from a coaly source rock like Åre.. Anyway, the results indicate that the samples were derived from a marine source, like the Spekk formation, but with obvious differences between proximal and distal parts of the source rock.

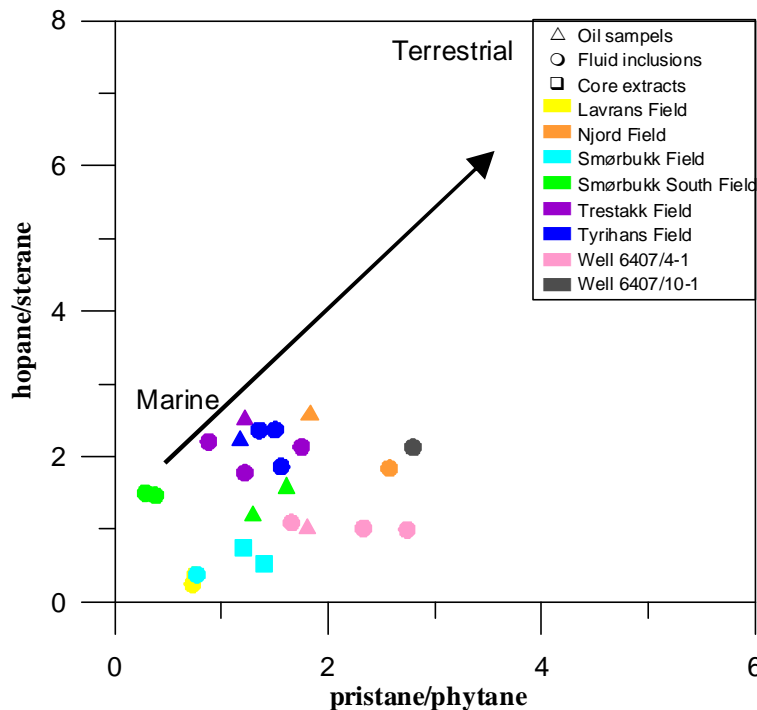


Figure 5.11. A plot of the facies parameters pristane/phytane versus hopane/sterane. A high value indicate strong terrestrial input, while lower values indicate more normal marine source rock facies. There is a trend in the studied fields from the Njord in the south-east to the Smørbukk and Smørbukk South in the north-west. Samples from Njord show the highest influence of terrestrial input.

Figure 5.11. combines medium range and biomarker facies parameters and it is obvious (as also discussed in earlier in this chapter) that the samples plot in the marine area, but with a different terrestrial influx. The Njord samples and sample Y1 from 6407/10-1 show highest terrestrial influence and this is not surprising since the paleo-coastline is towards the south-east and these samples are in the eastern part of the study area. The petroleum found in Smørbukk and Smørbukk South located towards the north-west show the least influence of terrestrial input. Karlsen et al. (1995) found the facies trend within the area to be from west to east, corresponding to the results found in this study.

Facies variations within the Spekk formation have been discussed by several authors (e.g. Karlsen et al., 1995) concluding that there are significant vertical and lateral changes. Because the petroleum are generated locally in most of the fields the facies differences are easily seen between both the oils and inclusions as well as between the fields.

6. Summary and conclusions

The data set includes oil and core samples from Lavrans, Njord, Smørbukk, Smørbukk South, Tyrihans North and South, Trestakk, well 6407/4-1 and well 6407/10-1 located in the Haltenbanken area. The aim was to compare trapped hydrocarbons and fluid inclusions within each field to determine if there are any maturity or facies differences between petroleum inclusions and oils or extracts, and to examine if there is any geographic distribution in the geochemistry of this region.

Extraction of hydrocarbons in the range C_{15+} from the inclusion samples was possible. But because of the low amount of organic material in the fluid inclusions the inclusion content could not be analysed on the GC-FID like the oils and core extracts, but had to be analysed on the GC-MS.

The oil and inclusion samples from the different fields show a wide variation in maturity ranging from petroleum generated early to late in the oil window. A regional maturity trend within the inclusion samples was found to go from the least mature in the south-east to the most mature in the north-west. An exception from this was well 6407/4-1 located in the south-east, which shows high maturities both for the oil and inclusions. The oil samples generally showed more uniform maturity than the inclusions and a specific trend was not observed. One sample differs from the others, the Njord oil show high maturities within the medium range parameters, whilst low maturities are observed within the biomarker parameters. This is a result of mixing between a low maturity oil and high maturity condensate, and is only observed in this sample.

Facies variations within the fields if found were small, but between the fields the organic facies signatures vary within the range from marine to “estuarine” depositional environments for the source rock. A trend was observed with higher terrestrial input to the source rock kerogen in the proximal east-western region, whereas in the more distal north-western regions the SR kerogen is inferred to be more amorphous and deposited under more reducing conditions. Knowing the paleo coastline is trending from south-west to north-east south of the Haltenbanken area, the difference between the fields reflects a shift from proximal to distal depositional environments. It is believed that a marine type II SR generated petroleum found in both inclusions and traps. No evidence was found for petroleum generated from the Åre formation, one should keep in mind that the Spekk formation with its overall lower maturity as compared to the Åre formation, would be expelling petroleum with much higher relative concentrations of biomarkers. This will reduce possible trace signals from early Åre derived petroleum in the traps and inclusions.

6. Conclusion

Thus, in general, the oil samples from the traps show the same facies signatures as the extracts from the petroleum inclusions, but at a higher maturity. This could correspond with the inclusion having trapped paleo-petroleum generated when the source rock were shallower and expelling petroleum of lower maturity.

This study has illustrated that integration of petroleum inclusions data and present-day petroleum samples can give information and knowledge on fluid distribution, HC migration and fluid properties in time and space, and as such improve our understanding of large scale HC movement in basins.

-
- Albrecht, P., Vandenbroucke, M. and Mandengue, M., 1976: Geochemical studies on the organic matter from the Douala Basin (Cameroon) - I. Evolution of the extractable organic matter and the formation petroleum. *Geochimica et Cosmochimica Acta*, **40**, 337-350.
- Alexander, R., Kagi, R. I. and Woodhouse, G. W., 1981: Geochemical correlation of Windalia oil and extracts of Winning Group (Cretaceous) potential source rocks, Barrow Subbasin, Western Australia. *AAPG Bulletin*, **65**, 235-250.
- Angard, K. A., 1996: Reservoir geochemistry of the Smørbukk, Smørbukk Sør, and the Heidrun fields-Haltenbanken, norwegian offshore continental shelf, K.A. Angard.
- Arbenz, J. K., 1992: Geological atlas of Western and Central Europe 1990; book review. *AAPG Bulletin*, **76**, 291-292.
- Bang, J., 1998: Lavrans interim report (doc.id.: RA98-444/REM).
- Bergan, M., 1999: Progress update document, Lavrans Field (doc.id.: RA99-384/NNA).
- Bhullar, A. G., Karlsen, D. A., Backer, O. K., Le Tran, K., Skålnes, E., Berchermann, H. H. and Kittelsen, J. E., 2000: Reservoir characterization by combined micro-extraction - micro thin-layer chromatography (Iatroscan) method : A calibration study with examples from the Norwegian North Sea. *Journal of Petroleum Geology*, **23**, 221-244.
- Blystad, P., Brekke, H., Færseth, R. B., Larsen, B. T., Skogseid, J. and Tørudbakken, B., 1995: Structural elements of the Norwegian continental shelf. Part II: The Norwegian Sea Region. *Norwegian Petroleum Directorate Bulletin*, 1-45.
- Bodnar, R. J., 1990: Petroleum migration in the Miocene Monterey Formation, California, USA: Constraints from fluid-inclusion studies. *Mineralogical Magazine*, **54**, 295-304.
- Bray, E. E. and Evans, E. D., 1961: Distribution of n-paraffins as a clue to recognition of source beds. Symposium on the chemical approaches to the recognition of petroleum source rocks., Pergamon, 2-15.
- Bray, E. E. and Evans, E. D., 1965: Hydrocarbons in non-reservoir-rock source beds. *Bulletin of the American Association of Petroleum Geologists*, **49**, 248-257.
- Brekke, H., Dahlgren, S., Nyland, B. and Magnus, C., 1999: The prospectivity of the Vøring and Møre basins on the Norwegian Sea continental margin. Petroleum geology of Northwest Europe; proceedings of the 5th conference., Boldy, S. A. R., Ed., The Geological Society of London, 261-274.
- Bukovics, C. and Ziegler, P. A., 1985: Tectonic development of the mid-Norway continental margin. *Marine and Petroleum Geology*, **2**, 2-22.
- Bukovics, C., Cartier, E. G., Shaw, N. D. and Ziegler, P. A., 1984: Structure and development of the mid-Norway continental margin. Petroleum geology of the North European margin., Spinnangr, A., Ed., Graham and Trotman, 407-423.
- Bøen, F., Eggen, S. and Vollset, J., 1983: Structures and basins of the margin from 62° - 69° N and their development. NPD - contribution no 8, Oljedirektoratet, 43.

-
- Clayton, J. L. and Bostick, N. H., 1986: Temperature effects on kerogen and on molecular and isotopic composition of organic matter in Pierre Shale near an igneous dike. *Advances in organic geochemistry, 1985; Part I, Petroleum geochemistry.*, Ruellkotter, J., Ed., Pergamon, 135-143.
- Cohen, M. J. and Dunn, M. E., 1987: The hydrocarbon habitat of the Haltenbanken-Traenabank area, offshore Norway. *Petroleum geology of north west Europe.*, Glennie Kenneth, W., Ed., Graham & Trotman, 1091-1104.
- Connan, J. and Cassou, A. M., 1980: Properties of gases and petroleum liquids derived from terrestrial kerogen at various maturation levels. *Geochimica et Cosmochimica Acta*, **44**, 1-23.
- Conoco Norway, I., 1986: Final well report, well 6507/7-5. Licence PL095, 174 pp.
- Corfield, S. and Sharp, I. R., 2000: Structural style and stratigraphic architecture of fault propagation folding in extensional settings: a seismic example from the Smørbukk area, Halten Terrace, Mid-Norway. *Basin Research*, **12**, 329-341.
- Cornford, C., Needham, C. E. J. and De Walque, L., 1986: Geochemical habitat of North Sea oils and gases. Habitat of hydrocarbons on the Norwegian continental shelf; proceedings of an international conference., Spencer, A. M., Ed., Graham & Trotman, 39-54.
- Cornford, C., Morrow, J. A., Turrington, A., Miles, J. A. and Brooks, J., 1983: Some geological controls on oil composition in the U.K. North Sea. *Petroleum geochemistry and exploration of Europe; International congress.*, Brooks, J., Ed., Geological Society of London, 175-194.
- Dahl, B. and Speers, G. C., 1985: Organic geochemistry of the Oseberg field. *Petroleum geochemistry in exploration of the Norwegian Continental shelf*, Thomas Bruce, M. E. A., Ed., Graham and Trotman, 185-195.
- Dalland, A., Worsley, D. and Ofstad, K., 1988: A Lithostratigraphic scheme for the Mesozoic and Cenozoic succession offshore mid- and northern Norway. Vol. 4, *NPD Bulletin*, Oljedirektoratet.
- Eglinton, G. and Murphy, M. T. J., Eds., 1969: *Organic geochemistry - methods and results.* 781 pp.
- Ehrenberg, S. N., 1990: Sandstone permeability viewed as a function of intergranular macroporosity; Garn Formation, Haltenbanken, mid-Norwegian continental shelf. AAPG annual convention with DPA/ EMD divisions and SEPM, an associated society; technical program with abstracts., Anonymous, Ed., American Association of Petroleum Geologists, 648.
- Ehrenberg, S. N., Gjerstad, H. M. and Hadler Jacobsen, F., 1992: Smorbukk Field; a gas condensate fault trap in the Haltenbanken Province, offshore mid-Norway. *Giant oil and gas fields of the decade 1978-1988.*, Halbouty Michel, T., Ed., American Association of Petroleum Geologists, 323-348.

-
- Ellenor, D. W. and Mozetic, A., 1986: The Draugen oil discovery. Habitat of hydrocarbons on the Norwegian continental shelf; proceedings of an international conference., Spencer, A. M., Ed., Graham & Trotman, 313-316.
- Elvsborg, A., Hagevang, T. and Throndsen, T., 1985: Origin of the gas-condensate of the Midgard Field at Haltenbanken. Petroleum geochemistry in exploration of the Norwegian Shelf., Larsen Rolf, M., Ed., Graham and Trotman, 213-219.
- Forbes, P. L., Ungerer, P. M., Kuhfuss, A. B., Riis, F. and Eggen, S., 1991: Compositional modeling of petroleum generation and expulsion; trial application to a local mass balance in the Smorbukk Sor Field, Haltenbanken area, Norway. *AAPG Bulletin*, **75**, 873-893.
- Gage, M. S. and Dore, A. G., 1986: A regional geological perspective of the Norwegian offshore exploration provinces. Habitat of hydrocarbons on the Norwegian continental shelf; proceedings of an international conference., Spencer, A. M., Ed., Graham & Trotman, 21-38.
- Hagemann, H. W. and Hollerbach, A., 1986: The fluorescence behaviour of crude oils with respect to their thermal maturation and degradation. *Advances in organic geochemistry*, 1985; Part I, Petroleum geochemistry., Ruellkotter, J., Ed., Pergamon, 473-480.
- Heum, O. R., Dalland, A. and Meisingset, K. K., 1986: Habitat of hydrocarbons at Haltenbanken (PVT-modelling as a predictive tool in hydrocarbon exploration). Habitat of hydrocarbons on the Norwegian continental shelf; proceedings of an international conference., Spencer, A. M., Ed., Graham & Trotman, 259-274.
- Hinz, K., Eldholm, O., Block, M. and Skogseid, J., 1993: Evolution of North Atlantic volcanic continental margins. *Petroleum geology of Northwest Europe; Proceedings of the 4th conference.*, Parker, J. R., Ed., The Geological Society of London, 901-913.
- Horstad, I., 1989: Petroleum composition and heterogenities within the Middle Jurassic reservoir in The Gulfaks field area, Norwegian North Sea, Department of Geology, University of Oslo.
- Hughes, W. B., Holba, A. G., Miller, D. E. and Richardson, J. S., Eds., 1985: Geochemistry of greater Ekofisk crude oils. *Petroleum Geochemistry in Exploration of the Norwegian Shelf*, Graham and Trotman, 75-92 pp.
- Hunt, J. M., 1996: *Petroleum geochemistry and geology*. W. H. Freeman and Company, 743 pp.
- Hvoslef, S., Larter, S. R. and Leythaeuser, D., 1988: Aspects of generation and migration of hydrocarbons from coal-bearing strata of the Hitra Formation, Haltenbanken area, offshore Norway. *Advances in organic geochemistry 1987; Part I, Organic geochemistry in petroleum exploration; proceedings of the 13th international meeting on organic geochemistry.*, Novelli, L., Ed., Pergamon, 525-536.
- Hydro, 2003: Njord field. Sjøholm, J., Ed.

-
- Jacobsen, V. W. and Van Veen, P., 1984: The Triassic offshore Norway north of 62 degrees N. Petroleum geology of the North European margin., Spinnangr, A., Ed., Graham and Trotman, 317-327.
- Karlsen, D. A., 2000: The Svale discovery: In the genetic context of other petroleum systems off Mid-Norway, 59 pp.
- Karlsen, D. A. and Larter, S. R., 1989: A rapid correlation method for petroleum population mapping within individual petroleum reservoirs - applications to petroleum reservoir description. Correlation in Hydrocarbon Exploration, Haresnape, J., Ed., 77-85.
- Karlsen, D. A. and Larter, S. R., 1991: Analysis of petroleum fractions by TLC-FID; applications to petroleum reservoir description. *Organic Geochemistry*, **17**, 603-617.
- Karlsen, D. A., Nedkvitne, T., Larter, S. R. and Bjørlykke, K., 1993: Hydrocarbon composition of authigenic inclusions: Application to elucidation of petroleum reservoir filling history. *Geochimica et Cosmochimica Acta*, **57**, 3641-3659.
- Karlsen, D. A., Nyland, B., Flood, B., Ohm, S. E., Brekke, T., Olsen, S. and Backer-Owe, K., 1995: Petroleum geochemistry of the Haltenbanken, Norwegian continental shelf. The geochemistry of reservoirs., England, W. A., Ed., Geological Society of London, 203-256.
- Karlsen, D. A., Backer-Owe, K., Skeie, J. E., Bjorlykke, K., Olstad, R., Berge, K., Cecchi, M., Vik, E. and Schaefer, R. G., in prep.: Petroleum migration, faults and overpressure.
- Karlsson, W., 1984: Sedimentology and diagenesis of Jurassic sediments offshore mid-Norway. Petroleum geology of the North European margin., Spinnangr, A., Ed., Graham and Trotman, 389-396.
- Khorasani, G. K., 1987: Novel development in fluorescence microscopy of complex organic mixtures; application in petroleum geochemistry. *Organic Geochemistry*, **11**, 157-168.
- Khorasani, G. K., 1989: Factors controlling source rock potential of the Mesozoic coal-bearing strata from offshore central Norway; application to petroleum exploration. *Bulletin of Canadian Petroleum Geology*, **37**, 417-427.
- Kvalheim, O. M., Telnaes, N., Bjorseth, A. and Christy, A. A., 1987: Interpretation of multivariate data; relationship between phenanthrenes in crude oils. Multivariate statistical workshop for geologists and geochemists., Kvalheim, O. M., Ed., Elsevier, 149-153.
- Larsen, V., Morkeseth, P. O. and Aasheim, S. M., 1987: Tyrihans. Geology of the Norwegian oil and gas fields., Spencer, A. M., Ed., Graham & Trotman, 411-418.
- Lilleng, T. and Gundestø, R., 1997: The Njord Field: a dynamic hydrocarbon trap. Vol. 7, *Hydrocarbons seals: Importance for exploration and production. NPF Special Publication*, Elsevier, Singapore, 217-229 pp.

-
- Mackenzie, A. S., 1984: Applications of biological markers in petroleum geochemistry. *Advances in petroleum geochemistry; Volume 1.*, Welte, D. H., Ed., Acad. Press, 115-214.
- Mackenzie, A. S., Quirke, J. M. E. and Maxwell, J. R., 1980: Molecular parameters of maturation in the Toarcian shales, Paris Basin, France; II, Evolution of metalloporphyrins. *Advances in organic geochemistry 1979.*, Maxwell, J. R., Ed., Pergamon, 239-248.
- Mackenzie, A. S., Maxwell, J. R., Coleman, M. L. and Deegan, C. E., 1984: Biological marker and isotope studies of North Sea crude oils and sediments. *Proceedings - World Petroleum Congress = Actes et Documents - Congres Mondial du Petrole*, **11**, 45-56.
- Mackenzie, A. S., Rullkoetter, J., Welte, D. H. and Mankiewicz, P., 1985: Reconstruction of oil formation and accumulation in North Slope, Alaska, using quantitative gas chromatography-mass spectrometry. Alaska North Slope oil-rock correlation study; analysis of North Slope crude., Claypool, G. E., Ed., American Association of Petroleum Geologists, 319-377.
- Mackenzie, D. P., 1978: Some remarks on the development of sedimentary basins. *Earth and Planetary Science Letters*, **40**, 25-32.
- McMaster, M. and McMaster, C., 1998: GC/MS - A Practical User's Guide. Wiley - VCH, 189 pp.
- Mello, M. R., Telnaes, N., Gaglianone, P. C., Chicarelli, M. I., Brassell, S. C. and Maxwell, J. R., 1988: Organic geochemical characterisation of depositional palaeoenvironments of source rocks and oils in Brazilian marginal basins. *Advances in organic geochemistry 1987; Part I, Organic geochemistry in petroleum exploration; proceedings of the 13th international meeting on organic geochemistry.*, Novelli, L., Ed., Pergamon, 31-45.
- Mo, E. S., Thronsen, T., Andresen, P., Backstrom, S. A., Forsberg, A., Haug, S. and Torudbakken, B., 1989: A dynamic deterministic model of hydrocarbon generation in the Midgard Field drainage area offshore Mid-Norway. Geologic modeling; aspects of integrated basin analysis and numerical simulation., Anonymous, Ed., Springer International, 305-317.
- Moldowan, J. M., Seifert, W. K. and Gallegos, E. J., 1985: Relationship between petroleum composition and depositional environment of petroleum source rock. *AAPG Bulletin*, **69**, 1255-1268.
- Moldowan, J. M., Fago, F. J., Carlson, R. M. K., Young, D. C., Van, D. G., Clardy, J., Schoell, M., Pillinger, C. T. and Watt, D. S., 1991: Rearranged hopanes in sediments and petroleum. *Geochimica et Cosmochimica Acta*, **55**, 3333-3353.
- Munz, I. A., 2000: Petroleum inclusions in sedimentary basins: systematic, analytical methods and applications. *Lithos*, **55**, 195-212.
- Munz, I. A., 2001: Petroleum inclusions in sedimentary basins: systematic, analytical methods and applications. *Lithos*, **55**, 195-212.

-
- Munz, I. A., Johansen, H., Holm, K. and Lacharpagne, J. C., 1999: The petroleum characteristics and filling history of the Frøy Field and the Rind discovery, Norwegian North Sea. *Marine and Petroleum Geology*, **16**, 633-651.
- Odden, W., Patience, R. L. and Van Graas, G. W., 1998: Application of light hydrocarbons (C (sub 4) -C (sub 13)) to oil/ source rock correlations; a study of the light hydrocarbon compositions of source rocks and test fluids from offshore Mid-Norway. *Organic Geochemistry*, **28**, 823-847.
- Patience, R. L., 2003: Where did all the coal gas go? *Organic Geochemistry*, **34**, 375-387.
- Pedersen, J. H., 2002: Atypical oils, unusual condensates and bitumens of the Norwegian Continental Shelf : an organic geochemical study, Geology, Natural Science, University of Oslo.
- Peters, K. E. and Moldowan, J. M., 1993: The biomarker guide. Interpreting molecular fossils in petroleum and ancient sediments. Prentice Hall Englewood Cliffs, N. J., 363 pp.
- Philippi, G. T., 1965: On the depth, time and mechanism of petroleum generation. *Geochimica et Cosmochimica Acta*, **29**, 1021-1049.
- Pittion, J. L. and Gouadain, J., 1985: Maturity studies of the Jurassic "coal unit" in three wells from the Haltenbanken area. Petroleum geochemistry in exploration of the Norwegian Shelf., Larsen, R. M., Ed., Graham and Trotman, 205-211.
- Planke, S., Skogseid, J. and Eldholm, O., 1991: Crustal structure off Norway, 62 degrees to 70 degrees north. Imaging and understanding the lithosphere of Scandinavia and Iceland., Lund, C. E., Ed., Elsevier, 91-107.
- Provan, D. M. J., 1992: Draugen oil field, Haltenbanken Province, offshore Norway. Giant oil and gas fields of the decade 1978-1988., Halbouty, M. T., Ed., American Association of Petroleum Geologists, 371-382.
- Radke, M., 1988: Application of aromatic compounds as maturity indicators in source rocks and crude oils. *Marine and Petroleum Geology*, **5**, 224-236.
- Radke, M. and Welte, D. H., 1983: The methylphenanthrene index (MPI); a maturity parameter based on aromatic hydrocarbons. Advances in organic geochemistry 1981., Speers, G., Ed., Wiley & Sons, 504-512.
- Radke, M., Welte, D. H. and Willsch, H., 1982a: Geochemical study on a well in the western Canada Basin; relation of the aromatic distribution pattern to maturity of organic matter. *Geochimica et Cosmochimica Acta*, **46**, 1-10.
- Radke, M., Vriend, S. P. and Schaefer, R. G., 2001: Geochemical characterization of Lower Toarcian source rock from NW Germany: Interpretation of aromatic and saturated hydrocarbons in relation to depositional environment and maturation effects. *Journal of Petroleum Geology*, **24(3)**, 287-307.
- Radke, M., Willsch, H., Leythaeuser, D. and Teichmueller, M., 1982b: Aromatic components of coal; relation of distribution pattern to rank. *Geochimica et Cosmochimica Acta*, **46**, 1831-1848.

-
- Requejo, G., Ed., 1992: Quantitative analysis of triterpane and sterane biomarkers: Methodology and applications in molecular maturity studies. *Biological Markers in Sediments and Petroleum*, Prentice Hall, 222-240 pp.
- Rønnevik, H. C., 1998: The exploration experience from Midtgard to Kristin - Norwegian Sea. Improving the Exploration Process by Learning from the Past - Norwegian Petroleum Society conference, Alexander-Marrack, P. D., Ed., Elsevier, 113-129.
- Seifert, W. K. and Moldowan, J. M., 1978: Applications of steranes, terpanes and monoaromatics to the maturation, migration and source of crude oils. *Geochimica et Cosmochimica Acta*, **42**, 77-95.
- Seifert, W. K. and Moldowan, J. M., 1986: Use of biological markers in petroleum exploration. Biological markers in the sedimentary record., Johns, R. B., Ed., Elsevier, 261-290.
- Sellwood, B. W., Wilkes, M. and James, B., 1993: Hydrocarbon inclusions in late calcite cements - migration indicators in the great-oolite group, Weald-basin, S England. *Sedimentary Geology*, **84**, 51-55.
- Shanmugam, G., 1984: Significance of terrestrial environments and related organic matter in generating commercial quantities of oil, Gippsland Basin, Australia. Society of Economic Paleontologists and Mineralogists First annual midyear meeting., Society of Economic Paleontologists and Mineralogists, 73.
- Skålnes, E., 1993: Petroleum geochemistry and filling history of the Hild field, Norwegian Continental Shelf, Department of Geology, University of Oslo.
- ten Haven, H.-L., De Leeuw, J. W., Rullkoetter, J. and Sinninghe Damste, J. S., 1987: Restricted utility of the pristane/ phytane ratio as a palaeoenvironmental indicator. *Nature (London)*, **330**, 641-643.
- Tissot, B., Califet, D. Y., Deroo, G. and Oudin, J. L., 1971: Origin and evolution of hydrocarbons in Early Toarcian Shales, Paris Basin, France. *The American Association of Petroleum Geologists Bulletin*, **55**, 2177-2193.
- Tissot, B. P. and Welte, D. H., 1978: Petroleum formation and occurrence : a new approach to oil and gas exploration. Springer-Verlag, 538 pp.
- Van Graas, G. W., 1990: Biomarker maturity parameters for high maturities: Calibration of the working range up to the oil/condensate threshold. *Organic Geochemistry*, **16**, 1025-1032.
- Walderhaug, O., 1994: Precipitation rates for quartz cement in sandstones determined by fluid-inclusion microthermometry and temperature-history modeling. *Journal of Sedimentary Research, Section A: Sedimentary Petrology and Processes*, **64**, 324-333.
- Waples, D. W. and Machihara, T., 1991: Biomarkers for geologists - A practical guide to the application of steranes and triterpanes in petroleum geology. Vol. 9, *AAPG Methods in Exploration*, AAPG, 91 pp.
- Welte, D. H., Horsfield, B. and Baker, D. R., Eds., 1997: Petroleum and basin evolution. Springer, 535 pp.

-
- Whitley, P. K., 1992: The geology of Heidrun; a giant oil and gas field on the mid-Norwegian shelf. Giant oil and gas fields of the decade 1978-1988., Halbouty, M. T., Ed., American Association of Petroleum Geologists, 383-406.
- Wilhelms, A. and Larter, S. R., 1994: Origin of tar mats in petroleum reservoirs; Part II, Formation mechanisms for tar mats. *Marine and Petroleum Geology*, **11**, 442-456.
- Ziegler, W. H., Doery, R. and Scott, J., 1986: Tectonic habitat of Norwegian oil and gas. Habitat of hydrocarbons on the Norwegian continental shelf; proceedings of an international conference, Spencer, A. M., Ed., Graham & Trotman, London, UK, 3-19.
- Aasheim, S. M. and Larsen, V., 1984: The Tyrihans discovery; preliminary results from well 6407/ 1-2. Petroleum geology of the North European margin., Spinnangr, A., Ed., Graham and Trotman, 285-291.
- Aasheim, S. M., Dalland, A., Netland, A. and Thon, A., 1986: The Smorbukk gas/ condensate discovery, Haltenbanken. Habitat of hydrocarbons on the Norwegian continental shelf; proceedings of an international conference., Spencer, A. M., Ed., Graham & Trotman, 299-305.

Appendix

Table of contents

Sample L1, well 6406-2-2 (incl 4487 m), Garn fm, Lavrans	2
Sample L2, well 6406-2-2 (incl 4492-93 m), Garn fm, Lavrans	6
Sample N1, well 6407-7-4 DST 2A, Tilje fm, Njord	10
Sample N2, well 6407-7-4 (incl 3038+3043 m), Njord	14
Sample S1, well 6506-12-9S (core extract 4416 m), Garn fm, Smørbukk	18
Sample S3, well 6506-12-9S (core extract 4472 m), Not fm, Smørbukk	19
Sample S4, well 6506-12-9S (incl 4472 m), Not fm, Smørbukk	23
Sample S5, well 6506-12-9S (core extract 4634.8 m), Tofte fm, Smørbukk	24
Sample S6, well 6506-12-9S (incl 4634.8 m), Tofte fm, Smørbukk	25
Sample S7, well 6506-12-9S (incl 4672m), Tilje fm, Smørbukk	26
Sample S8, well 6406-12-9S (core extract 4751.3 m), Tilje fm, Smørbukk	27
Sample S9, well 6406-12-9S (incl 4751.3 m), Tilje fm, Smørbukk	31
Sample SS1, well 6506-12-3 DST 1, Tilje fm, Smørbukk South	35
Sample SS2, well 6506-12-3 DST 6, Lysing fm, Smørbukk South	39
Sample SS3, well 6506-12-3 (incl 3872 m, coarse), Garn fm, Smørbukk South	43
Sample SS4, well 6506-12-3 (incl 3872 m, fine), Garn fm, Smørbukk South	47
Sample TN1, well 6407-1-3 DST 1, Garn fm, Tyrihans North	51
Sample TN2, well 6407-1-3 (incl 3648 m, coarse), Garn fm Tyrihans North	55
Sample TN3, well 6407-1-3 (incl 3648 m, fine), Garn fm Tyrihans North	59
Sample TS1, well 6407-1-2 (incl 3666.5 m), Garn fm, Tyrihans South	63
Sample TR1, well 6406-3-2 DST 2, Garn fm, Trestakk	67
Sample TR2, well 6406-3-2 (incl 3954.5 m), Garn fm, Trestakk	71
Sample TR3, 6406-3-2 (incl 3932 m, coarse), Garn fm, Trestakk	75
Sample TR4, well 6406-3-2 (incl 3932 m, fine), Garn fm, Trestakk	79
Sample X1, well 6407-4-1 DST 2, Garn fm	83
Sample X2, well 6407-4-1 (inclusions 3893 m, coarse), Garn fm	87
Sample X3, well 6407-4-1 (inclusions 3893 m, fine), Garn fm	91
Sample X4, well 6407-4-1 (inclusions 3893 m, ex coarse), Garn fm	95
Sample Y1, well 6407-10-1 (inclusions 2359.7 m)	99

Both the appendix and the thesis are found on the cd on the last page.

